https://theses.gla.ac.uk/

Theses Digitisation:

https://www.gla.ac.uk/myglasgow/research/enlighten/theses/digitisation/

This is a digitised version of the original print thesis.

Copyright and moral rights for this work are retained by the author

A copy can be downloaded for personal non-commercial research or study, without prior permission or charge

This work cannot be reproduced or quoted extensively from without first obtaining permission in writing from the author

The content must not be changed in any way or sold commercially in any format or medium without the formal permission of the author

When referring to this work, full bibliographic details including the author, title, awarding institution and date of the thesis must be given

Enlighten: Theses
https://theses.gla.ac.uk/
research-enlighten@glasgow.ac.uk

SEISMIC STUDIES OF LOCAL EVENTS RECEIVED AT THREE ARRAYS IN SOUTHERN CENTRAL SCOTLAND

by

ZUHAIR HASAN M. EL-ISA

B.Sc. CAIRO UNIVERSITY

M.Sc. STRATHCLYDE UNIVERSITY

Thesis submitted in fulfilment of the degree of Doctor of Philosophy of Science (by research) in the Geology Department, University of Glasgow.

Geology Department
University of Glasgow
Glasgow

November 1977

ProQuest Number: 10984507

All rights reserved

INFORMATION TO ALL USERS
The quality of this reproduction is dependent upon the quality of the copy submitted.

In the unlikely event that the author did not send a complete manuscript
and there are missing pages, these will be noted. Also, if material had to be removed,
a note will indicate the deletion.

ProQuest 10984507

Published by ProQuest LLC (2018). Copyright of the Dissertation is held by the Author.

All rights reserved.
This work is protected against unauthorized copying under Title 17, United States Code
Microform Edition © ProQuest LLC.

ProQuest LLC.
789 East Eisenhower Parkway
P.O. Box 1346
Ann Arbor, MI 48106 – 1346

Thesis
4696
Copy 1.

TO MY PARENTS

TO WHOM I WILL BE ETERNALLY GRATEFUL

ACKNOWLEDGEMENTS

I wish to thank Professor B. Leake of the Geology Department, with whose permission this work has been carried out. I am also grateful for the invaluable advice and constructive criticism of my supervisor, Dr. D. W. Powell. His assistance has been available to me throughout the course of this work.

Thanks are also due to Dr. A. McLean and Dr. J. Hall, of the Geology Department, for useful discussions; Mr R. Morrison and his staff, particularly Messrs. G. Gordon and R. Cumberland, for apparatus preparation and maintenance and assistance in the field; my research colleagues, F. Al-Haddad, B. Rashid, H. Al-Dabagh, M. Al-Omari, J. Wilcox, M. Wilson and my brother, S. El-Isa, for assistance in the field; Dr. Sharp of the Computing Department (Glasgow) for transcribing digitised tapes and writing a program to read them; Dr. Willmore of the Seismology Unit, I.G.S. (Edinburgh) for permission to use play-back and other facilities; Dr. B. Jacob (formerly of I.G.S.) for useful discussions and sending computer program; Mr G. Nielson (I.G.S.) for supplying LOWNET log sheets and much useful information; Messrs K. Chappel (N.E.R.C.), J. Davis, D. Houliston, J. Laughlin and Dr. C. Fife (all of I.G.S.) were very helpful during processing and digitising the data; Dr. Burton of (I.G.S.) for useful discussions and sending a computer program; Dr. Thirlaway of the U.K.E.A.E. for sending EKA tapes; Dr. R. King of Birmingham University for sending the timing device; Dr. R. Long of Durham University for sending M.S.F. radio receiver; N.E.R.C. committee for agreeing to lend apparatus from their seismic pool; EKA supervisors for their cooperation when EKA close

shots were fired; landowners of EKA and Broughton village for permission for access to the land; all those quarry owners and managers who gave information about their blasts and permission to time them.

My grateful thanks to Miss M. Kennedy for her accurate and efficient typing of this thesis.

And finally my grateful thanks to every member of my family. This work would not have been possible without their continuous moral and financial support.

C O N T E N T S

LIST OF FIGURES

LIST OF FIGURES (Contd.)

LIST OF FIGURES (Contd.)

LIST OF TABLES

S U M M A R Y

This work has been carried out to extend on the interpretation of the Upper Crustal structure under the Eskdalemuir Seismic Array and the surrounding area. A study of the dispersion of short period (about 1 sec.) surface waves from local events at different distances and azimuths was considered, but the lack of events showing such waves turned attention to the study of first P-arrivals from the same sort of events.

The thesis is in six chapters. Chapter I was given with an Introduction. In Chapter II, the general aspects of the geology of the area were discussed very briefly. Previous seismic work around EKA was summarised with special reference to LOWNET and LISPB models.

Seismic array technique, its advantages and methods of array data processing were discussed in Chapter III which also included a brief description of EKA and LOWNET and a detailed description of Broughton Array which was set up temporarily during the course of this work. Chapter IV gives detailed information about the data sources, origin time recording and play-back facilities.

Preliminary results of the analysis of some EKA local events showed some systematic velocity and azimuth variations and this revealed the need for detailed information about the shallow structure under the array itself. Six shots were fired in the vicinity of EKA. Chapter V has been devoted for the presentation

of the results of these shots, their discussion and interpretation. These demonstrated an anisotropy effect in the area of the array.

Chapter VI presents the results of all local events, received at the three arrays, their discussion, comparison and interpretation.

A velocity structure around EKA is proposed which involves (1) a rapid increase of velocity (0.8 km/sec./km) to about 1.6 km depth followed by a slow rate ($<$ 0.003 km/sec./km) to an undefined depth (2) a variation in the initial (zero depth) velocity with azimuth ranging from 5.0 to 4.4 km/sec. parallel and normal to the Lower Palaeozoic strike respectively. The Broughton data were consistent with this model if the Lower Palaeozoic structure under the Midland Valley is essentially flat-lying. The extent to which these conclusions are consistent with previous work is discussed.

Some of the methods of analysis are described in the Appendices (1 - 7), which also include two computer programs with their output results which form the basis for the interpretation and the above conclusions.

Burton & Blamey (1972)[80].

(2) a computer program which cross-correlates the outputs of different channels with the output of a reference channel, chosen to show a clear Rayleigh arrival and judged to be of high S/N ratio, and thus allowing for more accurate move-out determination and therefore a more reliable calculation of group velocity and angle of approach at the array (a copy of this program will be lodged in the Geophysics data room, Geology Department).

It should be mentioned that the picking of Rayleigh arrival for one of these events was complicated by a possible second S-arrival or an entirely different instantaneous arrival. The location and origin time of another event were doubtful and therefore they were rejected.

Results of the analysis of the other three (although not included in this thesis) showed that:

(1) group velocity-frequency function of the Rayleigh waves of these events strengthen the belief of them being dispersed, see Appendix (7) for an example.

(2) angles of approach at the array were shifted from the direct ray path up to 15° for one case.

(3) Further analysis on the first P-arrivals of these and other events, see Chapter VI, demonstrated the existence of the shift phenomenon.

Search for more local events continued, but unfortunately, no more surface waves were found, and thereafter, analysis was restricted to

first P-arrivals. Results from about 70 events (mainly quarry blasts and natural events) received from 25 different sources at distances ranging between 20 km - 165 km and propagation vector, see Fig. (4-2), ranging between 90^{o} - 210^{o}, showed that:

(1) azimuth anomaly is, to a large extent, systematic.

(2) apparent velocity seems to vary with both distance and azimuth.

(3) It was also found that the locations of some of these events were doubtful (seen through the very high azimuth anomalies, as high as 30^{o} in some cases) and therefore many events were rejected, see Chapter IV.

Azimuth anomalies and apparent velocity variations can be attributed to different causes, mainly anisotropy and lateral inhomogeneity effects. A complex velocity structure of some sort at any depth under EKA could be a reason.

A study of the shallow velocity structure under EKA seemed necessary to find out what effect this structure has on these observed azimuth and velocity variations. Six shots were fired in the vicinity of the array. Results from these shots demonstrated horizontal and vertical velocity variations, see Chapter V.

Most of the analysed local events originated in the Midland Valley which is separated from Southern Uplands by the major Southern Uplands Fault and where a 6.4 km/sec. refractor is known to exist at a depth of 7 - 8 km, see Bamford et al (1977)[21] and Crampin et al (1970)[36]. The existence of such a refractor, at a greater depth (12 km or more) beneath the Southern Uplands, see

Jacob (1969)[31] remains questionable. A seismic array close to the Southern Uplands Fault and to the south side of it could be useful in:

(1) studying arrivals from the different sources received at a different location in the Suthern Uplands, particularly those few Southern Uplands sources to help to define any regional anisotropy effects and/or any lateral inhomogeneity in the whole of the Southern Uplands.

(2) Receiving close to the fault from sources in the Midland Valley will help to study the same effects in that region. Sources close to the fault (at distances less than 50 km) will help to reveal more information about the shallow structure, i.e. at depths less than 7 - 8 km.

(3) Accurate travel times will be useful in defining and checking on any proposed structural model.

Broughton Array was set up near the town of Biggar and operated for a period of 65 days using the Geostore recording system, see Section (3.4). During that period and through direct contact with the quarry managers in the area, many recorded events on Broughton, EKA and LOWNET were identified and some of these were timed at the quarries, see Chapter IV. The analysis and interpretation of all local events are presented in Chapter VI.

CHAPTER II

REGIONAL GEOLOGY AND GEOPHYSICAL INTERPRETATIONS WITH SPECIAL REFERENCE TO SEISMIC STUDIES (EKA, LOWNET, LISPB)

2.1 Introduction

This thesis is concerned with transmission of seismic waves through the rocks of the Midland Valley and Southern Uplands of Scotland. The former is characterised by Upper and the latter by Lower Palaeozoic outcrop. The line of the Southern Uplands Fault separates them from the Rhinns of Galloway in the SW to Dunbar in the NE and represents the southern boundary of the Midland Valley Rift. The general nature and arrangement of the principal rock groups are shown in map Fig. (2-1), section Fig. (2-2) and table (2-1) which includes some relevant physical properties. For a general description of the Geology of Southern Uplands and the Midland Valley, and references to detailed studies, see Greig (1971)[1], Craig (1965)[2] and MacGregor & MacGregor (1965)[3].

2.2 Aspects of the Geology relating to Present Study (From the top)

Quaternary Deposits: represented by peat and boulder clay and occur at the seismometer array sites. At EKA, shot holes were augered or drilled into them without, generally, reaching bedrock, see Chapter V. Thicker unconsolidated deposits may occur on the seabed under the marine shots in the Forth and North Channel. In respect of these shots, therefore, Quaternary deposits will have caused some time delays. Otherwise, other sources and all detectors are sited below these deposits and first arrival ray paths are unlikely to pass through them.

Tertiary Dykes: A group of such dykes pass through Southern Uplands, close to EKA and could indicate some deep structural line. These dykes are of the order of 0.01 km wide, detectable magnetically, and are generally showing negative (reversed) anomalies. Such dykes, however, are too narrow in relation to seismic wavelengths to have any significant effect.

Upper Palaeozoic

Most of the quarries are into sills intruding rocks of this age group, see Section (4.1.3) and Appendix (1). The sedimentary succession and thicknesses are well known to the base of the Carboniferous Limestone Series as a result of coal workings. One of the most regular seismic sources is the N.C.B. opencase at Westfield (N.G.R. 312/670). At least some of the 'natural' events, see Section (4.1.5), are ground tremors brought about by mining operations, see Mashkour (1976)[4].

The concealed extent and thickness of underlying Carboniferous lavas are much less well known. Thickness estimates of Old Red Sandstone, especially the Lower, may be subject to large errors because of correlation problems in unfossilferous, laterally variable alluvial fan deposits and interbedded lavas, see Waterston (1965)[5]. Maximum thicknesses are, however, expected to occur close to the rift boundary faults, (George, 1960)[6]. Although the Lower O.R.S. rests with strong unconformity on the Southern Uplands Lower Palaeozoic rocks, it appears comparable on the Downtonian of the Midland Valley inliers (Lesmahagow).

A granitic pluton of Lower O.R.S. age intrudes these rocks at Distinkhorn within the Midland Valley. Three similar large plutons intrude the Lower Palaeozoic rocks of the S.W. Southern Uplands. Gravity anomalies over them indicate depth extents of 8–12 km, see Bott & Masson-Smith (1960)[7] and El-Batroukh (1975)[8]. Smaller but related bodies of granodiorite occur sporadically along the Northern Belt of the Southern Uplands as far as the east coast. It is geologically and gravitationally possible that these intermediate composition rocks underlie a wide area.

Lower Palaeozoic

The Upper Ordovician to Silurian rocks of the Southern Uplands are well compacted and jointed rocks, principally greywackes and shales. Some stratigraphic divisions show large thickness variation across the strike eg the Upper Ordovician greywackes of the Northern Belt, 2400 m thick, are represented by 21 m black shale near Moffat in the Central Belt (Walton, 1965)[9]. Except in the aureoles of the granitic plutons these rocks are barely metamorphosed and show well preserved sedimentary structures. Their tectonic structure is renowned for its complexity. Folding may be dominantly isoclinal, (Lapworth, 1882[10]; Peach & Horne, 1899[11]) or a combination of essentially monoclinal folds and revised faults (Craig & Walton, 1959)[12].

The foundation on which these sediments were laid may have been an oceanic crust of Arenig age (Wilson, 1966[13]; Dewey, 1969, 1971[14, 15]) and the Ballantrae ophiolite a remnant of it (Church & Gayer, 1973)[16]. Controversy over the concealed extent of such

rocks and the location of sutures between them and pre-existing continental blocks or directly between these blocks has recently been reviewed by Moseley (1977)[17].

Crust of continental thickness (30 km) now exists throughout the region (Bamford et al, 1976)[18], see also next Section. Within that crust, however, gravity (McLean & Qureshi, 1966[19]; Powell, 1971[20] and El-Batroukh, 1975[8]) and Seismic (Bamford et al, 1976[18]; Bamford et al, 1977[21]) evidences show a dense, high velocity basement at shallower depth under the Midland Valley (7-8 km) than under the Southern Uplands (12 km or more). Whether rocks like those under the Midland Valley exist under the Southern Uplands remains in doubt.

Era	System, Series, etc	Sediments Thickness	Contemporaneous Ingenous	Intrusive	Faults	Physical Properties
Quaternary	Recent Pleistocene	Alluvial, marine Glacial deposits 0–0.1 km	–	–	–	G 2
Tertiary	–	–	–	Dolerite Dykes	NW–SE faults	–
Mesozoic	Absent except offshore					
Upper Palaeozoic	Permain	Sandstone .6 km	Basalts	necks/plugs, basic sills & dykes	E–W faults	(S.S.) G = 2.44–2.68 V 3 km (Basalt) G = 2.8
	Carboniferous	S.S., shales L.S., Coal, Ironstones 3 km	Basalts 0–1 km	Volcanic necks, plugs, dykes	NE–SW faults control sedimentation	(L.S.) G = 2.76 V = 3–4 km/sec
	Upper O.R.S.	thicker in East S.S. Ironstones .3 km	–	–	–	G = 2.34–2.58 V = 2–4.2
	Unconformity					
	Lower O.R.S.	S.S. 1 km	Andesites	necks, plugs, sheets, dykes and major plutons (granite– granodiorite–diorite)	NE–SW	G = 2.6–2.73 V = 4–5
Major Unconformity – except within Midland Valley (Lesmahagow, Tinto)						
Lower Palaeozoic	Silurian Ordovician	(Downtonian (Valentian (Ashgillian (Caradocian (Unconformity				G = 2.6–2.77 V = 5.6–6.0
		(Arenig (oldest at outcrop in Southern Uplands)		Lavas and serpentimite & Gabbro		
	Dalradian of SW Highlands may underlie Midland Valley					G = 2.8, V = 6.4

Table (2–1) Succession, rock types, thicknesses and relevant physical properties*
G = density (gm/cm3); V = velocity of compressional waves (km/sec.)

* (See references 8, 22 and 23)

Scale 1: 625000

Fig. (2-1) Geological map of
Southern Central Scotland.

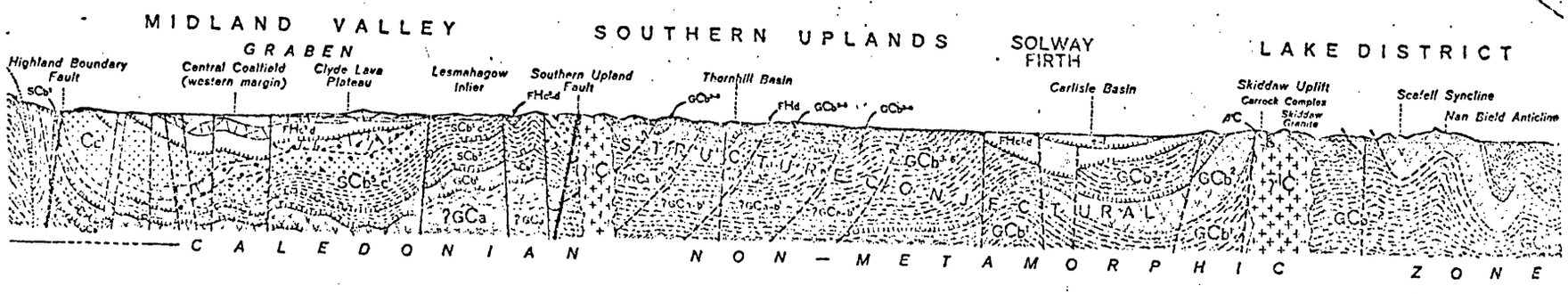

Horizontal Scale 1:1 000 000

Vertical Scale 3 times the Horizontal.

INDEX

FH Palaeozoic cover
sC Slightly to strongly folded L. Palaeozoic strata
GC Strongly folded L. Palaeozoic strata
C Intrusions of granitic & dioritic composition

Fig. (2-2) Diagramatic section across the Midland Valley and Southern Uplands showing the general relations of the main structural units - (from tectonic map of Great Britain & Nortnern Ireland, 1st edt., 1966).

2.3 Previous Seismic Work at EKA

Eskdalemuir Array was originally designed with distant sources in mind and has proved to be a powerful instrument in the studies of Mantle velocity structure. Several workers have pointed out that the array could also be used effectively for detailed crustal investigations but so far, it should be mentioned, however, that most of the seismic structural work, if not all, which has been carried out at the station has been concentrated mainly on deep crustal and mantle investigations. There is no detailed seismic study of the shallow structure under Eskdalemuir. Nevertheless, models have been published by different authors and certain assumptions have been made for the velocities of the shallow structure.

In their study of two British Earthquakes recorded at Eskdalemuir, Key et al (1964)[24] have recognised different phases arriving at the station, P_n, P* & P_g and S_n, S* & S_g. Using velocity filtering technique they concluded that deduced velocities of different phases do not agree with the calculated phase velocities. They attributed this to tilts in the layers below the array.

Agger & Key (1964)[25] have analysed EKA records of an earthquake epicentred in Paisley, near Glasgow. They gave a 5.75 km/sec. phase velocity across the array for P_g & P* arrivals and 7.80 km/sec. for P_n. S_g & S* have been found to travel across the array with a phase velocity of 3.5 km/sec. and S_n with a velocity of 3.9 km/sec.

In July 1962, a refraction shooting program using 320 lb depth charges was carried out for the calibration of Eskdalemuir Array.

Shots have been fired in the Irish Sea and the North Sea, see Fig. (2-4a). Records of these shots from Eskdalemuir and Rookhope, Durham, have been analysed by Agger & Carpenter (1964-5)[26]. From a plot of the reduced travel time, and choosing an arbitrary velocity of 8.0 km/sec., against range, their results seemed to fall into two distinct groups which they identified as P_g and P_n. Their deduced velocities at Eskdalemuir were:

P_n including second arrivals at ranges $110 \lesssim \Delta \lesssim 130$ km.

Western (10 observations) 7.84 ∓ 0.09 km/sec.

Eastern (4 observations) 7.68 ∓ 0.19 km/sec.

All (14 observations) 7.90 ∓ 0.12 km/sec.

P_g essentially first arrivals for $\Delta < 130$ km and second arrivals otherwise.

Western (8 observations) 6.10 ∓ 0.09 km/sec.

Eastern (7 observations) 6.04 ∓ 0.23 km/sec.

All (15 observations) 6.09 ∓ 0.06 km/sec.

combining all the data to get more first arrival P_g, and attempting a least square solution they gave P_g velocities as first arrival 6.47 ∓ 0.59 km/sec., and second arrival 6.29 ∓ 0.10 km/sec.

Using the time-term approach they found:-

P_n (16 shots): 7.99 ∓ 0.1 km/sec; P_g (23 shots) 6.12 ∓ 0.06 km/sec.

They referred also to the existence of another phase with a velocity of 7.75 km/sec. arriving from some shots between P_g and P_n which they associated with P* of Key et al (1964)[24].

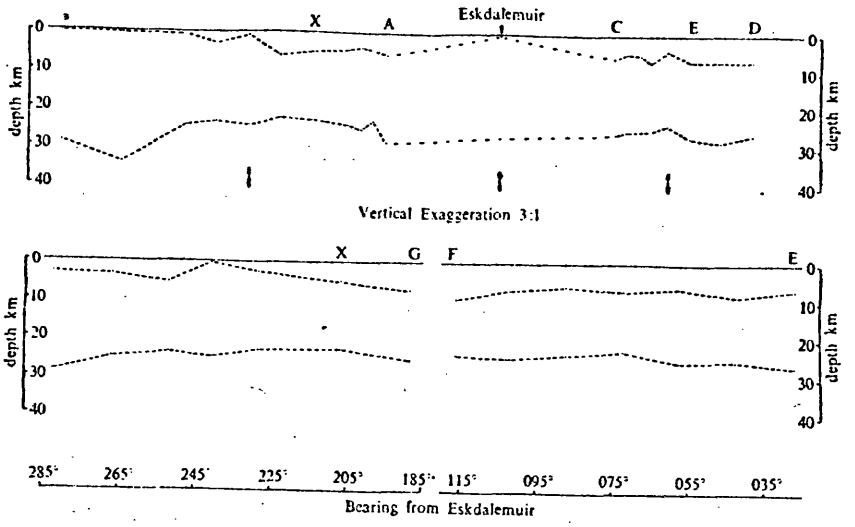

Fig. (2-3) Seismic velocity model around Eskdalemuir based on shots fired in the Irish Sea and North Sea.
After Agger & Carpenter (1964-5)[26].

Unfortunately, however, the nature of the experiment did not allow much to be said about the shallow structure since the ranges are relatively large. In their model the authors chose a 4.7 km/sec. sedimentary layer underlain by a crystalline rock layer of 6.12 km/sec. velocity. Both layers have uniform velocities and variable thickness and underlain by a uniform Upper Mantle of 7.99 km/sec. (See Fig. 2-3). Again the authors attributed the differences between the calculated P_g and P_n velocities and the phase velocities across the array to irregularities beneath the array itself.

Key (1967)[27] gave an investigation of signal generated noise recorded at Eskdalemuir using velocity filtering technique and considering the assumption that P-waves arriving at an irregular surface of topography at an angle of incidence of a few degrees, can generate local noise (surface waves) which cannot be distinguished from the primary signal on one station records. For theoretical treatment see Hudson (1967)[28].

The author demonstrated the lack of coherency of the P-signal, at the various seismometers, a few seconds after the first P-arrival, by subtracting the waveform of each individual signal from the normalized delayed sum-all signal, using records from an underground explosion (Bilby). This lack of coherency was associated with the arrival of another phase which was found to be of surface wave character. A detailed azimuth and velocity search for discreet signals in the 2-5.5 km/sec. velocity range which was carried out on the coda of the recording of an explosion in E. Kazateh, revealed a large number of noise sources. Key[27] associated these sources with the relatively steep surface gradients associated with high ground, the coast line and the sea-bed depression around Eskdalemuir. He gave a more detailed study of signals arriving from an event in Kamchataka, to conclude that noise signals have been originated from P-waves crossing a deep and narrow valley called Moffat Water (running in a NE-SW direction, 13 kms from the cross-over point of the array and with a bearing of 315°) at the point where the valley cuts through a basalt and dolerite dyke.

Hudson (1967)[28] discussed the mathematical aspects of the

application of the theory of scattering of a plane wave by a surface obstacle to a three-dimensional surface of any shape. He made a comparison of the theory with data from four events which allowed him to get an estimate of the breadth of the scatter. From a study of a relief map of the area surrounding the array, he showed that the Moffat river valley is the steepest piece of terrain for some miles in either direction, and this corresponds with the fact that the scattered signal from Moffat Water is the most prominent on Eskdalemuir records. Therefore, he concluded that the scattering is due to the steep nature of the sides of the valley.

Bott (1968)[29] in a review of geophysical surveys and their interpretation for the study of the geological structure of the Irish Sea basin, referred to the model of Agger & Carpenter[26], commenting that the variations in sediment thickness are in broad agreement with the gravity interpretation described in his paper. He reported also that the most important conclusion from Agger & Carpenter's work is that the crust appears to be thinner than the normal continental crust and also appears to be about 4 km thinner than beneath the Southern Uplands of Scotland.

Blundell & Parks (1969)[30] gave a comprehensive review of the seismic explosion studies for the crustal structure around the British Isles. They summarised the results of all previous work in Fig. (2-4). With regard to Agger & Carpenter's[26] work, they commented that " unfortunately, the experiment was not designed to obtain crustal information and the two stations were so situated in relation to the pattern of shots that the control of the velocity

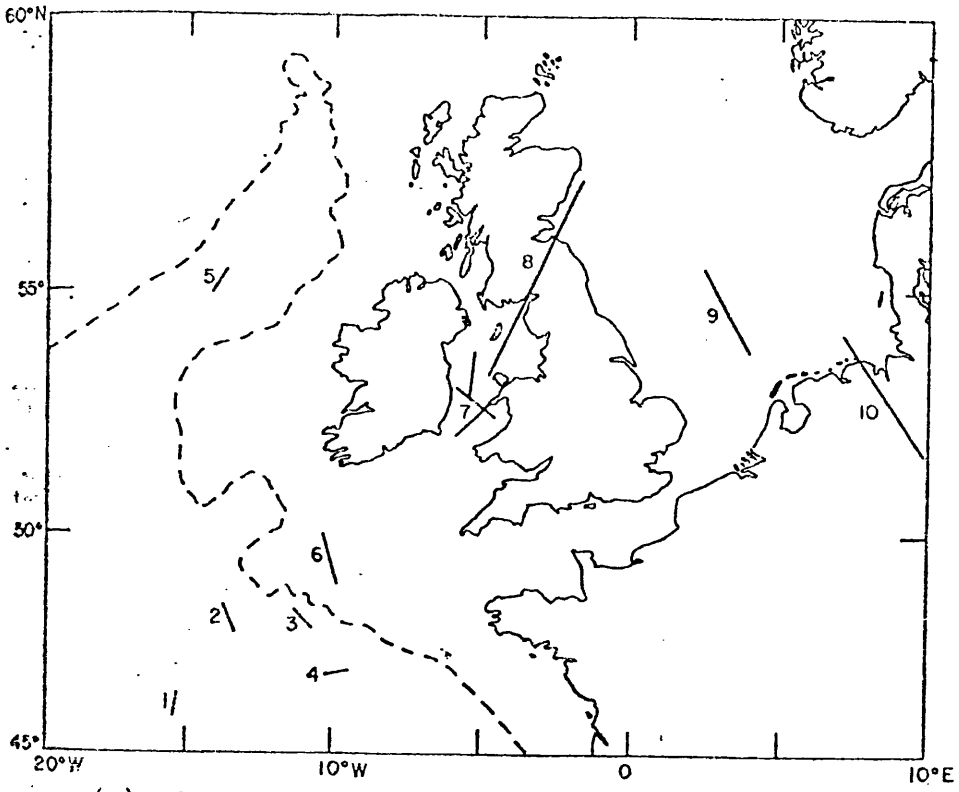

(A) Locations of seismic measurements. The broken line represents the 1000 m sea depth contour.

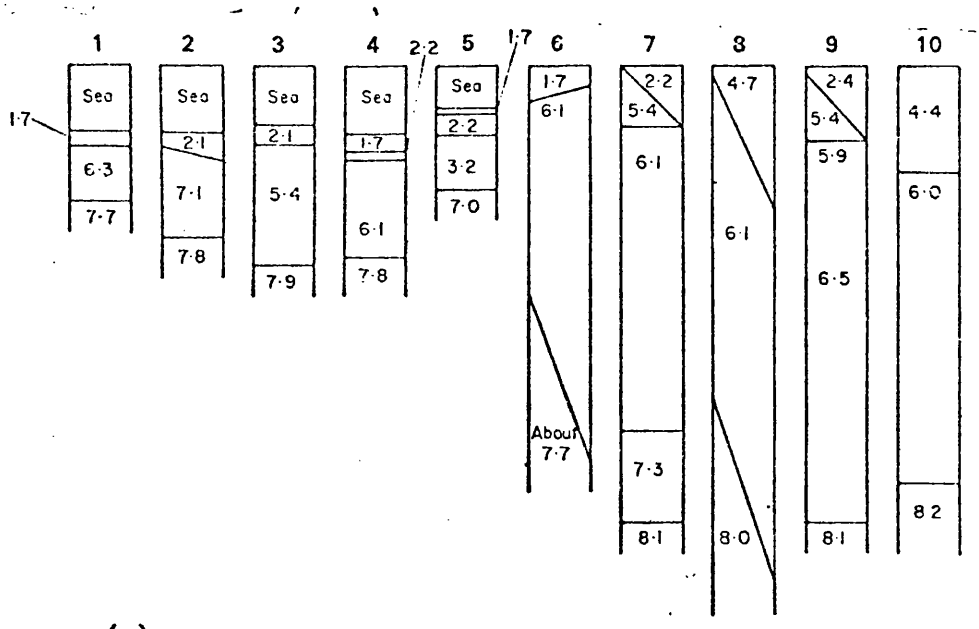

(B) Schematic diagram to summarize various representations of the crustal structure in the vicinity of the British Isles: (1) Line E-9, Lat. 46° 08′ N, Long. 15° 21′ W (Ewing & Ewing 1959), (2) Station 16, Lat. 47° 48′ N, Long. 13° 20′ W (Hill & Laughton 1954), (3) Station 9, Lat. 48° 20′ N, Long. 11° 20′ W (Hill & Laughton 1954), (4) Line D-12, Lat. 46° 53′ N, Long. 9° 50′ W (Ewing & Ewing 1959), (5) Line E-10, Lat. 54° 59′ W, Long. 14° 06′ W (Ewing & Ewing 1959), (6) SW Approaches (Bunce *et al.* 1964), (7) South Irish Sea, (8) Northern England (Agger & Carpenter 1965), (9) North Sea (Collette *et al.* 1965) and (10) North Germany (Willmore 1949). The numbers represent seismic velocities in kms^{-1}.

Fig. (2-4) Summary of previous seismic studies for the crustal structure around the British Isles as given by Blundell & Parks (1969)(30)

of P_g and P_n arrivals was poor. The line of charges fired in the Irish Sea was effectively unreversed and the requirement of interchange was not achieved. In addition, Agger & Carpenter had no short range observations. In view of all these uncertainties, the geological significance of the variations of crustal thickness in their model are very doubtful."

Blundell & Parks' experiment was carried out in 1965 and designed to permit the use of the time-term approach for the interpretation of the data. Their main goal was to study the crustal structure in the Irish Sea area. Recordings from 25 depth charges were carried out at three temporary stations in Wales and one in Ireland, the Rookhope Borehole, and the Eskdalemuir Array. Their results show that P_n was observed only at EKA and Rookhope and, as a result, the control on velocity is poor and the uncertainties in determining the time-terms are therefore large.

Their model of the crust in the region of the South Irish Sea is as follows: The upper 4 km contain a variety of rocks including considerable thickness of young sediments with a velocity of 5.4 km/sec. overlying a layer of heterogeneous rock to a depth of about 24 km with a P_g velocity, on average, of 6.1 km/sec., underlain by a layer of uniform material with the rather high velocity for P* of 7.3 km/sec. Because of the uncertainty in the velocity of P_n, the authors placed no great confidence in the figure of 30 km which they proposed for the base of the Crust.

Jacob (1969)[31] gave the results of the analysis of 71 Eskdalemuir

events, most of which were quarry blasts, see Fig. (2-5a). Using an array processing computer program, designed to make allowance for the curvature of the wave-front and the altitude variations between the seismometers, see Appendix (4), and calculating the distances between the shots and the array from the P-S time intervals, the author produced the apparent velocity-distance graph shown in Fig. (2-5b). The graph shows that the data is split into two sets. The first set lies approximately in the range 5.5-6.0 km/sec. indicating that the phase velocity is increasing gradually with range. The second group has a less definite trend in velocity with range, in the interval $50 < \Delta < 180$ km, with an average phase velocity of 6.44 km/sec. None of this group has less than 6.2 km/sec. velocity.

Applying Wiechert-Herglotz inversion method (reviewed and compared with other methods of determining velocity structure by Johnson & Gilbert (1972)[32]) to the first group (slow), the author indicated a gradual increase in velocity from 5.54 km/sec. at the surface up to 5.94 km/sec. at a depth of about 12 km. To account for the other group (fast) the author produced the model shown in Fig. (2-6a) which gave the reduced travel-time curve of Fig. (2-6b). For this structure, the 6.44 layer will give a second arrival in the range $49 < \Delta < 83$ km and first arrival when $\Delta \geq 83$.

The author considered two points to deduce a generalised picture of the structure in the area. Firstly, the closest source of his fast group is at 56 km range at the time when such a range is expected to give a second arrival from the 6.44 layer. Jacob reported that

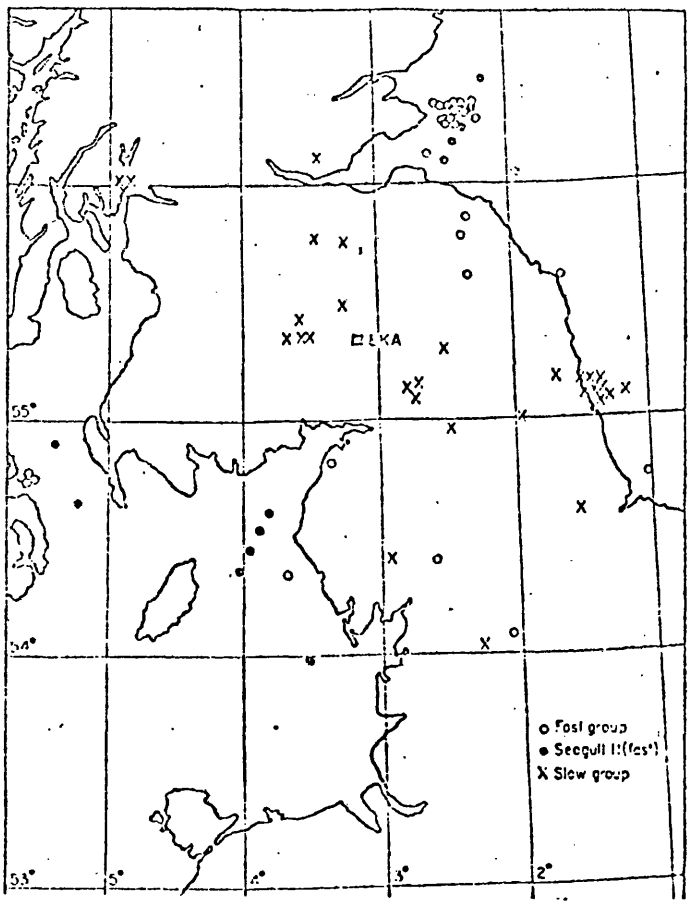

(a)

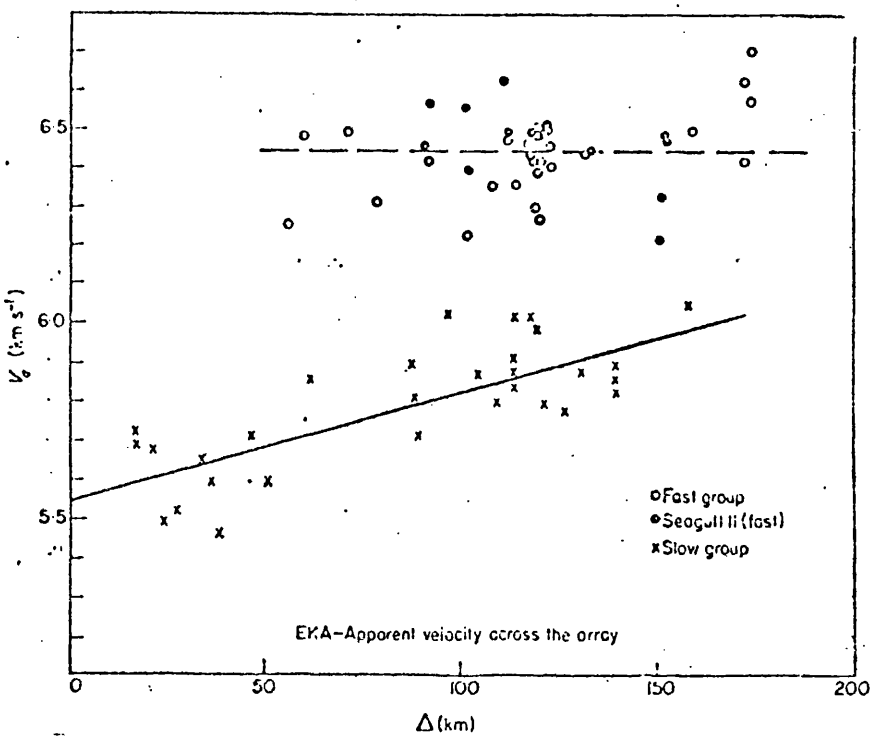

(b)

Fig. (2-5) (a) Location of all events with respect ot EKA
(b) Apparent velocity Vs. Distance
After Jacob (1969)[31].

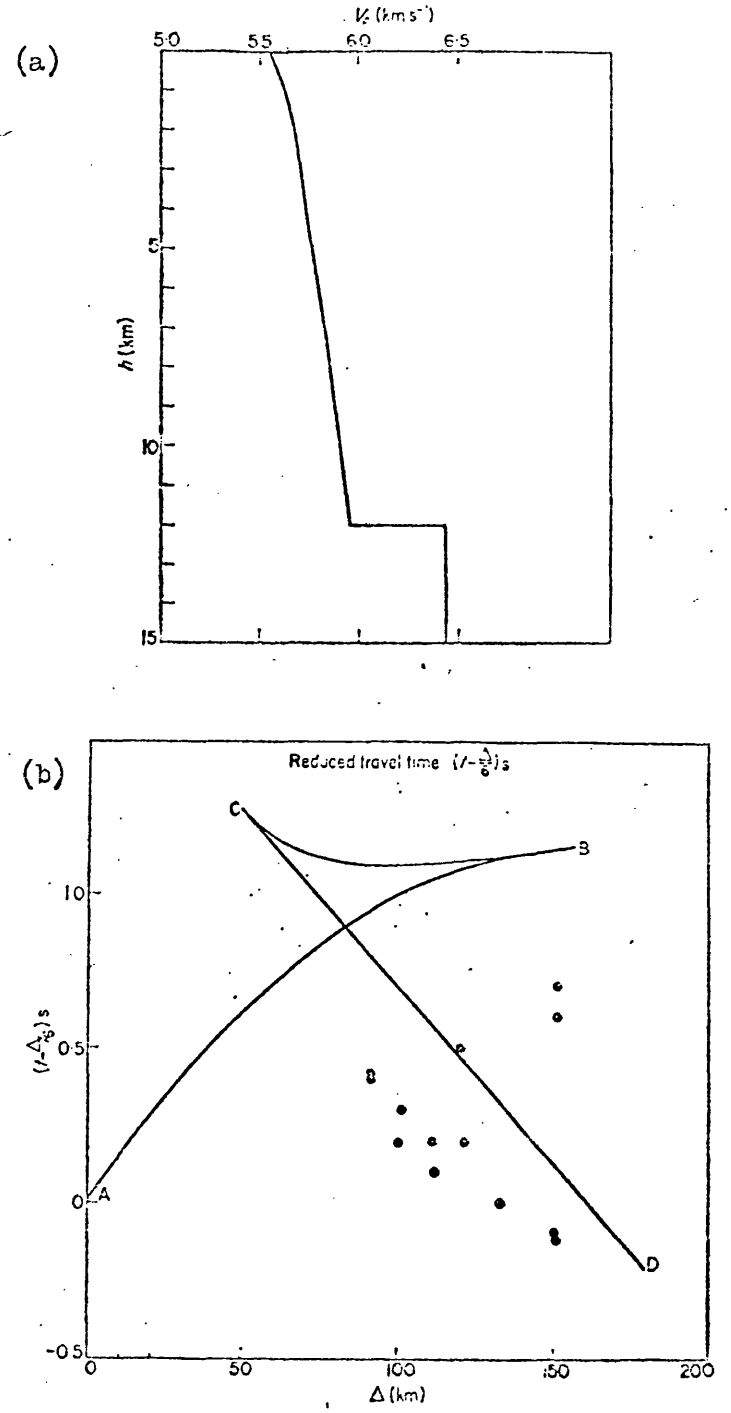

Fig. (2-6) (a) Velocity-depth function under EKA.
(b) Reduced T-X graph for the above model
After Jacob (1969)[31].

if a calculated first arrival at 5.7 km/sec. velocity has not been missed, then the closer fast sources may be sited in an area where the fast layer comes closer to the surface. Secondly, since both fast and slow groups occur in the 100°–160° azimuth interval, this would rule out anisotropy as a solution. Therefore the author suggested that the structure could be represented by a saddle of high velocity rock with a depth of 12 km below EKA shoaling to the NE and probably also to SW and deepening to the SE and NW. He documented his suggestion by recalculating the reduced travel-times for the Agger & Carpenter's[26] shots (which are shown as dots on Fig. (2-6b)) to deduce that the early arrival times support the suggestion that the 6.44 layer may shoal towards the NE and SW.

It should be mentioned, however, that the author did not give an explanation for the appearance of slow and fast sources (see Fig. 2-5) at almost same azimuths and ranges. Something which in a sense does not agree with his model.

Corbishley (1970)[33] has shown that if the slowness of the Jth event recorded within the Kth distance from an array, h, is $dT/d\Delta_k$, then at the ith seismometer a site correction R_{hi} incorporating both a constant and an azimuthally varying term can be defined from the residuals ε_{hi} by fitting a sine curve using least squares.

$$R_{hi} = S_{hi} + \varepsilon_{hij} = A_{hi} + B_{hi} \sin (\alpha_{hj} + E_{hi}) \quad \ldots (2\text{-}1)$$

Where α_{hj} is the azimuth of the jth event from the array h and

S_{hi} is a correction associated with each seismometer and A_{hi}, B_{hi} and E_{hi} are constants.

In a following publication, the same author[34] derived average slowness curves ($dT/d\Delta_k$) for D = 30° - 104° using data from 478 earthquakes and underground explosions recorded at the four U.K.A.E.A. arrays. Slowness curves were corrected for station bias by means of equation (1). As far as Eskdalemuir station is concerned, two main conclusions were reached at:

(1) Corrections for individual seismometer sites are related to the altitudes of these sites.

(2) The teleseismic data strengthens the assumption of a three plane-layered model of Agger & Carpenter[26].

Willmore (1973)[35] gave a review of seismic studies around the British Isles from 1965. He concluded that the main features of that work are: (1) The Mohorovicic discontinuity is shallowing towards the west (2) There is some indication of an increase of P_n velocity with range (3) also indications of lower-crust velocities ranging from 6.9-7.3 km/sec. have been found in some parts of the area.

2.4 LOWNET MODEL (MIDLAND VALLEY)

One of the main objects of LOWNET is to study the crustal structure of the Midland Valley using time-term analysis, see Section (3.3). A time-term survey in the area has not been completed yet (Neilson, Oct. 1977, personal communication). Crampin et al (1970)[36] reported: " Despite the varied geology in the area, the variation in time-terms between sites is small enough to yield some estimate of crustal structure from a preliminary plot of travel-times." Their travel-time results of some recorded explosions are shown in

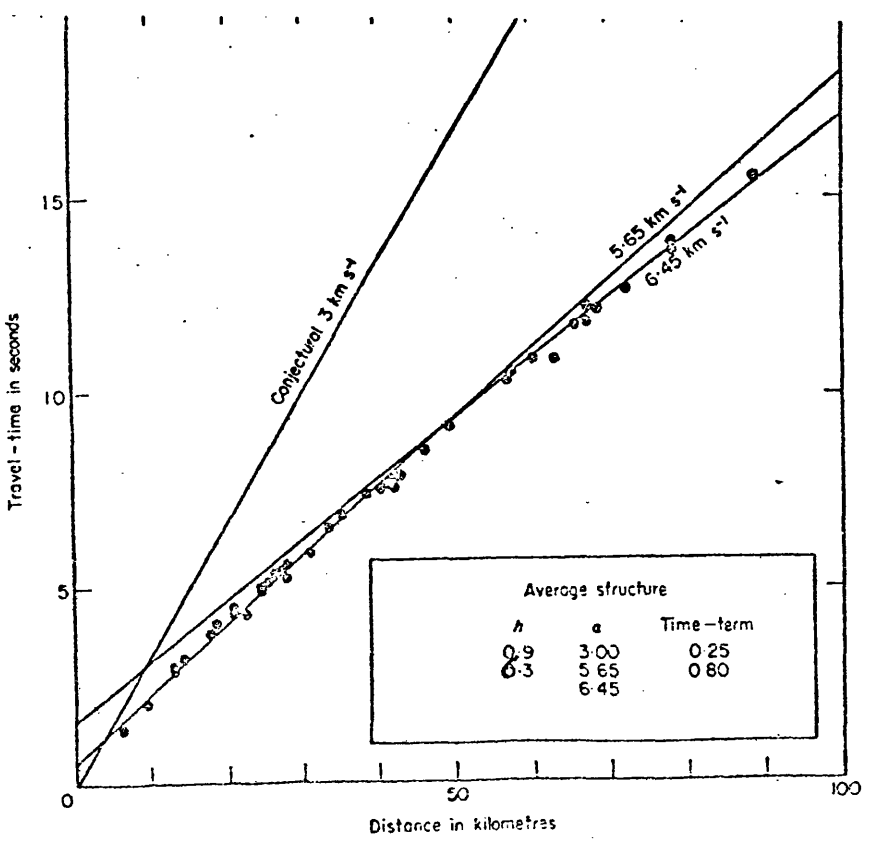

Fig. (2-7) Travel-time diagram for explosions recorded on LOWNET. Parameters of Model for Midland Valley are given inside the box.

After Crampin et al (1970)[36].

Fig. (2-7) from which they derived average time-terms, velocities and thicknesses. From these results they suggest a three-horizontally layered model with the parameters shown in box Fig. (2-7). They indicated, also, that first arrivals from the 6.4 km/sec. layer are received at distances of about 50 km.

2.5 LISPB RESULTS (RECENT PUBLICATIONS)

The Lithospheric Seismic Profile in Britain, referred to as " LISPB " was completed in summer 1974. A full description of the experiment with some preliminary results have been given in Bamford et al (1976)[18]. Recent results concerning the Upper Crustal Structure of northern Britain have been given in Bamford et al (1977)[21].

In their model (Fig. 2-8) for Midland Valley, the authors[21] gave a 4-5 km/sec. velocity for a top most layer of varying thickness ($\leq$ 3km). This layer corresponds to Old Red Sandstone/Lower Carboniferous sequences and is underlain by a 5.7 - 5.9 km/sec. velocity, Lower Palaeozoic layer with a definite discontinuity at a depth of the order of 7-8 km where the velocity increases to 6.4 km/sec. Both boundaries are reported to be sharp discontinuities.

Refractions from the 6.4 km/sec. layer are seen at distances of about 50 km in the Midland Valley but not seen in the Southern Uplands until beyond 120 km and then with high apparent velocity (6.7 - 6.9 km/sec.) The upper crustal velocity structure in the Southern Uplands therefore consists of two layers. A thin top layer (5.0 km/sec.) followed by 5.8 - 6.0 km/sec. material to depths greater than 10 km - all, presumably, Lower Palaeozoic type rocks.

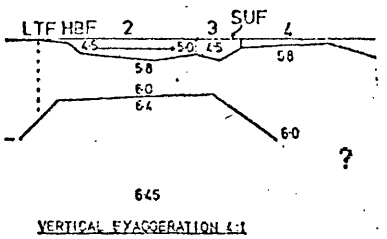

Fig. (2-8) Upper crustal structure - Midland Valley and Southern Uplands

After Bamford et al (1977)[21]

The top of the 6.4 km/sec layer beneath the Midland Valley slopes down to the south near the S.U. fault at an angle shown around 15° but which may be steeper (Bamford, 1977, personal communications). Apart from this, and contrary to Jacob's interpretation of EKA data, a 6.4 km/sec. layer is not recognised under the Southern Uplands.

CHAPTER III

SEISMIC RECORDING

3.1 Seismic Arrays

3.1.1 Introduction

Borg & Bath (1971)[37] defined a seismic array as " the one which consists of a number of seismometers arranged in a regular geometric pattern, with central recording, and where the signals from the individual sensors show such similarity in wave shape as to permit an ensemble treatment ". They stressed on signal similarity where regular geometric pattern and central recording can be dispensed with.

The idea of using seismic arrays originated from the requirement to measure velocities and amplitude absorption more accurately. The time differences and amplitude ratios, upon which these parameters are respectively based, are most precisely measured between stations with identical seismometers and over distances at which signal similarity is retained.

Such comparative studies have been done both regionally and world-wide by using records of independently recording stations. This dates back to the beginning of the application of seismic prospecting techniques where the need for closely spaced seismometers with central recording was obvious.

In the 1930s several investigators suggested triangular arrays for microseismic research. For continuous teleseismic recordings, the

multi-sensor technique was applied during and after World War II by the U.S. Navy for locating and tracking tropical storms by the generated microseisms[37]. Triangular nets of ordinary seismograph stations began to be used during the 1950s for correlation of surface waves[37,38], particularly after the development of the time-domain phase velocity methods for surface waves by Press (1956b)[39].

The technical possibilities and problems of nuclear tests were discussed in the conference of experts at Geneva in 1958 which resulted in the involvement of seismology for nuclear test detection. This introduced a new era in the field of seismic array techniques. It is from this conference that the term Geneva-type station stems, i.e. array station[37,40].

A seismic array was installed on Solisbury Plain, in February 1961, to test the effectiveness of a practical array. To test recording, shots were fired at distances of 100 - 200 kms[41,42]. Another array was installed by the United Kingdom Atomic Energy Authority (U.K.A.E.A.) at Pole Mountain, Wyoming, U.S.A. in December 1961. Recordings were made of the 3.5 kT Gnome nuclear explosion near Carlbad, New Mexico at a distance of 1000 kms. This array was discontinued in September 1963[41,43]. Results from these two arrays were encouraging enough to put into practice the idea of establishing larger and more fully instrumented arrays at Eskdalemuir in the United Kingdom and somewhere else. The construction of Eskdalemuir station commenced in the Autumn of 1961 and the array became operational in May 1962[43].

In the 1960s many arrays were installed in different parts of the world. Different shapes were considered and tried such as triangular, rectangular, circular, cross (semi-cross), L-shaped, ... etc. An array could be constituted by grouping subarrays as in the case of LASA, near Miles city in Eastern Montana, where the array comprises (21) subarrays of (25) short period vertical seismometers and a three-component set of long period seismometers[44]. Different sizes of arrays were practiced also. "Size", here, refers to the number of the arrays seismometers. This varied from a few up to hundreds of seismometers. The area covered by an array, best referred to seismologically as the "aperture", varied also from few up to hundreds of kilometers.

Signals from different sensors of the array are usually transported into a central recording either by cables or through radio links.

3.1.2 Advantages of Seismic Arrays

The advantages of using seismic arrays can be grouped in the following:

(1) Central recording is convenient as it provides immediate access to all records. This is particularly important for quick preliminary location of all sorts of events.

(2) Small aperture, big sized, arrays provide more details on the variation of the slowness ($dT/d\Delta$) with epicentral distances. On the other hand large aperture arrays provide the facilities for a clearer understanding of the Earth's structure, particularly the Earth's Crust, over large areas, at least the area covered by the array. Therefore, arrays are useful in the studies of both vertical and lateral inhomogenities.

(3) They are also used to distinguish between natural earthquakes and artificial explosions. They also provide information about azimuths, epicentral distances, origin times and magnitudes of all sorts of events.

(4) Array techniques can be used by Universities and Research Centres, on a temporary basis and with reasonable costs, especially after the development of long-period (long time) multichannel recording equipments. (See Section 3.4).

(5) Arrays proved to be a convenient answer for one of the most awkward problems in seismology, the noise, and for the detection of weak arrivals. A considerable amount of work has been published on this subject. Different techniques have been applied, all of which utilize the simple fact that " by introducing time delays to compensate for the signal propagation time across the array and (summing or multiplying or both) the outputs from each sensor, an improvement in S/N ratio is obtained.

It should be mentioned, however, that rapid advances in computer technology (both analogue and digital) in the last two decades have made possible rapid and also real-time array processing not previously feasible.

3.1.3 Array Data Processing Techniques

Different array data processing techniques have been developed and adapted for different arrays within the last decade or so. All of them aim to improve our ability to extract reliable information from these data and are based upon signal similarity between different

sensors for at least the first cycle or few cycles. This requires careful consideration, especially in dealing with large aperture arrays, since large distances between sensors might introduce certain geological conditions (such as sedimentary layering and/or anisotropic effects) which will make this expectation unlikely. Jansson & Husebye (1968)[45], in their discussion of the application of array data processing techniques to SLASA arrays, reported that if the signal similarity is not maintained over a number of cycles, SLASA arrays cannot be used because errors in station corrections, travel-time curves, etc make it impossible to determine the proper time shifts necessary for the array processing.

Different techniques can be grouped under two headings:

(a) Linear which include frequency filtering and array summation, and has the advantage that no information is destroyed. The most commonly used method of processing the output of a U.K.A.E.A. type array[46] has been described by Birtill & Whiteway (1965)[41]. The method is to form linear partial sums from each of the two array lines, multiply these together and average the output with either a square or exponential window for 1 - 2 S. The linear sums preserve the signal waveshape and the correlator output provides an improved S/N ratio. Therefore linear processing is preferred in the case of incoherent noise. Wiechert et al (1967)[47] suggest that background noise is largely incoherent at short periods if the array site is relatively quiet and the spacing between the different sensors is large. Wilson (1967)[40] reported that

in the case of incoherent noise, simple summing of the output of different sensors scattered over an area with dimensions of a few kilometers should increase S/N ratio by $\sqrt{n}$, where n is the number of seismometers.

(b) Non-Linear methods, such as cross-correlation. These methods are usually used if the noise is coherent, and have the disadvantage of distorting the signal. Nevertheless, non-linear methods have been widely used for the enhancement of S/N ratio in the past fifteen years or so. These methods imply appropriate phasing and attenuating the noise which will be subtracted to produce an enhanced signal. It should be noted, however, that the appropriate phasing varies with the direction of arrival. An outstanding technique which has been discussed and used by different authors, is known as "Velocity Filtering" or "Frequency-Wavenumber Filtering". (See Savit et al (1958)[48] and Bath (1974)[38] pp 265 - 269. This technique is based on the fact that although noise is coherent, it crosses the array with different velocity which is usually less than the velocity of the desired signal.

Muirhead & Datt (1976)[49] discussed what is known as the non-linear Nth root method, which was suggested earlier by Muirhead (1968a)[50]. The method is based on taking the Nth root of the sensor outputs (with the sign preserved) before phased summing. The authors conducted their numerical experiments on synthetic signals and noise. However, they believed that for event detection, this process is much better at handling non-Gaussian noise and is only very marginally worse

than linear processing when it is Gaussian. For event processing they reported the advantage of suppression of sections of the record where the S/N ratio is low enabling more precise azimuth and slowness measurements to be made.

Iyer (1968)[51] concluded that U.K. methods of array processing are seen to be equivalent to simplified Fourier transforms in wave-number space. The technique of multiplying array data by a Fourier operator and integrating is shown to be a simple and effective way of computing frequency wave number spectra of space time signals.

3.2 The Eskdalemuir Seismological Station

3.2.1 Introduction

In the year 1959, the United Kingdom Atomic Energy Authority began a program for detection and identification of nuclear explosions. A Geneva-type station, referred to later as a U.K.A.E.A.-type, was first installed in Salisbury Plain in early 1961, followed by a larger station at Pole Mountain in the same year. Experience from these arrays was sufficiently promising to support the establishment of larger, more fully instrumented arrays at Eskdalemuir, south of Scotland; Yellowknife, Canada; Gauribidanur, India and at Tennent Creek, Australia.

Each array consists of two perpendicular lines of ten vertical component seismometers spaced at 0.896 km in the case of Eskdalemuir and 2.5 km for the others. Full description of sites, station design, instrumentation and operation for these arrays is available in Literature For Eskdalemuir, see Truscott (1964-5)[43].

The design of any seismic array will depend mainly on the intended use of that array. Haubrich (1968)[52] described the problem of array design in two steps: (a) the number of seismometers and where they should be placed, and (b) what processing scheme should be applied to the output data.

The choice of a suitable site should be the best compromise between many requirements. First of all the site should be away from all noise sources, good coupling at all seismometer pits should be achieved and the geology of the site should be homogeneous and uncomplicated by major elastic discontinuities. Accessibility and local topography also should be considered. The spacing between different seismometers, their configuration and the aperture of the array are mainly controlled by the sort of events we are interested in, and the background noise of the area of the array.

Truscott (1964-5)[43] reported that the site at Eskdalemuir has been chosen to fulfil the following requirements:-

(1) It should not be closer than:
   a) 10 miles to the sea
   b) 5 miles to any railway line
   c) 1 mile to any "A" class or well-used "B" class roads.

(2) To be free from large numbers of trees or woods; scattered individual trees being acceptable. Rivers and streams must not be near possible pit locations.

(3) Contours to permit siting of pits within $\pm$ 200 ft (61 m) of a mean level.

(4) Cables to be buried but not necessarily directly routed.

(5) Service facilities of electrical power, telephone and water to be available.

(6) Good access by road to recording laboratory.

3.2.2 General Description of the Array

The array is sited on Llandovery rocks of Silurian age (Lower Palaeozoic), isoclinally folded, highly cleaved and compacted but no metamorphism is evident on the surface. Typical rock types are frits, shales, mudstones, greywackes and conglomerates. When the site was first chosen, most of its land was used for sheep farming. Few years after several private companies and the Forestry Commission have acquired parts of the land which have now become subject to afforestation programs.

The average annual rainfall is 2.54 meters and the terrain has an irregular network of drainage ditches and forestry roads.

The noise at the site has been reported to be relatively low and to vary between 3 and 20 mm for the 1-3 C/S band depending on weather conditions[41]. Truscott (1964-5)[43] represented the background noise at the site under typical conditions in Fig. (3-1).

The complete installation comprises an array of 20 seismometers, recording laboratory and seismological vault. The array consists of two, almost, straight lines of especially constructed pits excavated down to well consolidated rock, levelled off with a 6-inches thick concrete layer where a cylindrical steel shell,

covered by a fibre glass lid with inverted U-band vents, is planted upright to house the seismometer. Every precaution has been taken to prevent the pits from water drainage.

The two lines intersect at right angles, see Fig. (3-2) and Fig. (3-3), forming a semi-cross with an aperture of about 10 km. There are eleven equidistant pits on each line, spaced about 0.896 km, making a total

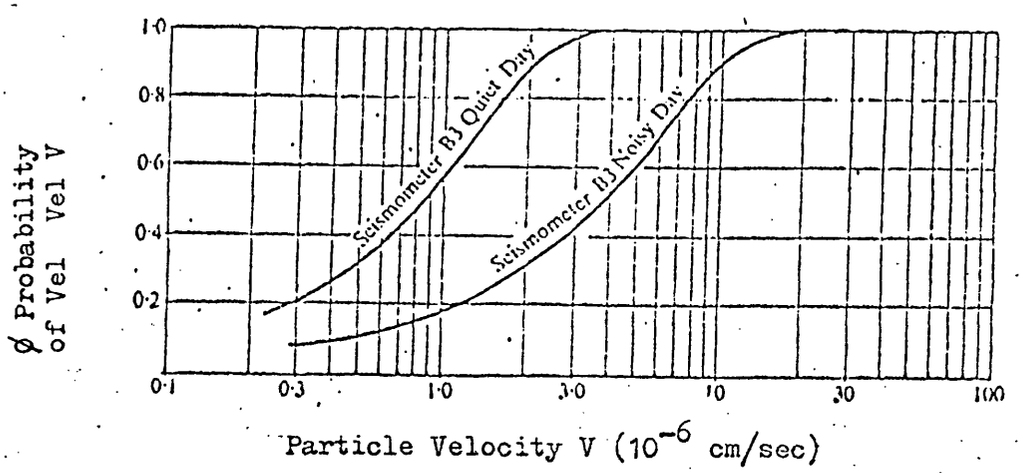

Fig. (3-1) Eskdalemuir noise probabilities (band pass $\frac{1}{3}$–3 c.p.s.). After Truscott (1964-5)[43].

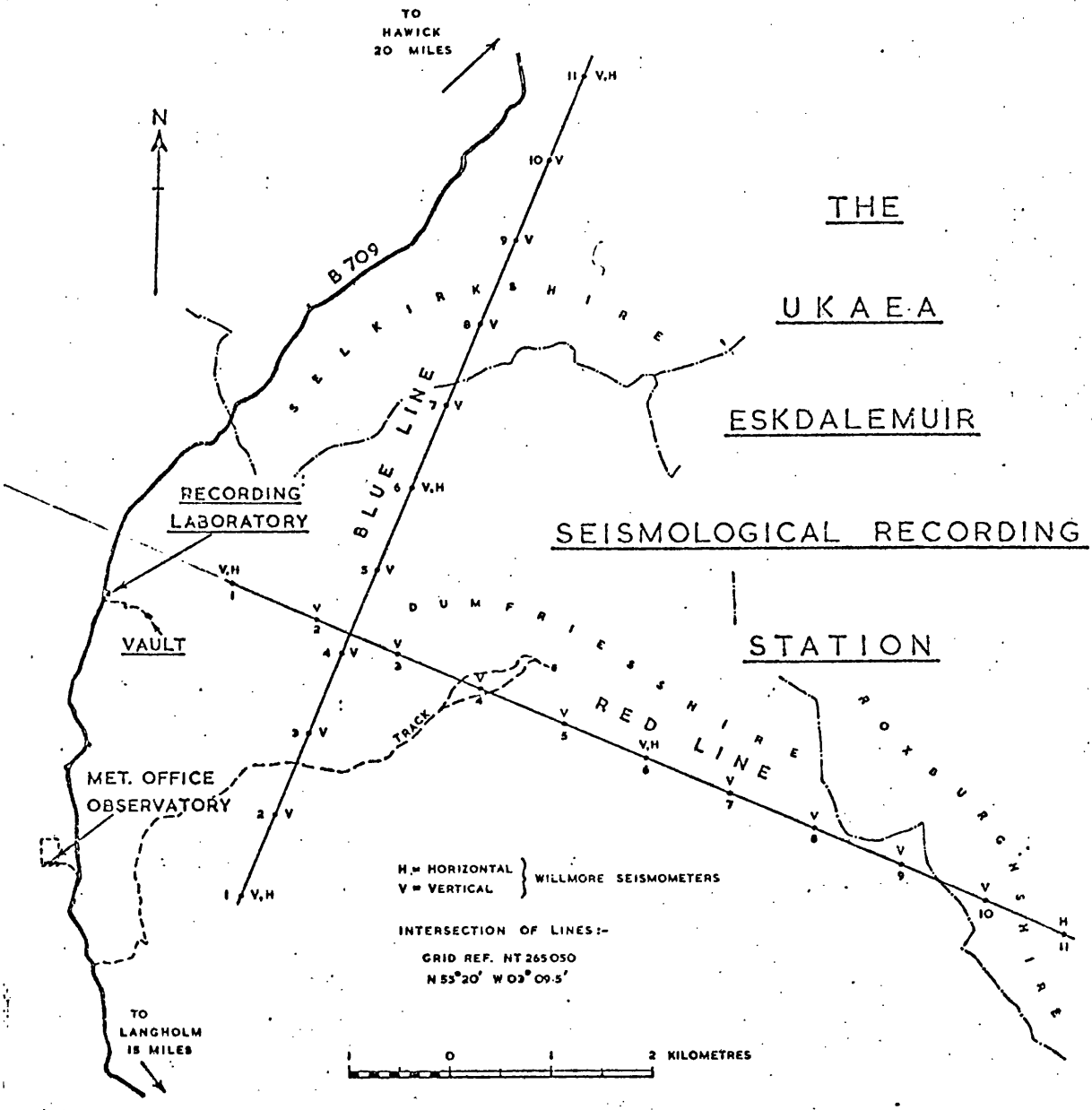

Fig. (3-2) Eskdalemuir Seismic Array Station.

PIT	CARTESIAN COORDINATES X (KM)	Y	SEISMOMETER TYPE	ELEVATION (METERS)
CP	0.000	0.000		305.0
B1	-1.049	-2.659		274.7
B2	-0.717	-1.829		313.2
B3	-0.521	-0.952		312.4
B4	-0.056	-0.168		298.9
B5	0.276	0.662		310.1
B6	0.606	1.493		337.7
B7	0.937	2.323		436.2
B8	1.313	3.281		405.4
B9	1.598	3.984		398.0
B10	1.929	4.815		327.4
B11	2.260	5.645		342.9
R1	-1.174	0.471		355.7
R2	-0.342	0.136		349.8
R3	0.489	-0.199		321.6
R4	1.320	-0.534		337.7
R5	2.151	-0.869		306.9
R6	2.983	-1.204		395.5
R7	3.814	-1.539		348.6
R8	4.645	-1.874		419.5
R9	5.477	-2.210		428.6
R10	6.308	-2.545		383.4
R11	7.140	-2.880		350.4

Millmore Mark II

Cross-over Point (CP): 55 19' 59.48" N)
03 09' 31.52 W) Grid reference NT 265050

Table (3-1) Cartesian coordinates of different pits with respect to CP - Eskdalemuir Array

length of about 9 km. Pits number (10) on each arm are not instrumented now. Seismometers were removed to pits (11) a few years ago. The two lines were referred to as " RED " for the NW-SE line and " BLUE " for the other. The maximum altitude difference between one pit and the next is (99) meters for the blue and (89) meters for the red. The pit coordinates and elevations are given in table (3-1).

3.2.3 Instrumentation and Recording

Each pit, apart from R_{10} and B_{10}, is instrumented with a vertical Willmore Mk II short period seismometer, adjusted to a natural period of one second and damping factor of 0.6, a telemetry sender unit which contains a preamplifier, an amplitude modulated (am) tone modulator, calibration circuits, filters, voltage stabilisers and line driver circuits. A separate unit contains lightning protection circuits. Power for the senders is fed from the station laboratory via the telemetry transmission cables.

In the year 1970, new cables (known as spiral 4) and Mk II am tone system were installed to replace the old multi-cored cables known as the de system and the Mk I system. With the new system, frequency multiplexing is used to transmit two am tones along one cable corresponding to two seismometers' output. For a detailed description of the telemetry systems and their characteristics, see (18).

The recording station is a single storey brick building which contains the main laboratory, battery room, store room, office, ... etc. Electrical power, telephone and water are available. Should power

cuts occur, a standby diesel powered alternator, housed in the adjacent garage, is automatically brought into operation.

The main recorder is a 24-track EMI TD 516 deck. The 24 tracks are obtained by using two 12-track record heads with the heads mounted so that the tracks interlace. One track is used for the station clock code, two for error correction, one for the strong motion seismometer (which is situated in the vault) and the remaining twenty for the array seismometers. Incoming signals are amplified, filtered (low pars 15C/S cut-off) and frequency modulated.

One inch (2.54 cm) width polyester base magnetic tapes, 7200 feet (2194.5 m) long, are used for recording. Tapes are usually mounted on 14 inches (35.56 cm) reels. Recording speed is 0.3 in./sec. (0.762 cm/sec.), giving a recording time of 80 hours. The carrier frequency is 270 C/S with a peak deviation of $33\frac{1}{3}\%$.

The clock-coder in use has been designed and developed at AWRE, Blacknest. The unit has a fast warm up crystal oscillator which operates at 5 MH_Z. It takes only 30 minutes to reach its specified accuracy of less than $\mp$ 1 part in 10^9 per ^0C. The coder generates a fast code in Vela format. The output from the clock-coder is recorded in a form which gives 1 sec., 10 sec. and 1 min. markers, together with a code one per minute which describes the absolute time in days, hours and minutes.

A correlator system is available at the laboratory and is used to produce the replay of 8 channels from the short period tape deck on to a paper chart recorder. The summed output of the 8 channels with automatic gain correction and also a cross-correlation output is

therefore obtainable for any event of interest.

Tapes are collected and transported monthly to Blacknest to be filed and stored. Processing facilities are available there where detailed analysis of selected events are carried out. Also play-back facilities are available at I.G.S., Edinburgh and elsewhere.

3.3 LOWNET

This is a permanent radio-linked short-period siesmometer network operating in the central of Scotland (Midland Valley) and recording on an analogue, 2.54 cm (1 inch) magnetic tape. The network has been partially operating since January 1969 and fully since September of the same year. At present, it consists of seven vertical Willmore Mark II seismometers, placed on high ground with line of sight to the Royal Observatory, Edinburgh, where the recording takes place. A three-component set of seismometers is lodged in the Observatory Vault EDI, see Fig (3-3).

The network is used mainly for (a) time-term refraction studies of the crustal structure in central Scotland, (b) for monitoring the minor seismic activities which have been reported, in the area, as early as the eighteenth and nineteenth centuries, see Davison (1924)[54] and continuing into the twentieth century, see Dollar (1950)[55] and Crampin and Willmore (1973)[56] and (c) the network could be used as an array of 100 km aperture to determine apparent velocities and azimuths of teleseisms.

Crampin et al (1970)[36] gave a detailed description of LOWNET, equipment, sites and the results of a study of some explosions and

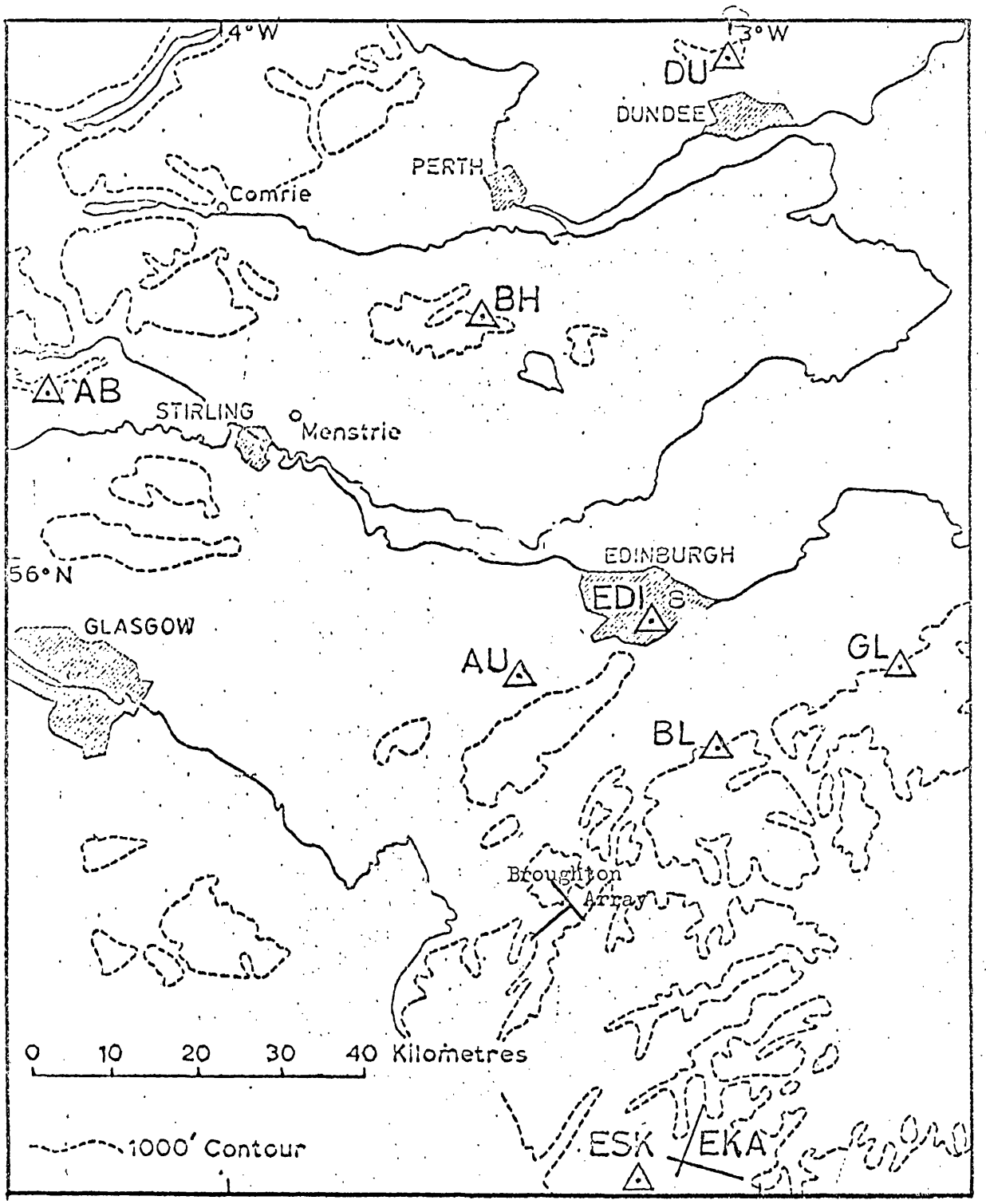

Fig. (3-3) Map of Southern-Central of Scotland showing the three seismic arrays, LOWNET, EKA and Broughton.

natural events recorded on the network, see Section (2.4). A computer program " FAMG " is used to determine the epicentre, depth, magnitude and travel time of any event recorded by the network, see Crampin (1970)[57] and Crampin (1973)[58].

3.4 Broughton Seismic Array

3.4.1 Introduction

Results from local events received at EKA, see Chapter II, show an azimuthal shift varying in sign and magnitude and variations in apparent velocity in both direction and distance. Results from EKA close shots, see Chapter I, indicate an azimuthal velocity variation in the vicinity of Eskdalemuir.

Results from an array south of the Southern Uplands Fault, near the town of Biggar, would help to define the following factors:

(1) Seeing wavefronts differently affected by possible anisotropy than those for the same events at EKA, details in Chapter VII.

(2) Studying the apparent velocities from the same sources at different distances and azimuths.

(3) The nearest likely geological factor to EKA is the line of S.U. fault. If the block to the north of the fault had a velocity of 6.0 km/sec. and that to the south a 5.8 km/sec., then 15° ray re-orientation could be expected at critical angle refraction. Apparent re-orientation of this amount occur, however, at nearer normal than parallel incidence. The proposed array will receive as critical angle refractions, from sources to the NE and close to the north side of the fault.

(4) We also hoped to time the blasts at the sources, see Chapter IV, and thus achieve as accurate origin times and locations as possible.

3.4.2 Description of Site and Station Layout

Three sites were considered for the location of a temporary seismic array in the area south of the town of Biggar. The main factors which controlled the search for a suitable site were:-

(1) The number of the sensors will be nine vertical, short-period seismometers, arranged on two 5-6 km long perpendicular straight lines, forming either a semi-cross or a T or L-shaped array and preferably with one seismometer common to both lines.

(2) One of the lines is to run parallel to the strike of the rocks in the area (about 40° - 50°).

(3) Recording is to be central where the recording device will be lodged in a well-secured place (base station) and all the other stations will be connected to it by radio, apart from the nearest one, which might be connected by cable. Therefore, a line of sight from every outstation to the base should be achieved.

(4) Height differences between seismometers not to be large.

(5) All seismometers should be on geologically homogeneous rock and coupled to it, away from noise sources, easily accessible and secured against vandalism.

(6) Permission to be permitted by the land-owners for access to their land.

(7) The array will be used mainly to record local events (quarry blasts and natural events) at different distances and azimuths and originating mainly in the Southern Uplands and the

Midland Valley.

The area around Broughton village was found to be the best compromise between all these requirements and was finally selected, see map of Fig. (3-3).

Site Description

The array was sited on greywackes and shales of Ordovician (Upper Llandeilo - Caradoc) age. These rocks form a part of what is geologically known as the Northern Belt of the Southern Uplands, which is made up of thick greywacke successions thinning in a south-easterly direction, and associated with Upper Llandeilo or Caradocian volcanicity, see Walton (1961)[59]. At outcrop, these rocks are well compacted, steeply dipping (generally SE) and unmetamorphosed. Typical rock types are greywackes, shales, conglomerates, grits, sandstones and limestones.

The altitude of the seismometer pits varied between 259 m and 346.5 m. Most of the ground is used for sheep pasture. There are few trees and little of the land is used for agricultural purposes. The ground is crossed by an irregular network of drainage ditches and little streams which join the River Tweed. All seismometers were kept at considerable distances from drainage ditches and streams to minimise the noise effect. Seismic noise sources are little and the site can be fairly described as " quiet ".

Array Layout and Pit Construction

The idea was to install all seismometers on bedrock, preferably on two perpendicular straight lines and with equal spacings between seismometers. Conditions, however, were not favourable since peat and boulder clay sediments were up to a few feet thick in some places. Therefore, some pits were moved from the original proposed sites for the seismometers to be on bedrock and on line of sight with the base station to ensure radio connection.

Nine seismometers were available with eight radio links which allowed the installation of eight seismometers on two, almost straight, lines intersecting at the point with NG coordinates of (313.42/635.32) and making a 90^{o} angle, see Fig. (3-4). These seismometers were connected by radio to the recording base station, which was installed on Dreva Craig Hill. A Post Office Engineers tent was borrowed and used to house the recorder (Geostore). The ninth seismometer was placed, off both lines, at Dreva Craig, some 50 m from the Geostore and connected to it by cable. The lines, referred to as "S" and "N" for parallel and normal to strike respectively, were of lengths of 6.20 km for the first (measured from the cross-over point i.e. S_5 - CP) and 6.10 km for the second i.e. (N_1 - N_4). Maximum spacing and altitude differences between two successive seismometers were 1.77 km and 0.08 km for S-line and 2.87 km and 0.16 km for N-line, in respective order. The location, height and coordinates of each seismometer are given in table (3-2).

Pits were excavated through topsoil down to bedrock, levelled off with cement, 10-20 cm thick. A wall was built around each pit and

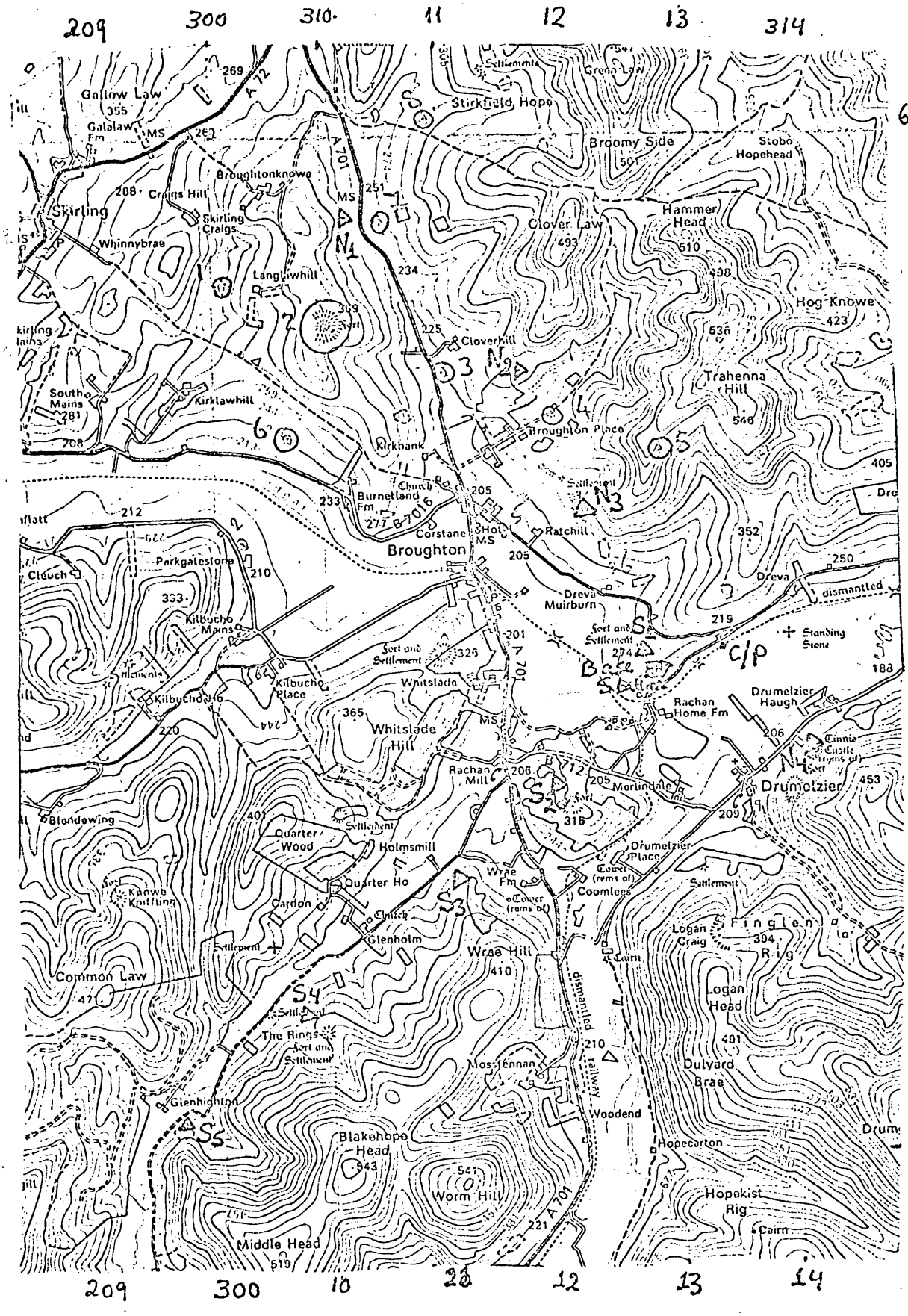

Fig. (3-4) Broughton Array - Seismometers locations.

Station	Location	Coordinates N.G. Lat./Long.	Height (meters)	Bedrock	Seismometer Type	Link	Comments
S_1	Dreva Craig	312.710/635.340	266.7	↑ Greywacke ↓	WMK III	Cable	Base Station
S_2	Rachan Hill	311.940/634.100	288.0		HS-10-2	Radio	
S_3	Wrae Hill	311.140/633.350	261.2		WMK III	"	Old Quarry
S_4	The Rings	309.790/632.200	283.5		HS-10-2	"	
S_5	Glenhighton	308.740/631.300	259.1		WMK III	"	
N_1	Langlaw Hill	310.250/639.130	266.7		WMK III	"	Old Quarry
N_2	Cloverhill	311.610/637.780	346.6		HS-10-2	"	
N_3	Ratchill	312.230/636.630	308.5		HS-10-2	"	
N_4	Drumelzier	314.130/634.470	259.1		HS-10-2	"	
CP		313.420/635.320	190.5				Cross-over-point not instrumented

Table (3-2) Broughton Seismic Array
Seismometers locations, coordinates and heights

wooden boards were used to cover them. Little ditches were dug for water drainage when necessary. Every precaution was taken to protect the seismometers from water, wind and sheep. In some cases, fences were built around the pits. Seismometer N_1 was placed in a concrete slab, built on rock, in an unused quarry. That was the only case where a pit was not excavated. Seismometer N_3 was probably placed on a large boulder. A nearby better (bedrock) site was missed due to snow on the ground when setting up. The depths of different pits varied from 20 - 50 cm. Cables connecting seismometers with transmitters and receivers with the Geostore were always buried.

3.4.3 Instrumentation and Power Supply

Each pit was instrumented by a vertical short-period seismometer, adjusted to a natural period of 1 sec. and connected to an amplifier modulator (amp. mod.) which converts the seismometer's output to a train of pulses and transfers it through a cable into a radio transmitter of a certain frequency which transmits the signal to a radio receiver with the same frequency, installed at the base station and from which the signal is fed through a cable to the recorder. Seismometer (S_1) was connected through amp./mod. to recorder by cable. The equipment involved in the array could be grouped in three categories: detection, amplification and transmission; receiving and recording and maintenance equipment.

Detection, Amplification and Transmission Equipment

(A) Seismometers

Two types of vertical, short-period seismometers were used. Four of them were of Willmore Mk III type and the other five of HS 10 type. Both instruments are adjustable frequency and based on the idea that earth movements will cause relative movements between the casing of the instrument and a suspended permanent magnet mass which will generate an E.M.F. as an output fed to the amp. mod. The output of the W Mk III is greater than 4 V/cm/sec., with sensitivity variation of less than 1% over a temperature range of $-40^{\circ}c - {}^{+}50^{\circ}c$, using a coil of 16 Kohm resistance. The output of the HS-10 is of the order of 3.73 V/cm/sec. when fitted to a coil of 4000 ohm resistance. For safety reasons, it is recommended that the HS-10 should be carried upside down when transported. W Mk III is supplied with a clamping facility for these reasons and therefore when used it should be unclamped.

(B) Amplifier-Modulator (amp. mod.)

The seismometer's output is directly fed into an amp. mod. where the input is amplified and converted to a series of pulses (frequency modulated signal centred on 676 H_Z). This simple audio frequency output signal is not only suitable for transmission by wire or radio, but also for direct recording on magnetic tape. Power can be fed along the same part of wires that carry the output signal. The unit is designed for low power consumption and is packed in a waterproof container.

Two different types of amp. mods. were used at Broughton, known as " prototype and production", having different gain settings to cope with the noise level in the area and the type of seismometer. In our case all amp. mods. were adjusted to a gain of "7" for production type and "3" for prototype (This was the case for both W Mk III and HS-10 seismometers). The amp. mods. outputs were fed through cables, connected direct to the input terminals of the geostore for station "S" , and to the input terminals of U.H.F. transmitters for the other outstations. All amp. mods. were covered by plastic bags and housed inside the pits for protection against water.

(C) U.H.F. Transmitters

For each of the eight radio linked outstations, the output from the amp. mod. was connected to the input terminal of a miniature U.H.F. transmitter, housed in a metal can strapped to the aerial mast above ground level or to the antenna. The coaxial output from the transmitter was convected directly to a multi-element Yagi array (antenna). The antenna was fixed on top of the mast and directed towards the corresponding receiver at the base station and in line of sight with it. Different transmitters had different frequencies. In some cases, fences were built round the transmitter for protection against sheep.

Receiving and Recording

(A) U.H.F. Receivers

Radiated signals from transmitters' antennae were received by similar antennae fixed on top of masts over the ground, near the recorder, at the base station. These antennae were directed towards the corresponding transmitters and each convected to a metal can housed receiver arranged in a similar way as the transmitter. Outputs from these receivers were connected by cables to the input terminals of the geostore. Two or three receiver antennae were strapped to one mast to reduce the size of area covered by masts. Power was fed to the receivers from the recorder supply via the same cables carrying the outstations' output.

(B) M.S.F. Radio Receiver

This is a timing device which receives the 60 KHz short wave standard time signal transmitted by the M.S.F. Rugby station, and delivers it to the geostore for referencing the interval encoded time signal. The radio has an accuracy of better than 1 m sec. at 650 km from the transmitter in the presence of moderate background noise. With a pass-band frequency width of 25 c/sec., the radio can work under temperature range of 0^{o} - $^{+}45^{o}$c, supplied by a 4.5 volt dry battery and with a consumption of 0.8 mA.

(C) Geostore Field Recorder

This is an analogue recording device, designed for long term collection of frequency modulated seismic data, with very low power consumption and suitable for temporary or permanent seismic networks.

All geostore components are light weight, designed for easy installation, fully protected against the impress of dirt or water and each is easily accessible for routine checks and maintenance. Housed together with a time encoder in a completely waterproof aluminium cabinet, the field recorder unit weighs 23 kgm, measures 52 cm width, 27.5 cm height and 44 cm depth, and uses a 1.27 cm ($\frac{1}{2}$ inch) width, 730 m (2400 ft.) length, magnetic tape wound on 10.16 cm (4 inch) diameter spool, which accommodates a total of 14 tracks, 11 of which are used for seismic data, one for time and the other two for flutter compensation to improve the signal to noise ratio. Two seven-track interleaved heads are fitted and either uni or bi-directional recording may be employed. In the second case only five seismic data channels are available and the recording time is doubled.

The recorder accepts, on the seismic channels, only frequency modulated input signal with a centre carrier of 676 H and a maximum deviation of 40%. This, however, does not apply to an external standard radio time signal. Recording speeds of 0.05953, 0.11906 and 0.23813 cm/sec. (15/640, 15/320 and 15/160 in/sec.) are provided giving maximum recording time of 680, 340 and 170 hours respectively (bi-directional operation) and half these times for uni-directional. A 37 way socket is provided which, in conjunction with the geostore field test box (see Section 4.3.4) will monitor selected points within the recorder in order to verify correct functioning of the equipment.

A 12 volt power supply is required to operate the equipment,

normally a standard car battery. Another 12 volt battery is required for the outstation supply. Three power supply cables are provided, one for the outstations and two for the recorder supply, as a facility for changing batteries without disturbing recording or time code. The equipment has been designed to keep power supply down to 1.5 W. Input sockets are provided for the eleven data channels. These sockets also send power to the outstations' radio receivers or, for cable links, to the amp. mod.

The time encoder is an integral part of the recorder and provides time code data, an accurate flutter compensation signal, and a capstan servo reference frequency. The timing signals from the encoder are accurate to one part in 10^6 over the full operating temperature range, and recording is in accordance with " Vela Uniform Code " for one minute time frames. Timing is in days, hours, minutes and seconds which can be read numerically, see Fig. (3-5). The time code generator has a visual display which is enabled by a key switch where push buttons enable the date/time to be updated. Facilities are provided to allow the recording of a broadcast standard radio time signal (via an external receiver e.g. the M.S.F.). This may be done either continuously or once every hour on the hour and for a limited time.

A desiccator is screwed inside the recorder to dry out the air inside the recorder case if the humidity is high when the lid is closed. A routine check on the running of the recorder can be carried out by observing a red light plug connected to the side of the case and without opening the lid.

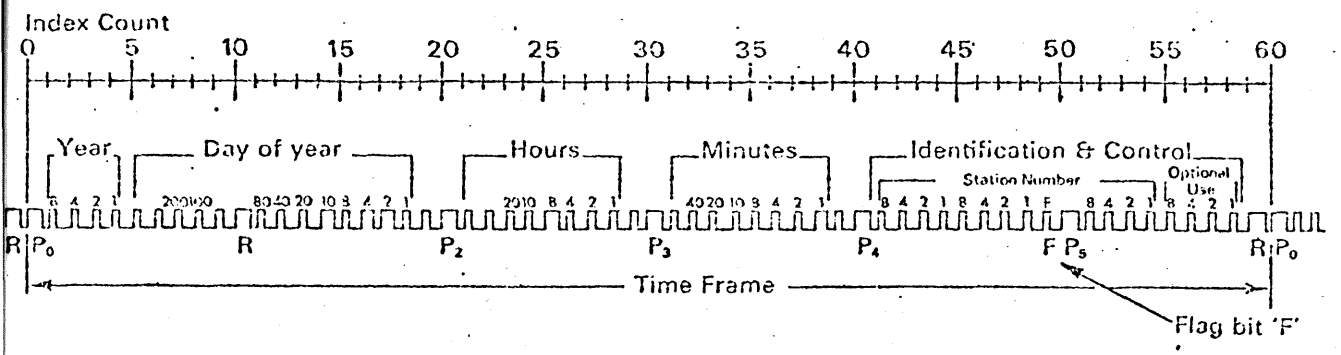

Time decoded reads:

Year = Zero

Day of year = 16

Hours = 8

Minutes = 1

$P_0 - P_5$ = 0.8 sec. duration - '10 sec. marks' -

Position Identifiers

R = 0.8 sec. duration - 'End of frame marks' -

Reference

R & P_0 denote '1 minute mark'

Binary coded decimal bits - 'One' = 0.5 sec.

'Zero' = 0.2 sec.

Unused bits = 0.2 sec.

Clock rate (Bit rate) = 1PPS

Clock interval = 1 sec.

Time frame interval = 1 min.

Flag bit 'F' denotes abnormal recording format

when value is 'One' (See index count 49)

Fig. (3-5) Vela standard time code for use with Magnetic Tape Recording

At Broughton Array, nine channels were used for seismic data and one channel for standard radio time signal. The recording speed was chosen to be 0.11906 cm/sec. (15/320 in./sec.) giving a maximum recording time of 170 hours and a 16 Hz frequency bandwidth, see Fig (3-6). Standard radio time signal was recorded continuously. The geostore, the M.S.F. radio and the batteries were housed in a Post Office Engineers tent, specially borrowed for this purpose and this proved to be efficient against wind and rain, and the geostore was kept dry and safe during the period of the experiment. All cables connecting the geostore with seismometer " S " and the receivers of the others were buried a few centimeters in the ground.

Power Supply and Cable Connections

Each transmitter was supplied by a 12 volt car battery with maximum capacity of 40 A/H. The amp. mod. was fed by the same battery via the signal cable. Total power consumption, from that battery, was of the order of 0.1 A/H. Two batteries of the same type were used to supply the geostore, the receivers and the amp. mod of seismometer S_1, making a total power consumption of about 0.45 A/H. Although batteries were supposed to supply power for over a week, it was more convenient to charge them weekly. Twenty batteries were used, 10/week.

Army type " D 10 " cable connections were used to connect amp. mods. with transmitters, receivers with geostore and amp. mod. of seismometer S_1 with geostore.

Fig. (3-7) shows the overall picture of the geostore seismic data

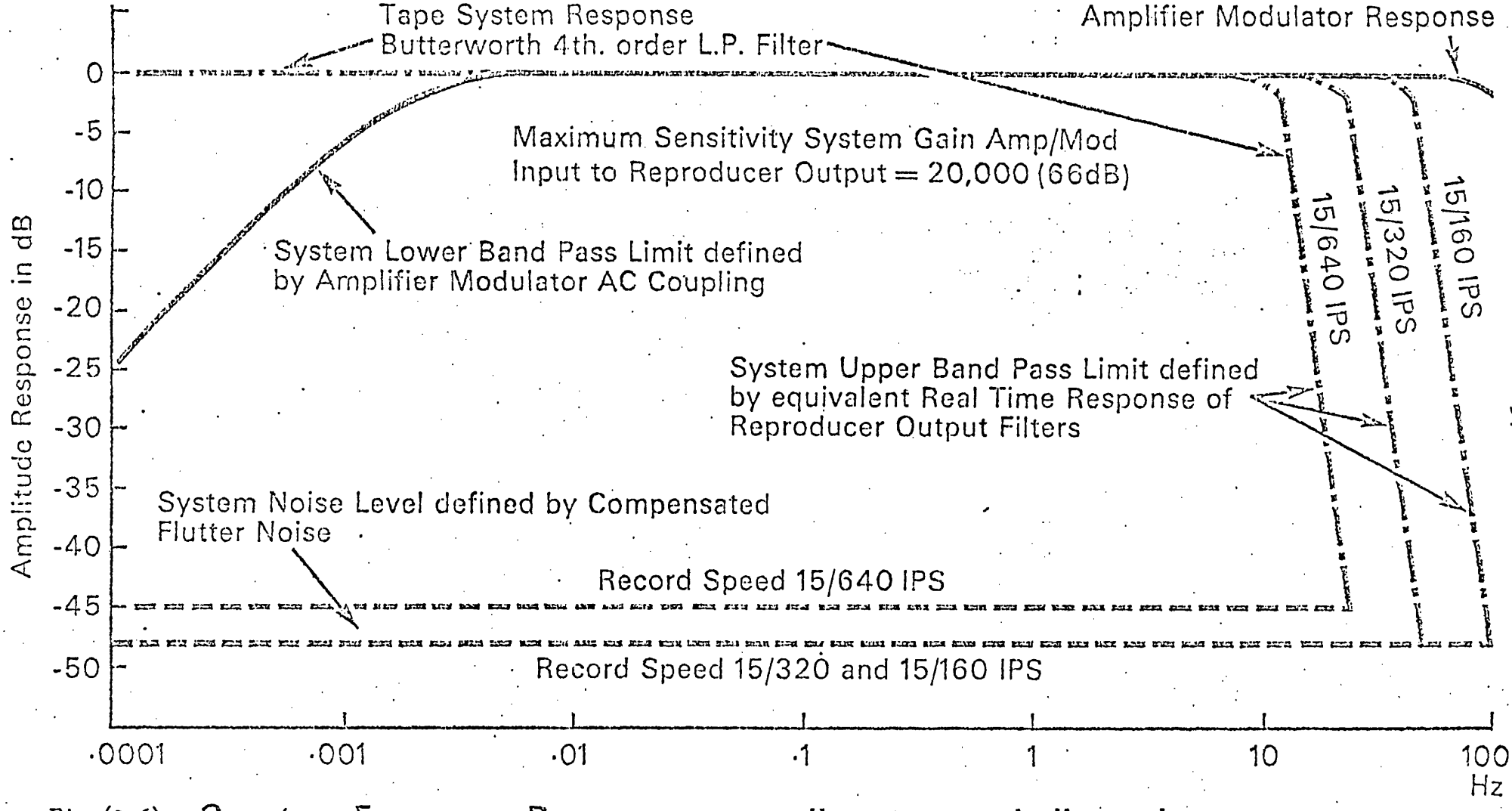

Fig.(3-6) Geostore Frequency Response – overall system excluding seismometer

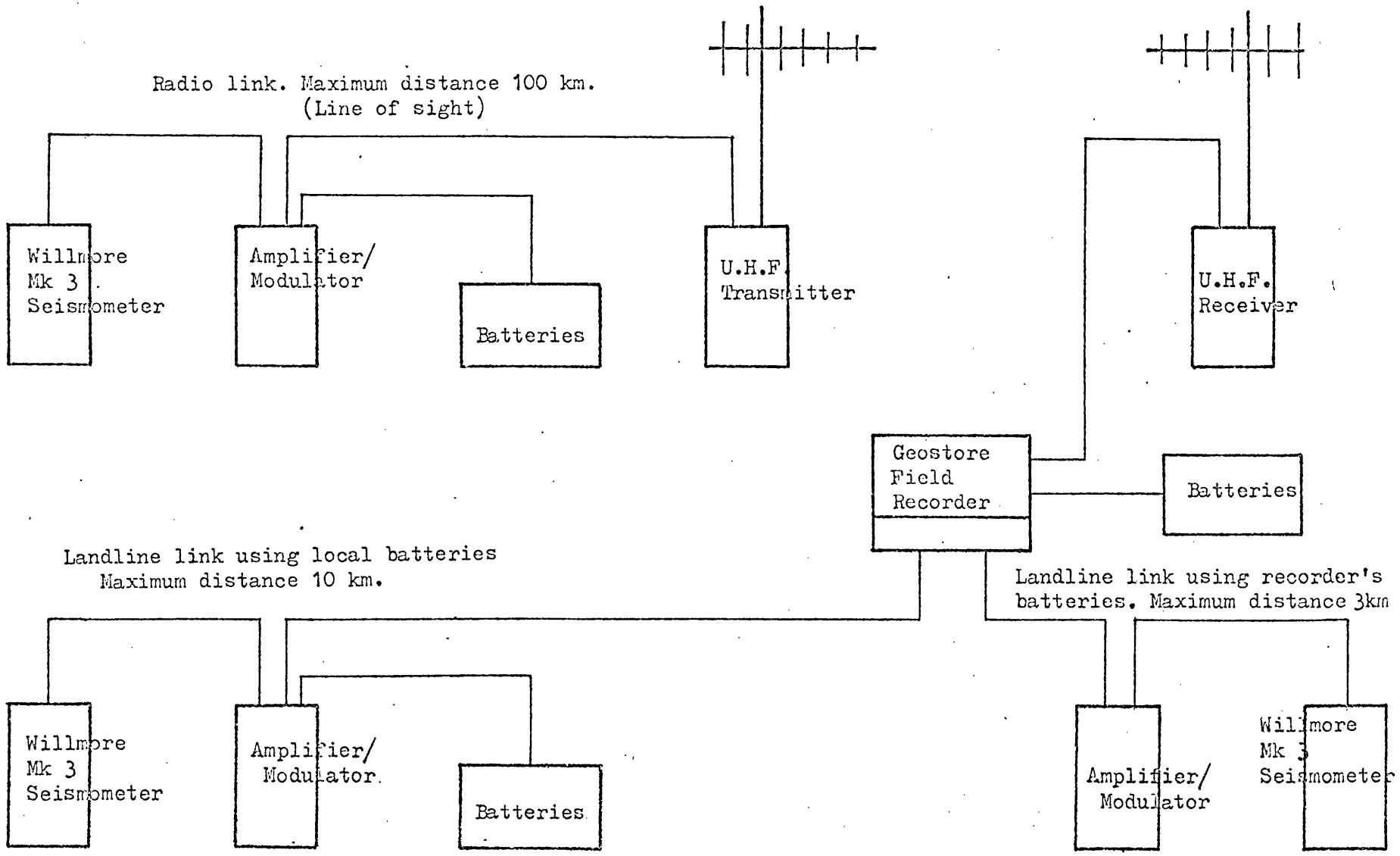

Fig. (3-7) Geostore Seismic Data Field Recording System.

field recording system.

Maintenance Equipment

Test equipment and tools were essential for routine maintenance and checking the performance of the array. A kit of tools, wires, fuses, tape, a voltmeter and three field test boxes were used throughout the experiment. The field test box is a self-contained and very compact one which can be used as a " short-run" seismograph station, and it may be used to monitor any channel whilst geostore system is in use. Outputs from this box include power for driving the amplifier modulator or radio, test signal for the amp. mod. to confirm its gain accuracy and test signals for setting up radios and the field recorder. Inputs include the seismometers output signals which can be checked on the field test box pen recorder, and the field recorder head currents which can be monitored in both frequency and amplitude on each of the 14 channels.

Checking on functioning of network was carried out weekly as also changing tapes and batteries.

3.4.4 Array Performance

The array operated partially with siesmometers N_1, N_2, N_4, S_1, S_3 and S_5 on 31/1/1977 (16 hr. 46 m. U.T.), and fully on 2/2/1977 (15 hr. 40 m.) and was discontinued on 6/4/1977 (12 hr. 51 m.). Ten tapes were used successfully for continuous recording during that period. Many seismic events were recorded, ranging from local to teleseisms (only local events were processed). Fig. (4-4) shows a local event recorded at the array. A statistical survey, carried out

on 119 selected events recorded on all the tapes, showed that the average recording of all the channels was 71.5%.

Some faults and breakdowns were experienced in the system throughout the experiment and are summarised as follows:

(A) Geostore

(1) Channel (1) showed to be noisy at the start of the experiment and therefore was not used.

(2) Channel (10) was found faulty on 3/4 and not used thereafter.

(3) Two days' recording was lost due to battery failure (22 - 23 March).

(B) Seismometers

On only one occasion seismometer N_1 was found on its side. This was a possible wilful interference.

(C) Amp./Mods.

Occasional high frequency noise was noticed on play-back of seismometer N_1. This is believed to have been caused by an amp./mod. fault.

(D) Radio Telemeter Links

Occasional transmission/reception failures occurred and found to have been caused by:

(1) fuse failure (one case) at transmitter N_1.

(2) untuned transmitter (one case) at S_5.

(3) wet receiver (one case) at N_3.

(4) possible high moisture causing intermittent transmission (one

case) at S_3.

(E) Cables

Damage occurred in only two cases. One was caused possibly by sheep at N_1 and the other (S4) by strain when at first stretching the cables between the trees at the base station was attempted.

CHAPTER IV

SOURCES, ORIGIN TIME RECORDING AND DATA PROCESSING

4.1 Sources

4.1.1 Introduction

As outlined in the introduction to this thesis (chapter I), our first interest was in local events received at EKA from different azimuths and distances and showing short-period (about 1 sec.) surface waves. Surch for such events began through transcribed EKA and LOWNET records filed in the I.G.S. (Edinburgh) and containing different events. These events varied from local to teleseisms. The latter category was ignored. Local events were mainly quarry blasts, special marine shots and LOWNET fixed earth tremors. Play-backs were carried out for more than (70) of these and showed that events of the last category (ie earth tremors) are the only likely ones to show surface waves. Unfortunately, these were only a few.

First P-arrivals of these events were considered next. Results revealed the need for (1) more events at various azimuths and ranges, see chapter (VI). (2) shots to be fired at short ranges in the vicinity of Eskdalemuir array, see chapter (V), and (3) the study of other events, preferably from the same sources, recorded at different location in the Southern Uplands, see Section (3.4) and chapter (VI).

The data used for this thesis are summarised in the following sections. Fig. (4-1) shows the location of all sources, apart from the close

Scale 1: 625000

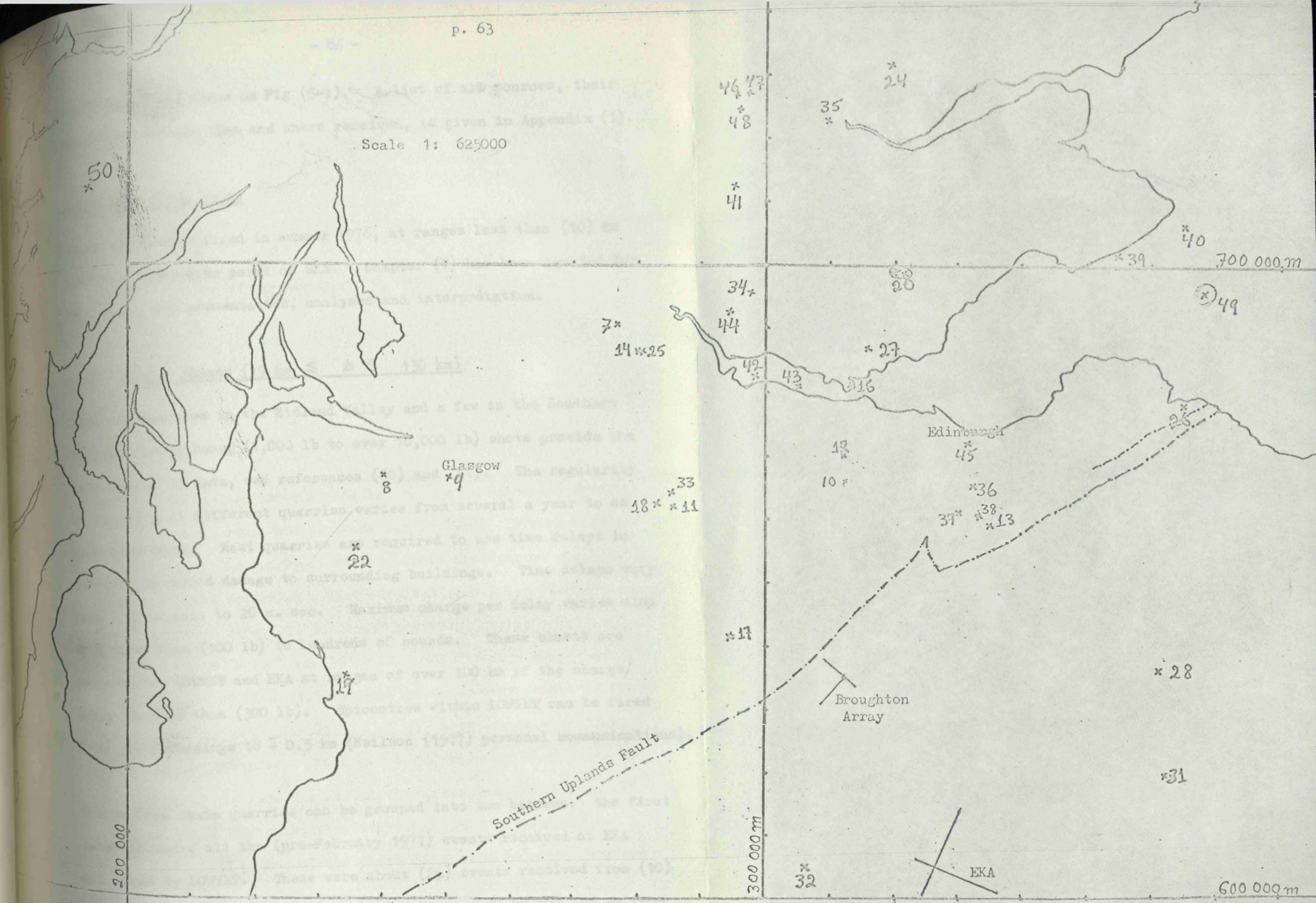

Fig. (4-1) Map of Southern Central of Scotland showing the locations of all local sources (apart from the SOSP I & II shots).

shots which are shown on Fig (5-1). A list of all sources, their locations, origin time and where received, is given in Appendix (1).

4.1.2 EKA Close Shots

These shots were fired in summer 1976, at ranges less than (10) km from the cross-over point of EKA. Chapter (V) has been devoted for this data, its presentation, analyses and interpretation.

4.1.3 Quarry Blasts (19 km $\leq \Delta \leq$ 130 km)

Numerous quarries in the Midland Valley and a few in the Southern Uplands firing heavy (1,000 lb to over 10,000 lb) shots provide the main source of data, see references (60) and (61). The regularity of blasting at different quarries varies from several a year to as many each week. Most quarries are required to use time delays in blasting to avoid damage to surrounding buildings. Time delays vary from 0.7 m. sec. to 20 m. sec. Maximum charge per delay varies also from less than (100 lb) to hundreds of pounds. These blasts are recorded on LOWNET and EKA at ranges of over 100 km if the charge/delay is more than (300 lb). Epicentres within LOWNET can be fired from its recordings to $\mp$ 0.5 km (Neilson (1977) personal communications).

Events from these quarries can be grouped into two batches: the first batch includes all the (pre-February 1977) events received at EKA and fixed by LOWNET. These were about (25) events received from (10) different quarries at distances ranging between 20 km and 126 km from EKA cross-over point and propagation sectors ranging between 90° and 210°, see Fig. (4-2).

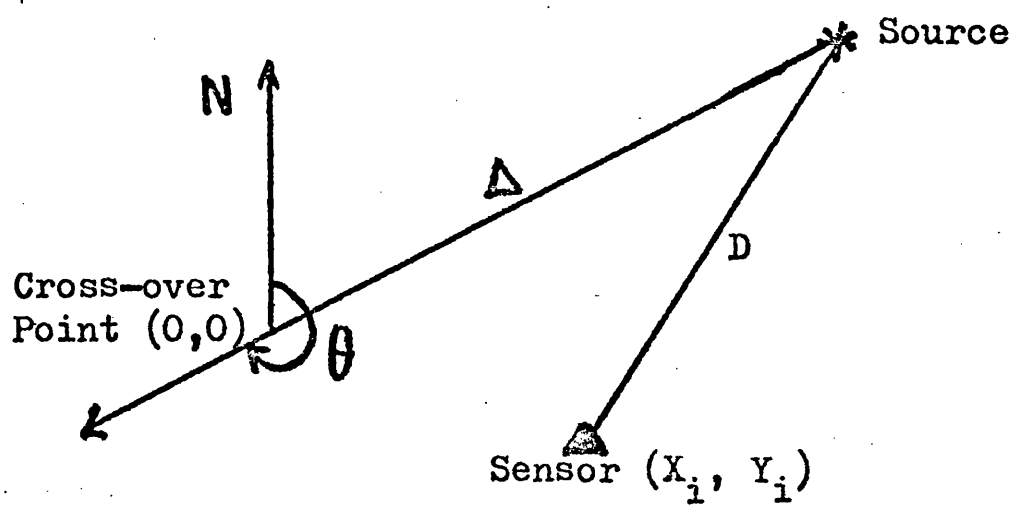

Fig. (4-2) Propagation Vector ( )

The second batch spanned essentially the period during which Broughton array was operating (1st February - 6th April 1977). Through direct communication with the quarry operators, close checking on the location of these blasts was possible. This resulted in (1) the identification of over (60) events from (22) different quarries, giving propagation vector ranges of 90° - 248° and 89° - 224° and distance ranges of 20 km - 126 km and 19 km - 81.5 km from the cross-over points of EKA and Broughton Array respectively. (18) of these events were timed at (14) different quarries. Figures (4-3/5) show the recordings of a quarry blast (Craig Park Q.) at EKA, Broughton and LOWNET respectively. (2) Some of the LOWNET identifications were found to be wrong. Therefore about (15) events of the first batch were rejected from the analysis.

54d. 16h. 46m.

R1

2

3

4

5

6

7

8

9

R11

F

54d. 16h 46m.

B1

2

3

4

5

6

7

8

9

B11

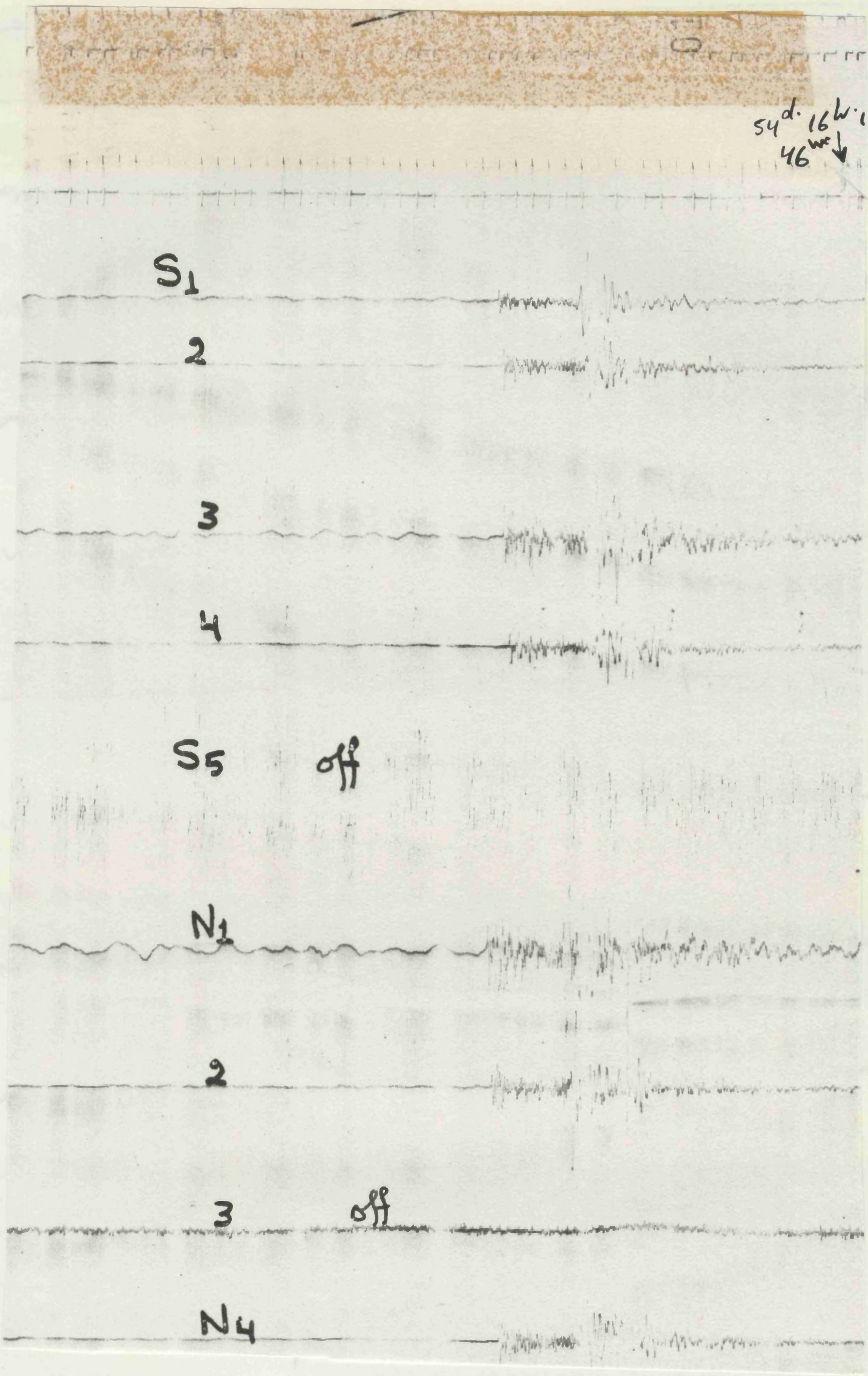

Fig. (4-4) Broughton record of the above mentioned blast at Craig Park Quarry.

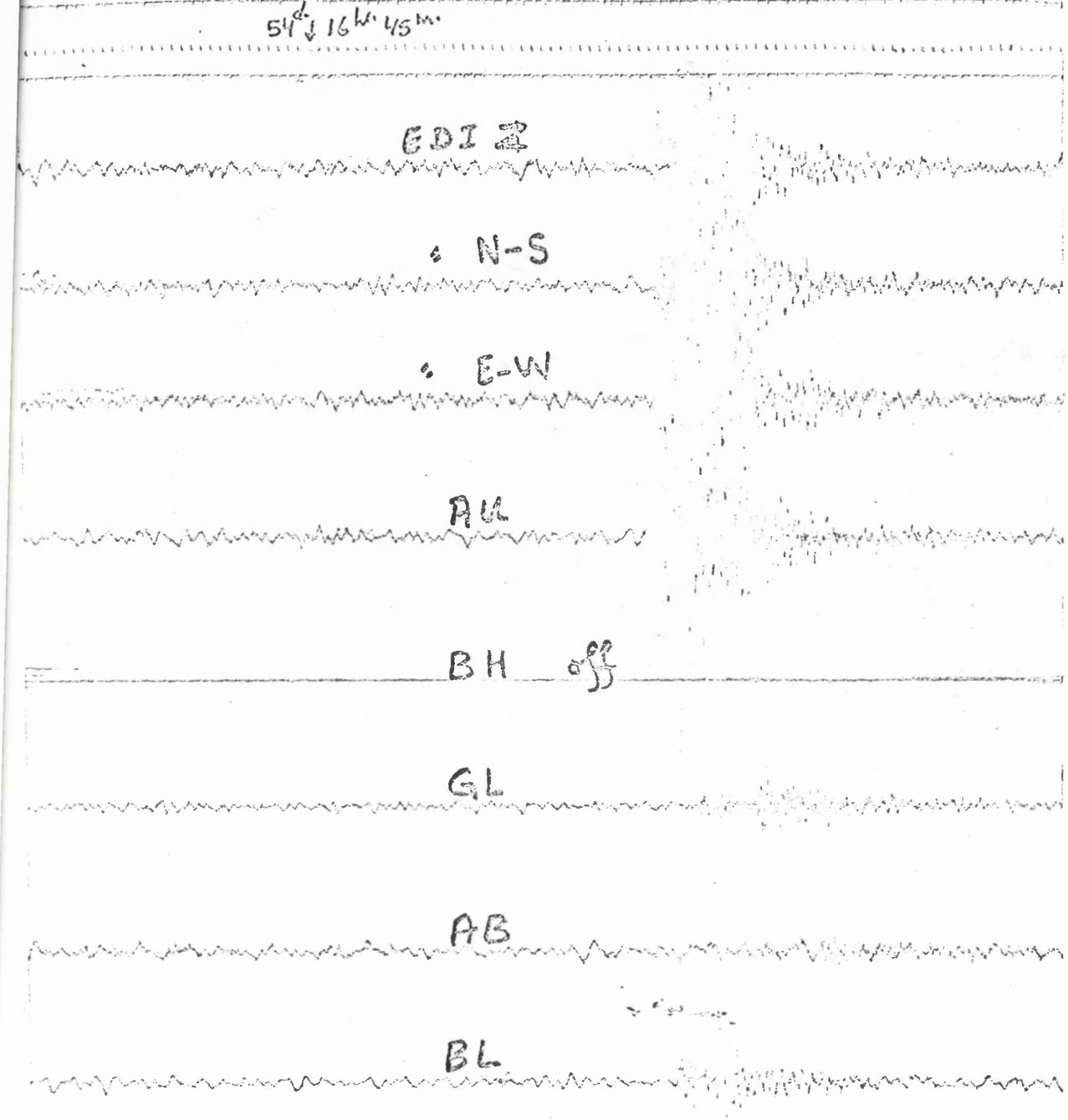

Fig. (4-5) LOWNET record of the same blast of Craig Park Quarry.

4.1.4 Marine Shots ($100 \text{ km} \leq \Delta \leq 340 \text{ km}$)

With the kind permission of I.G.S. (Edinburgh), shots (22 - 36) of SOSP (II) project in the North Channel were made available for my use. Also a few Navy shots, near the Isle of May, and some shots of SOSP (I) project were also permitted. EKA records of these shots were of importance. They enlarged the range of propagation sectors to 54° - 248°.

4.1.5 Natural Events ($56 \text{ km} \leq \Delta \leq 165 \text{ km}$)

There is a considerable seismic activity in the Midland Valley, some of which has been associated with the mining activity, see Mashkour (1976)[4] and references therewith. Tremors are recorded on both EKA and LOWNET where the second is used to determine the epicentres of such events. Accuracy of determination is of the order of $\mp$ 0.5 km, providing that the event has been recorded at five sensors, or more, of the network (Neilson (1977) personal communication). About (15) (pre-February 1977) EKA records of such events were analysed but the location of more than half of these were doubtful and therefore were rejected.

4.2 Origin Time Recording

As mentioned in the previous section, (14) different quarries were visited, during the period when Broughton Array was in operation, attempting to determine the origin times of their blasts.

Timing Device

With the kind cooperation of the Geology Department, Birmingham University, their timing device was available for our use during the period of our experiment at Broughton. The device consists of:-

(1) An M.S.F. radio, see Section (3-4-3).

(2) Seismometer of any type.

(3) A mixer box, with variable gain control, which amplifies the seismic signal output and mixes it with the output of the M.S.F. radio. The mixed output is fed and recorded on:-

(4) An ordinary, one channel, cassette recorder.

To time any blast, the seismometer was planted as near as possible to the centre of the shot pattern, mostly of the order of (10 m) and surrounded by a wall of stones to avoid any possible damage. A (100 m - 150 m) cable connected the seismometer with the recorder box which was generally placed near the shot firer. The instrument was switched on a few minutes before the shot and off a few minutes after.

A difficulty was experienced in timing some blasts, where the M.S.F. time signal disappeared through a background noise of television and/or radio programs. That resulted in the loss of a few timed blasts. This is believed to have been caused by either (1) battery voltage being too low to drive the oscillator gated by the M.S.F. pulses and/or (2) the long cable connecting the seismometer with the box, where the cable might have acted as a receiver. Thereafter, the battery was replaced and a short cable was used. The seismometer

was located about (100 m) from the shot and small corrections were made to the origin times.

All timed blasts, at the quarries, were played back using either the facilities of I.G.S. (Edinburgh), see Section (4.3), or a single channel hot-stylus device at Glasgow University. Timing accuracy was of the order of $\mp$ 0.01 sec.

It should be mentioned that the M.S.F. minute markers were not decoded at the time of the experiment. To avoid confusing the timed blast with any near simultaneous event on the seismic tapes, an accurate hand watch was used to time the blast to the nearest minute.

4.3 Data Processing

With the kind permission and cooperation of the U.K.A.E.A., all wanted EKA tapes were transported to Edinburgh for my use and with the kind permission of I.G.S. (Edinburgh), all LOWNET tapes and playback facilities for all types of tapes were accessible. Two playback systems were used, one which handles geostore 1.27 cm ($\frac{1}{2}$ inch) Broughton tapes, referred to as Geostore Replay System, and the other handles 2.54 cm (1 inch) EKA and LOWNET tapes and referred to as Analogue Processing System. Both systems, described in detail by Houliston, et al (1976)[62], will be briefly described in this section.

4.3.1 Geostore Replay System

The geostore reproducer comprises a mains operated tape deck and an electronics unit. Two different head assemblies are offered with the tape deck, the choice of which depends on whether uni or bi-directional

recording was employed in the field i.e. providing simultaneous playback of 7 or 14 channels respectively. A subtractive flutter compensation system is used to reduce the base line noise and thereby improve the S/N ratio on all data channels. A monitor switch enables any one channel to be switched independently to a pre-amplifier unit (housed in the rear of the equipment) which automatically adjusts the gain and bandwidth to suit the level and frequency of the signal. This switched gain/bandwidth facility allows reproduction of signals at speeds in the range of 2.38/25, 4.7625, 9.525, 19.05 and 38.1 cm/sec. (15/16, $1\frac{7}{8}$, $3\frac{3}{4}$, $7\frac{1}{2}$ and 30 in./sec. respectively). Inserts for the demodulators cards are also available for these speeds. The output may be fed to an ink-jet recorder, computer or any other analysing equipment.

The 16-channel ink-jet recorder provides a visible display of the analogue magnetic tape. A fine jet of ink is directed at a moving paper chart. A galvanometer switch, consisting of a small permanent magnet mounted upon a glass capillary tube, is provided to control the oscillation of the ink-jet. The ink flow is adjustable and controlled by a pump which feeds it to the capillary tube jet via a fitter.

This system was used for playing back Broughton Array tapes from which about (120) selected events were reproduced in an analogue form on paper. These events were timed quarry blasts, known untimed quarry blasts, LOWNET fixed natural events and quarry blasts and few special marine shots. The replay speed was selected at 2.38/25 cm/sec. (15/16 in./sec.) corresponding to a speeding factor of (20). The ink-

jet gain was mostly chosen to be at 2.5 volt/cm and found to be more appropriate for small and distant quarry blasts recordings. Paper speed was always selected at 1000 mm/sec. Time channel was reproduced as first and last traces to increase the accuracy of time measurements (± .01 sec.). M.S.F. radio signal was also made on every record.

A few selected events, with possible surface waves, were transcribed on another tape in a digital form using the PDP11/50 computer available in I.G.S. Limitations concerning speeding up factor, frequency limit and a computer maximum capacity of 12,000 samples/sec., limited the number of digitised channels for any events to (6) including the time channel at a digitising rate of 120 samples/sec.

4.3.2 Analogue Processing System

This system was developed to provide processing facilities for seismic network data recorded on 2.54 cm (1 inch) tapes. The system consists of a 24-channel replay unit connected to a programming board to facilitate the interconnections between various instruments, stereo listening for event detection, 24 analogue band pass filters, a 16-channel ink-jet recorder to provide visual playbacks, time decoder to decode and display time channel, two particle motion analysers, an automatic analogue playback control unit and bass-lift circuits for wave velocity response modification.

The unit is capable of replaying 24-track tapes at various speeds 19.05, 38.1 and 76.2 cm/sec. (7.5, 15 and 30 in/sec.) which are 25, 50 and 100 times the recording speed of EKA tapes and 64, 128 and

256 times the recording speed of LOWNET tapes. Two replay heads provide the data for amplification and demodulation, one track per head being used for flutter compensation. The band-pass filters provide optional analogue filtering within the range 0.01 H_z - 100 KH_z , with an attenuation slope of 24 db octave. The ink-jet recorder is the same one described in Section (4.3.1).

The replay speed for both EKA and LOWNET tapes was selected at 19.05 cm/sec. (7.5 in/sec.). Filtering was applied within the range 0.1 H_z - 16 H_z for both tape types. Ink-jet gains, mostly used, were 1 volt/cm or 2.5 volt/cm., depending on the size of the event. Paper speed was always selected at 1000 mm/sec. Time channel was always played back at the top and bottom of each record, for more time-measurement accuracy.

When playing-back an EKA tape, the operation was carried out twice to cover all the channels (20 seismic + time channel) since the ink-jet recorder can display only 16 channels at a time.

For the convenience of anyone wishing to reproduce EKA data, the (24) tape tracks correspond to the channels as shown in table (4-1)

Track Plug Socket on I.G.S. Playback	EKA Tapes
1	R1
2	B1
3	R2
4	B2
5	R3
6	B3
7	R4
8	B4
9	R5
10	B5
11	EC
12	EC
13	R6
14	B6
15	R7
16	B7
17	R8
18	B8
19	R9
20	B9
21	R11
22	B11
23	BB
24	TIME

Table (4-1) EKA records - tracks and corresponding channels

CHAPTER V

ESKDALEMUIR ARRAY SHALLOW STRUCTURE

5.1 Introduction

Preliminary analysis of P-waves of about (50) local events and Rayleigh waves of five of these received at Eskdalemuir Array from different azimuths and ranges (some of which were repeated) revealed the existence of an azimuthal anomaly or shift (bearing of direct source to receiver ray - observed) varying in sign and magnitude from one source to another and ranging from ($^{-}5^{\circ}$ to $^{+}15^{\circ}$). In other words, waves travelling from different sources, originating in the Midland Valley, Southern Uplands and off-shore, seemed to have been refracted from their straight line routes to Eskdalemuir.

At that stage, an explanation of the azimuthal anomalies of Rayleigh waves were considered of foremost importance. Their periods varied within the range (0.5 sec. - 1.5 sec.) and therefore required any causative structure to lie within the upper 0-3 km of the earth's surface, anywhere between the sources and Eskdalemuir. On the other hand, P-waves may be affected by deeper structures as their emergent ray angles from the vertical are in the range 40° to 70°.

Azimuth anomalies of seismic waves from array data have been reported by different authors (more details in Chapter VI). Such anomalies have been attributed to different causes such as: non-homogeneous and anisotropic conditions within the wave path; lateral heterogeneity in the media such as dipping planes and/or a complex velocity

structure of some sort immediately beneath the recording station.

An explosion experiment in the vicinity of Eskdalemuir seemed to be a convenient way to study the shallow velocity structure within the Lower Palaeozoic bedrock beneath the array, utilizing P-waves and aiming to:

(1) identify any lateral inhomogeneity such as dipping refractors.

(2) study the effect of depth on velocity, i.e. significance of layering.

(3) and to study the velocities in different directions, i.e. possible anisotropy.

Resources available permitted a pattern of six untimed shots providing enough energy to be detectable across the whole array, i.e. ranges up to about 10 km giving information to depths of about 1 km. Since all seismometers are founded on the steeply dipping Lower Palaeozoic bedrock (shales & greywackes) no effect from superficial deposits (at most a few metres of peat, boulder clay, alluvium, sand or gravel) is anticipated on the apparent velocities measured at over 100 m range. There is no expectation of any other change of rock type within the top kilometre of depth. Velocity changes with depth, therefore, are only to be expected from joint and crack effects. Lateral changes in velocity may be due, in addition, to any contrast between shale and greywacke beds.

5.2 Description of Shot Pattern and Operational Details

Four reversed inline shots were fired on the two arms of the array and two shots in between (see Fig. (5-1)). Distances between shots

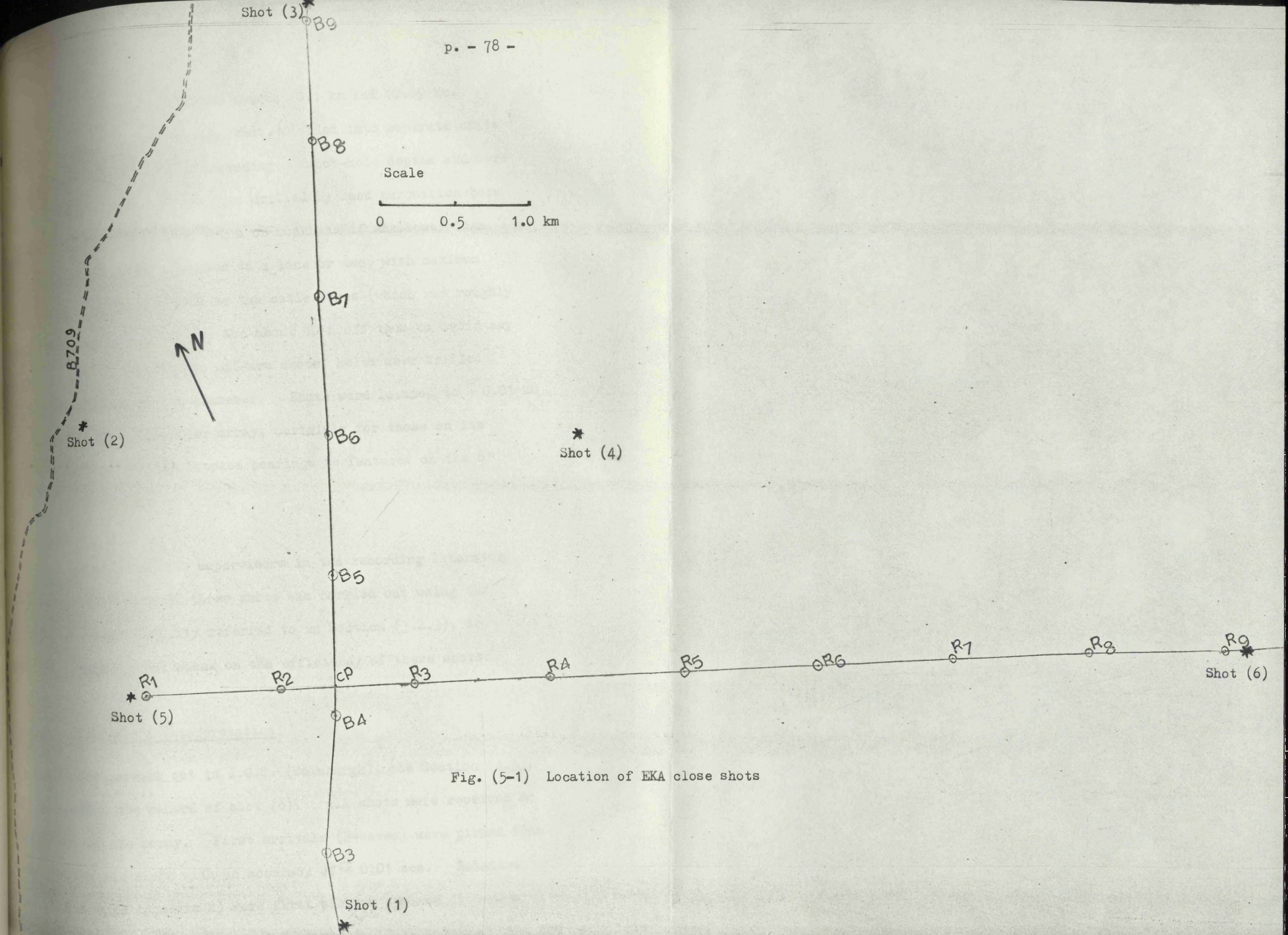

Fig. (5-1) Location of EKA close shots

different seismometers varied between 0.1 km and 10.09 km. Charge sizes averaged around 4 kg/shot, divided into separate units of roughly 0.2, 0.4 or 0.6 kg depending on shot-hole depths and were fired instantaneously. Holes were drilled by hand percussion bore through peat or earth down to 1-2 m or rockhead if shallower than this. Shot patterns were limited to a line or two, with maximum length of about 15 m, parallel to the cable lines (which run roughly with the two arms of the array) and about 10 m off them to avoid any possible damage. For the two off-arm shots, holes were drilled within circles of about 7 m diameter. Shots were located to $\pm$ 0.01 km in relation to the seismometer array, certainly for those on its arms and probably, through compass bearings to features on the 6" maps, for the other two.

With the cooperation of the supervisors in the recording laboratory, instantaneous play-back of three shots was carried out using the available play-back facility referred to in Section (3.2.3), to verify the recording and check on the efficiency of these shots.

Data Analysis & Interpretation

Play-backs were carried out in I.G.S. (Edinburgh), see Section (4.3). Fig. (5-2) shows the record of shot (6). All shots were received on every sensor of the array. First arrivals (P-waves) were picked from records of the six shots with an accuracy of $\pm$ 0.01 sec. Relative arrival times (see Appendix 2) were first plotted against distances for each shot. Origin times were calculated on the assumption that the T-X slope between the nearest pair of seismometers to the shot projected through the point (0.0). Three of the inline shots were about 0.10 km

R1
2
3
4
5
6
7
8
9
R11
B1
2
3
4
5
6
7
8
9
B11
21' 50"

from the nearest seismometer, the fourth was about 0.48 km. The nearest seismometers to the off-line shots, 2 & 4, were at 1.66 km and 1.58 km respectively. For the inline shots accuracy of origin time determination is believed to be $\mp$ 0.01 sec. which is the difference between the travel times to the nearest seismometer at 4.3 and 3 km/sec. For the other shots accuracy is of the order of $\mp$ 0.02 sec.

5.3.1 Vertical Velocity Variation
T-X Graphs/Inline Shots

First inspection of the travel-time-distance graphs of the inline shots suggested that three linear segments could be fitted to each. It should be mentioned, however, that the third segment (with lowest slope) of each curve was fitted to only two or three points at most. Velocities associated with different segments are given on the graphs, see Fig. (5-3 A).

(A) Plus - Minus Method

Utilizing the results obtained from the T-X graphs of Fig. (5-3A) and considering a two-layer model, the plus-minus method has been applied to the reversed inline shots, see Hagedoorn (1959)[63]. Results are given in table (5-1) and Fig. (5-4). Commenting on these, the following points should be made:

(1) The refractor velocity under the Blue arm differs significantly from that under the Red (+ 0.36 $\pm$ 0.03 km/sec.). The higher velocity is in the direction closer to the local geological strike (20° compared with 70°) (more details later). This difference means that the basic assumptions of this method of

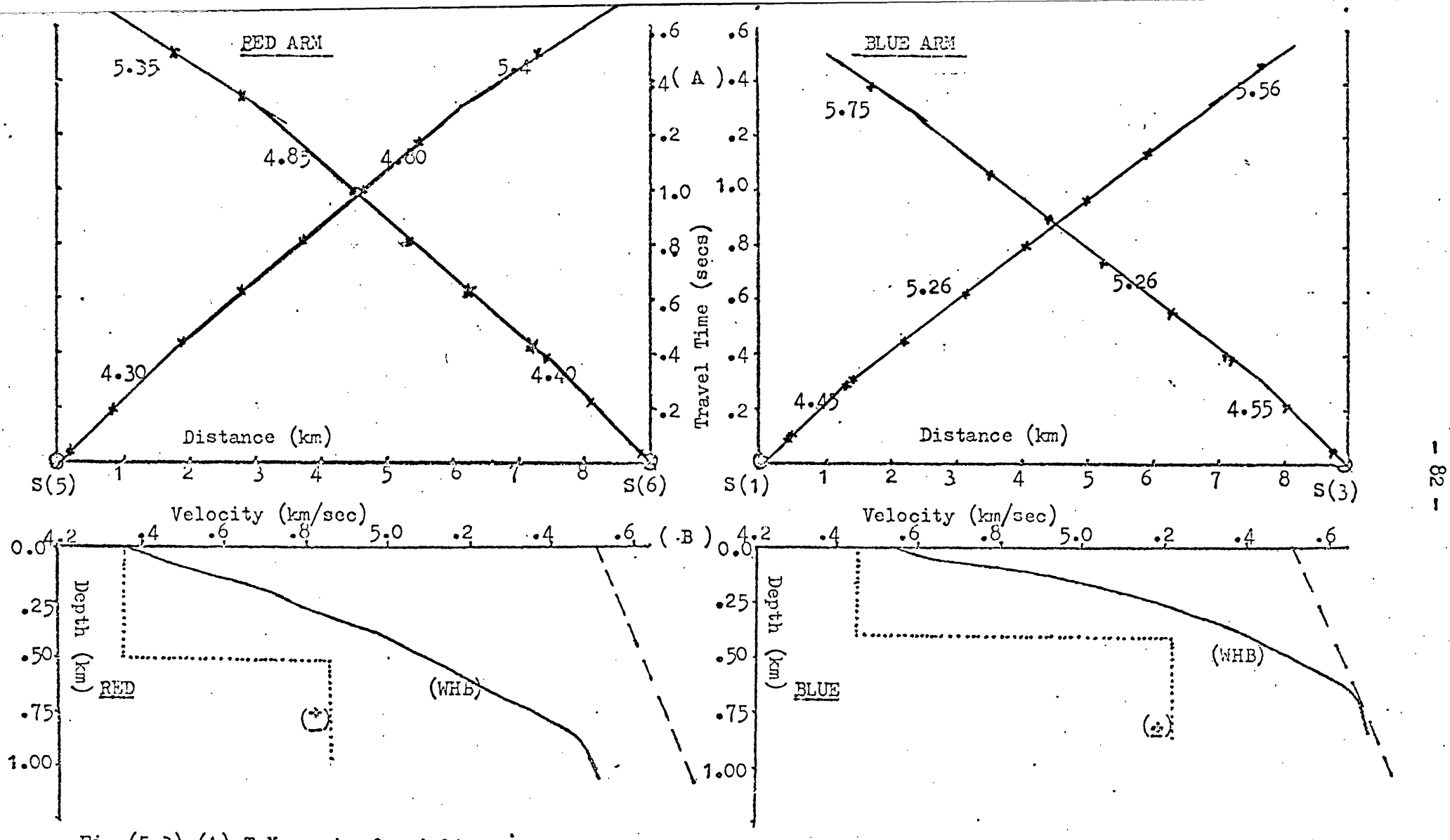

Fig.(5-3):(A) T-X graphs for inline shots, numbers on segments refer to their velocities in (km/sec);
(B) Velocity-Depth functions, dotted lines = (±) results, solid lines = WHB integral, dashed lines are Jacobs[31].

Pit	tA secs.	tB secs.	tAB =	K = 0.5 * $V_1/(1 - V_1^2/V_2^2)$ = 4.918	(-) value i.e. tA - tB - tAB	+ value = tA + tB - tAB	Depth to refractor = (K* (+) value) (km)
R_3	0.432	1.167	1.510 secs.		- 2.245	0.089	0.440
4	0.614	0.994			- 1.890	0.098	0.480
5	0.794	0.809			- 1.525	0.093	0.460
6	0.982	0.645			- 1.173	0.117	0.580
R_7	1.172	0.438			- 0.776	0.100	0.490

(a) Red arm, A = shot (5), B = shot (6)

V_1 = 4.35 km/sec., V_2 = 4.86 $\mp$ .02 km/sec.

B_4	0.277	0.919	1.109 sec.	K = 4.0425	- 1.751	0.087	0.350
5	0.466	0.740			- 1.383	0.097	0.390
6	0.637	0.560			- 1.032	0.088	0.360
B_7	0.824	0.402			- 0.687	0.117	0.470

(b) Blue arm: A = shot (1), B = shot (3)

V_1 = 4.45 km/sec., V_2 = 5.22 $\mp$ .02 km/sec.

Table (5-1): Results from $\mp$ method. Last column gives the depth to the refractor under different pits.

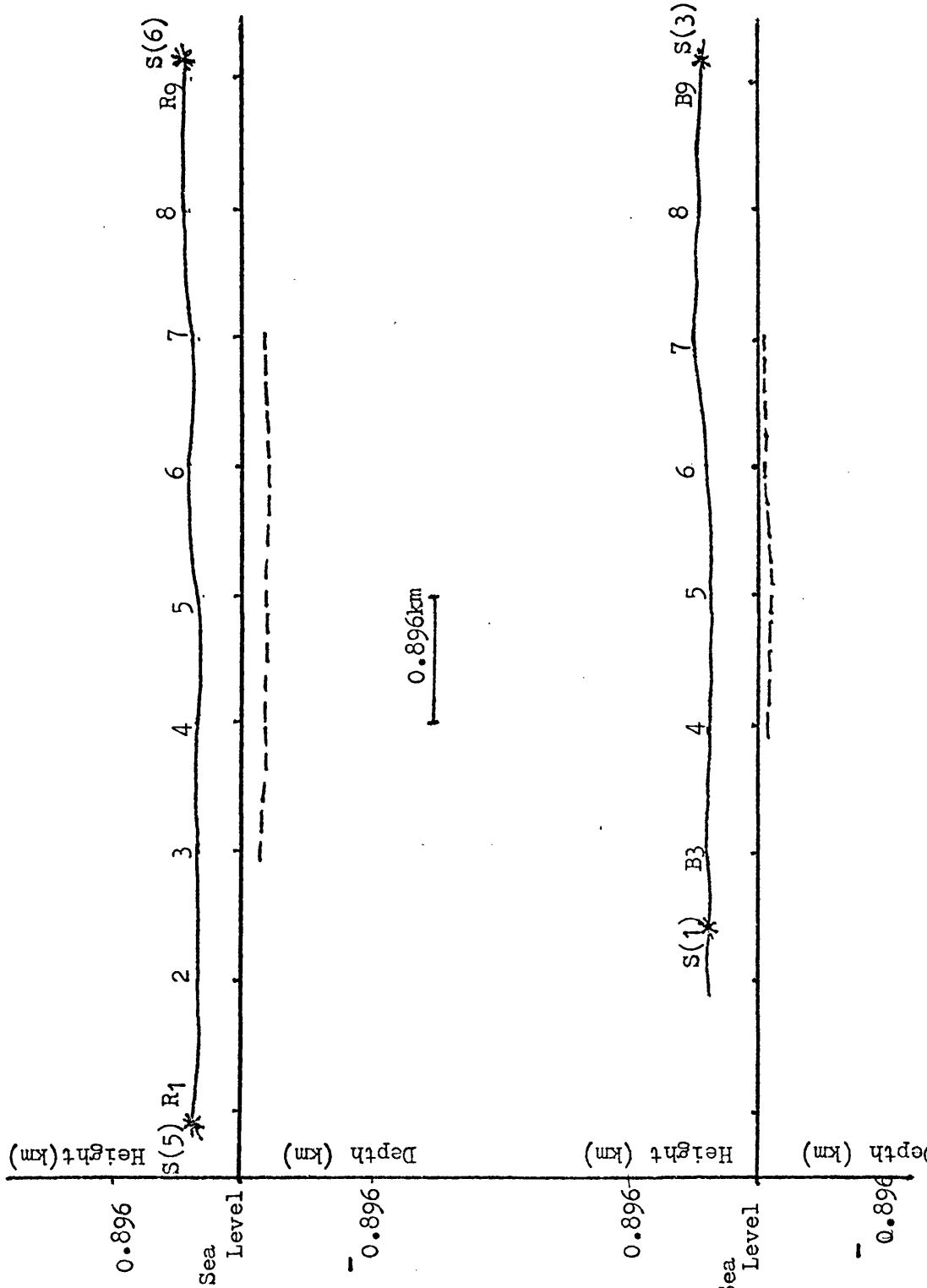

Fig.(5-4) Vertical section along the two arms showing depths to refractor under different pits as calculated through ($\pm$) method.

analyses are not met. Refractor depths under one arm cannot, strictly, be compared with those under the other when the velocities differ.

(2) From a reference datum the apparent amplitude of relief on the refractor is 66 m on Red and 58 m on Blue (table 5-2, col. 7) with a maximum apparent slopebetween adjacent seismometers of 4°. On the Red arm the refractor appears to be slightly deeper near the centre of the reversed spread (R5 & R6). The unreversed off-line ray paths cannot be used to add unambiguously to this pattern.

(3) The most sustained apparent slopeon the refractor is shown towards ESE along Red (Re to R6). This is little more than one degree. A dip in this sense would tend to produce both azimuth shifts and apparent velocity differences in the senses observed for arrivals from the northerly quadrants. The maximum azimuth shift i.e. arrival along strike with a 2° dip and a velocity contrast of 0.8 would, however, only be $1-2^{\circ}$ compared with $10-15^{\circ}$ observed. Similarly the maximum velocity difference would be about 2% compared with 10% observed (allowing for range).

(4) Corbishley (1970)[34] found from teleseisms i.e. arrivals at nearly vertical incidence that time delays between EKA Seismometers correlate with their elevations which is indicative of a surface layer velocity of 2.94 ± 1.3 km/sec. This is a low figure for the well-compacted rocks on which the seismometers are founded. Lack of original times combined with the wide seismometer spacing exclude the possibility of direct determination of near (tens of metres) surface velocities from

	Sea Level Datum		Elevation Difference from B4 (ED) (km)	Elevn. Delay (ED/V_1) secs at		Structure Difference from B6 (SD)(km)	Structure Delay SD $\frac{(V_2 - V_1)}{V_2 V_1}$ (secs) at V_2 = 5 km/sec V_1 = 4 km/sec	Structure & Elevn. Delays (secs) at V_1 = 4 km/sec V_2 = 5 km/sec	Difference from B4 (secs)
	Elevation km	Refractor depth km		3.0 km/sec	4.0 km/sec				
R_3	.322	- .118	+ .023	.008	.006	.096	.0048	.0108	.0093
4	.338	- .142	+ .039	.013	.010	.120	.0060	.0160	.0145
5	.307	- .153	+ .008	.003	.002	.131	.0066	.0086	.0071
6	.396	- .184	+ .097	.032	.024	.162	.0081	.0321	.0306
7	.348	- .142	+ .049	.016	.012	.120	.0060	.0180	.0165
B_4	.299	- .051	0	0	0	.029	.0015	.0015	0
5	.310	- .080	+ .011	.004	.003	.058	.0029	.0059	.0044
6	.338	- .022	+ .039	.013	.010	0	0	.0100	.0085
7	.436	- .034	+ .137	.036	.034	.012	.0006	.0346	.0331
Col. 1	2	3	4	5	6	7	8	9	10

Col. (5) - Col. (6) = .024 secs. ; Col. (5) - Col. (10) = 0

Table (5-2) Delay times at different pits assuming different velocities for the top layer.

the present measurements. It is found, however, that the algebraic sum of the differences in delays due to using a surface velocity of 4.0 rather than 3.0 km/sec. is cancelled by the additional delays introduced by the structure on the 5.0 km/sec. refractor taking an average figure and for this purpose assuming that depths under Red and Blue can be compared.

At less than vertical incidence and neglecting the effect of refractor dip (delay = $\Delta h \left(\frac{V2 - \sqrt{V2^2 - V1^2}}{V1 \sqrt{V2^2 - V1^2}}\right)$, delays due to variations in top layer thickness will be decreased by up to $\frac{1}{3}$ (at the critical angle), i.e. in the worst cases (B7 & R6 relative to B4) will lie between + 0.036 and 0.024 sec. Assuming critical angle refraction and elevation differences only, calculated apparent velocities, see Jacob (1969)[31] and Appendix (4) differed by up to 0.03 km/sec. from those found by neglecting the elevation effect entirely.

(B) Continuously Increasing Velocity with Depth

The data (Appendix 2 and Fig. (5-3A)) could be considered to represent sample points on smooth T-X curves instead of linearly segmented ones. The slightly greater apparent refractor depths under the middle of the Red arm could reflect the progressively decreasing T-X gradient. In-line shots at different ranges into the array arms would, in principle, resolve this ambiguity. Whilst these are not available, the increase in apparent velocity with range for more distant (20-150 km) sources, see Jacob (1969)[31] and Chapter VI, supports the continuous velocity variation model at

greater depth (3 to 10 km).

The inversion of a suitable T-X graph to yield the implied velocity depth function may be achieved by applying the Wiechert-Herglotz-Bateman (WHB) integral. This may be formulated as:

$$Z(v) = \frac{1}{\pi} \int_{0}^{\Delta} \cosh^{-1}\left(V \cdot \frac{dt}{dx}\right) .dx \quad \ldots\ldots\ldots (5\text{-}1)$$

Where $1/V = \left(\frac{dt}{dx}\right)$ $x = \Delta$, see Grant & West (1965)[64], p. 139.

The program used here for evaluating this integral is listed in Appendix (3). In-put to it requires a series of T-X sample points such that each successive time increment is less than the previous. Such series have been estimated from the in-line data for each array arm, see Appendix (3).

The results (Fig. (5-3B)) appear to indicate:

(1) a rapid (1.3 to 1.4 km/sec./km), though slightly decreasing rate of velocity increase over the first 0.7 to 0.9 km.

(2) a reduced rate (0.3 km/sec./km) near the limit of depth penetration (0.8 to 1.0 km).

(3) a greater velocity under the Blue array arm than under the Red at every depth within the range (+ 0.3 to 0.4 km/sec.).

These velocities, however, appear to be too high when compared with the refractor model. A simpler approach which allows the theoretical travel times to be calculated for comparison with the observations is to find the best value of linear rate of increase in velocity with depth (K) for each line taking the appropriate values of Vo i.e. 4.35 km/sec. for Red and 4.50 km/sec. for Blue. On this basis,

using equation (5-2) K was found to be about 0.8 km/sec./km for both arms.

The velocity-depth curve under EKA derived from the linear relation between apparent velocity and range ($20 \lesssim \Delta \lesssim 120$ km) extrapolated to zero range shows velocity increasing from 5.54 to 6.0 (or 6.2) km/sec. at a decreasing rate over the depth range 0 to 10 or 12 km, see Jacob (1969)[31] and Fig. (2-6A). This is in general agreement with laboratory measurements on greywackes over a range of pressure (5.4 km/sec. at 0.01 k bar to 6.13 km/sec. at 10 k bar, see Anderson & Liberman (1968)[65]. High initial rates of velocity increase have been found in granitic gneiss (1.0 km/sec./km) in the first 0.3 km, see Smithson & Shive (1975)[66]. These effects are considered to be due to the closure of cracks (joints, bedding, cleavage-fracture) under pressure, see Hall & Al-Haddad (1976)[67].

The velocity-depth curves derived here appear to join the curve found for greater depths at about 1 km below the surface (slightly greater under Red) (Fig. (5-3B)). The higher velocities under the Blue arm could be due to the orientation pattern of cracks, see Schenk & Schenkova (1974)[68]; thus more frequent cracks may be expected to be parallel with the steeply inclined bedding (strike 20° off Blue) and reduce, relatively, the velocity of paths across them (the Red arm lies at 70° to the strike). At depths over 3 km, however, where velocity increments with pressure become small (Fig. (2-6A)) such an azimuth effect should also be much reduced but see Chapter VI on apparent velocity variation with azimuth).

5.3.2 Azimuthal Velocity Variations

Whilst a T-X plot of all the data points (Fig. (5-5), 6 shots into 20 seismometers) shows a mean velocity of 5 ± 1 km/sec. with a possible 3 to 4 km/sec. top layer between 0 and 0.07 km thick, in-line measurements indicate higher velocities under the Blue than the Red arm. In off-line azimuths the travel times are, in general, known for only a single range along a particular line. In order to compare them the average linear rate of increase of velocity with depth (K = 0.8) has been used. On this basis the implied zero-depth velocity, Vo, has been calculated for each travel time, T, and range, X, from the equation:

$$Vo = \left(\frac{K.X}{2}\right) / \text{ Sinh } \left(\frac{TK}{2}\right) \quad \ldots\ldots\ldots\ldots\ldots (5\text{-}2),$$

see Nettleton (1940)[69], p. 259.

$$Vo = \left(\frac{K.X}{2}\right) / \text{ Sinh } \left(\frac{TK}{2}\right)$$

1940)[69], p. 259.

These velocities are plotted against ray azimuth from the geological strike direction (N 50 E - S 50 W) in Fig. (5-6) where some systematic variation becomes apparent when the Red and Blue seismometer points are treated separately and all points from ranges < 1.8 km are omitted. Each set of lines then shows a Vo range approaching 1 km/sec. between a minimum 70/80° and a maximum, best seen on Blue, 10/20 from the strike direction. The Blue set, however, lie about 1 km/sec. above Red representing differences, in the same sense for each shot, in the interpolated cross-over times. The mean cross-over time difference (Red-Blue) is 0.07 ± 0.005 sec. and the mean Vo difference is (-0.85 ± 0.05 km/sec.). Each difference depends only on relative arrival times at Red and Blue seismometers read from an analogue play-back of both onto the same chart. Errors here should not exceed ± 0.02 sec. and despite rechecking no explanation of the large and systematic difference

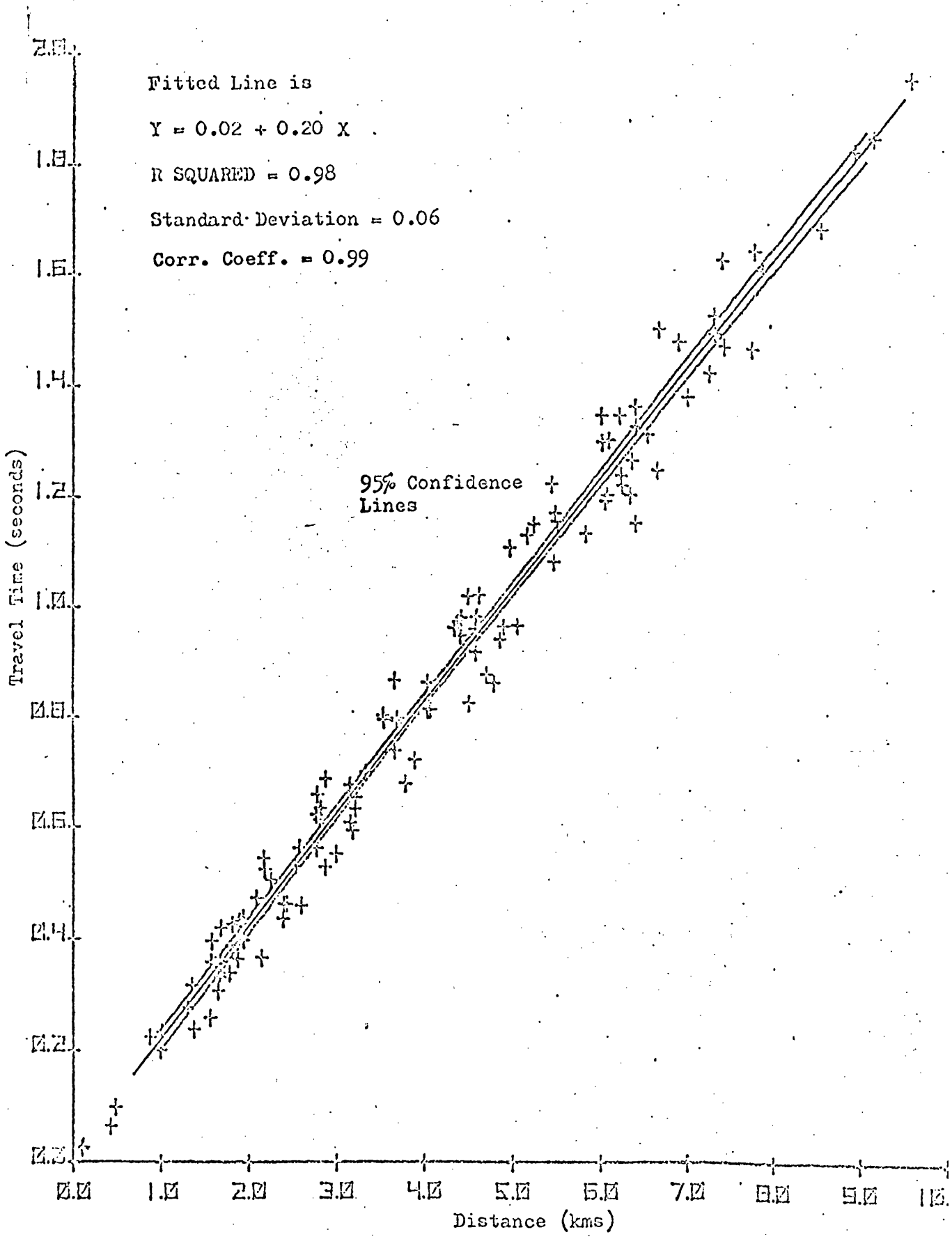

Fig. (5-5) T-X graph, all close shots.

Fig.(5-6) Velocity Vs. angle between geological strike (N50°E/S50°W) and ray path.
Solid lines = Blue seismometers,
Dashed " = Red "
$S_{1,..,6}$ = Shot 1,..,6.

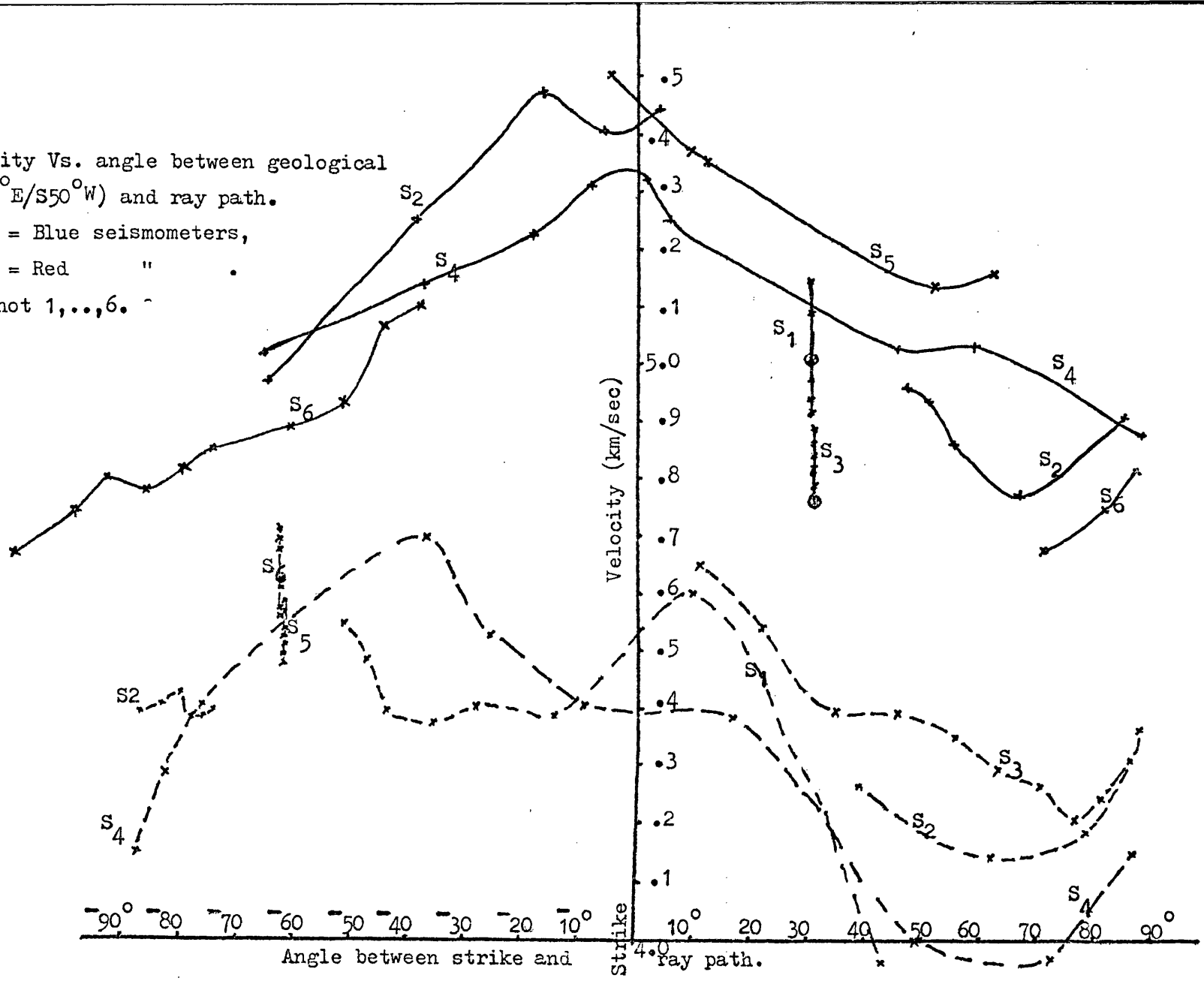

strike (N50°E/S50°W) and ray path.

Solid lines = Blue seismometer;

Dashed " = Red " ;

$S_{1,..,6}$ = Shot 1,..,6.

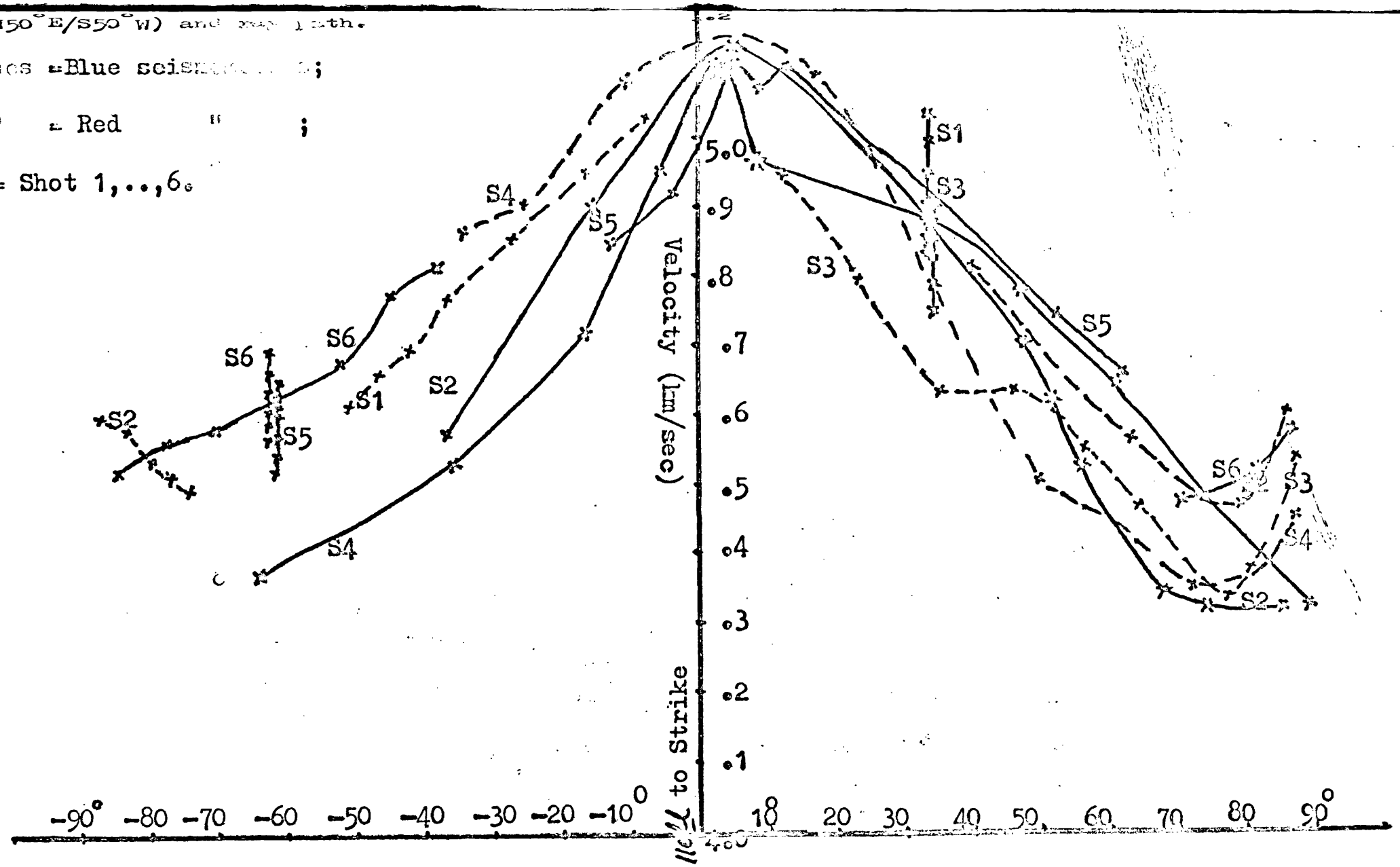

theoretical)

—— Observed

—·—· Theoretical curve showing the variations in qP velocity for propagation through transversely isotropic olivine scaled to an amplitude of 0.85 km/sec. After Crampin (1976)(82)

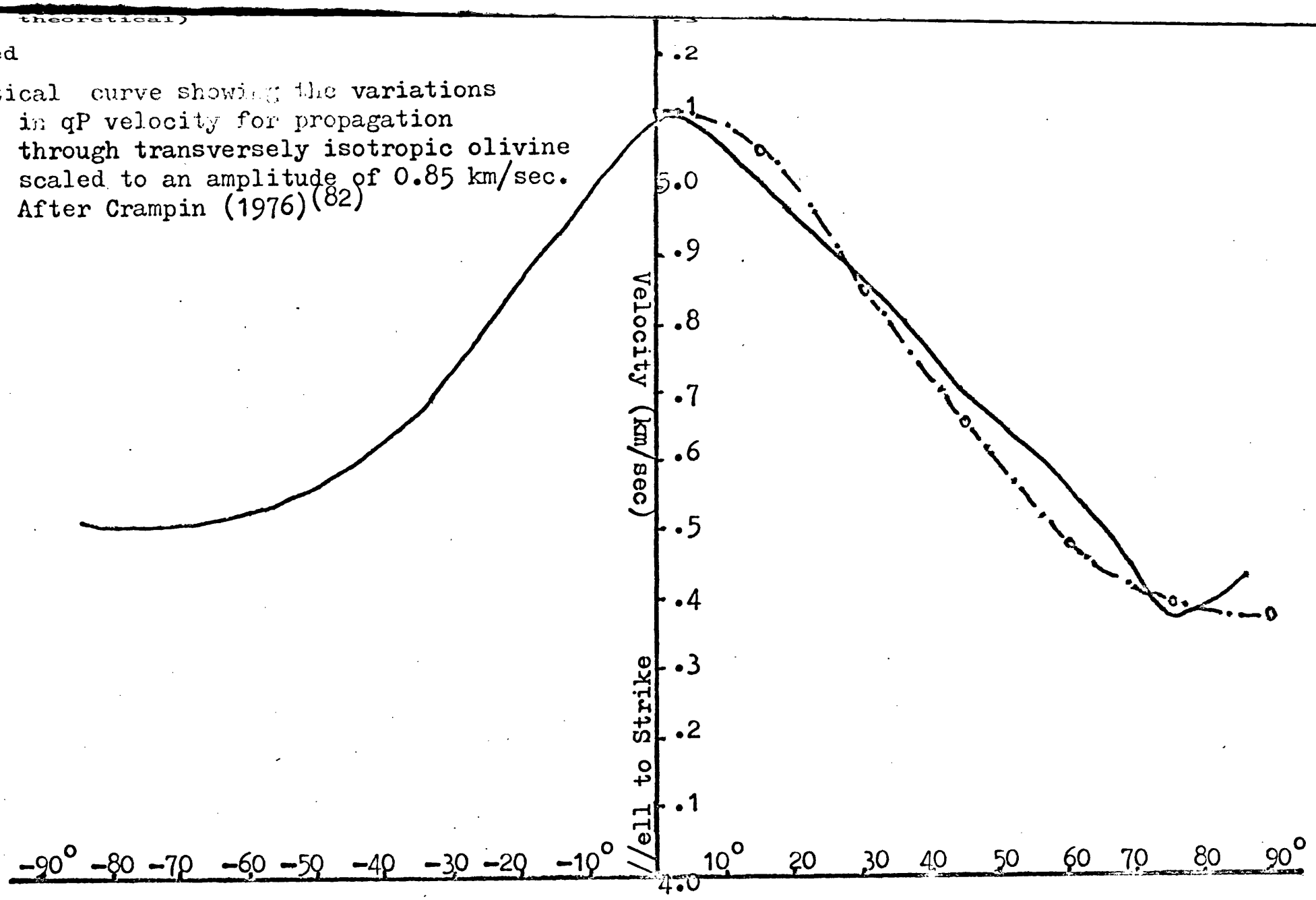

has been found. The most direct estimate of its value is given by the time differences on three reversed ray paths involving a Blue and Red seismometer + 0.123 ∓ 0.03 (Red-Blue). Estimates of Vo for one arm and one shot at constant azimuth are:

Shot 1 (Blue 5.03 ± 0.06 km/sec; shot 5 (Red) 4.60 ∓ 0.06 km/sec

Shot 3 " 4.89 ∓ 0.06 km/sec; shot 6 " 4.59 ∓ 0.06 km/sec

Mean = 4.96 ± 0.06 km/sec; Mean = 4.595 ∓ .6 km/sec

On reading the above, Dr. B. Jacob suggested that a misalignment of the tape heads on the I.G.S. (Edinburgh) playback system could have produced such a time difference. New analogue playbacks, provided by Dr. Thirlaway, from the original tapes at M.O.D., Blacknest have, in fact, confirmed this. For the fire shots (2, 3, 4, 5 & 6) of 7 September, the first arrivals for red on these new playbacks were found to average 0.05 sec. earlier, relative to Blue, than on the original playbacks. Relative to each other, arrival times on Red had not changed. The same applies to Blue. Since for shots 1, 3, 5 & 6 the origin times were estimated relative to either Blue (1 & 3) or Red (5 & 6) times, there has been no need to change the travel times used in Section 5.3.1. Similarly on Fig. (5-6) the in-line Vo values for these shots are unaffected. The ranges for each of these 4 sets of points are an indication of the uncertainties applicable to individual off-line points. For the off-line seismometer travel times, however, those from shots 1 & 3 into Red have been shortened by 0.05 sec. and those from shots 5 & 6 into Blue lengthened by 0.05 sec. in producing Fig. (5-6A). For shots 2 & 4, off-line with respect to both Red and Blue, the travel times have been shortened and lengthened by 0.025 sec. into Red and Blue respectively in the calculations of Vo for Fig. (5-6A).

To read travel times from Appendix (2), the origin times have now been taken as follows:

Shot(1)	Blue	13hr 06' 28.05"	Shot(2)	Blue	11hr 20' 02.45" - 0.025"
	Red	" " "		" " "	+ 0.025"
Shot(3)	Blue	13hr 48' 40.82"	Shot(4)	Blue	15hr 34' 45.10" - 0.025'
	Red	" " "		" " "	
(5)	Blue	17hr 24' 45.70"	Shot(6)	Blue	19hr 21' 46.75" - 0.05"
	Red	" " "		" " "	

Conclusions to be drawn from this analysis, Fig. (5-6A) are:

(1) Calculated as Vo, from eqn (5-2), where K = 0.8 km/sec/km, the velocity varies systematically with azimuth from a maximum around 5.1 km/sec parallel with the geological strike to a minimum around 4.4 km/sec normal to the strike. Towards the maximum range, where its effect is most, changing K by $\mp$ 0.1, affects Vo by not more than $\mp$ 0.03 km/sec so that this conclusion is not particularly sensitive to the rate of increase of velocity with depth, in fact, it is apparent in the uncorrected travel times (K = 0).

(2) An average variation derived as points at 10° azimuth intervals from averages of all the calculated points in those intervals is shown on Fig. (5-6B) in comparison with the theoretical variation in velocity for a transversity isotropic material (see Crampin (1976)[82], Fig. (2) for olivine parallel to (001) with the b & c axes randomly orientated) scaled to the same amplitude (.85).

(3) Anisotropy of this amount would produce wave front shifts up to 10° from the normals to ray paths in the sense shown on Fig. (6-3). The theoretical estimation of these shifts is based on the relationship given on page 106 which compares closely with that given by Crampin (1977)[83], Fig. (3) for the variation in angle (PHI1) between group velocity and propagation vector with propagation vector for qP in anisotropic material.

(4) The problem which arose because of the time difference between Red and Blue cross-over times have been explained by a misalignment of the heads of the replay system. Correction for this has not changed the data or conclusions about velocity variation with depth of Section (5.3.1) as these were based on time differences along either the Red or Blue arms.

CHAPTER VI

PRESENTATION OF RESULTS AND INTERPRETATION
ALL LOCAL EVENTS
EKA, BROUGHTON & LOWNET

6.1 Introduction

First P-arrivals of most local events, see map of Fig. (4-1), Appendix (1) and Chapter IV, were picked with an accuracy of $\mp$ 0.01 sec. and less than that for weak arrivals. Travel times and average velocities were calculated for all timed shots. A computer program " CLOSE ", see Appendix (4), designed to handle array data and makes allowance for the curvature of the wavefront and the altitude variation between the seismometers, has been used to calculate the apparent velocities and angles of approach (with accuracies of $\mp$ 0.002 km/sec. and $\mp 0.3^{o}$ respectively) for all local events received at Broughton and EKA. Since most of the sources lie within the distance ranges 20 km $\lesssim \Delta \lesssim$ 126.85 km and 20 km $\lesssim \Delta \lesssim$ 90 km from EKA and Broughton respectively, it is anticipated from previous work (table 6-1) that first arrivals at both arrays will be either P_g or P* except for a few possible P_n from over 130 km.

It should be mentioned that for these events linearly interpolated cross-over times from the Red and Blue arms agree to within the expected reading error, but that from Red is systematically later by up to 0.02 sec.

The results for each array (apparent velocities (Va), azimuth shifts ($\Delta\theta$)) are first considered separately. Travel times to both arrays and some LOWNET stations are considered together in a following section.

Phase	Southern Uplands		Midland Valley	
	Velocity(km/sec)	Range(km)	Velocity(km/sec)	Range(km)
P_g	5.8–6.0	20–80	5.93 ∓ 0.03	20–50
P*	6.7–6.9	80–130	6.4	50–90
P_n	7.9–8.1	130	$\sim$ 8	90

Table (6–1) Seismic crustal phases – their expected velocities and ranges at Broughton and EKA as seen from previous work, see references 21, 26 and 31.

6.2 EKA

6.2.1 Va Against Distance (Δ) and Azimuth (θ)

Apparent velocities, calculated by the program "CLOSE", for 62 events from 41 different source locations are plotted against distance in Fig. (6–1) More than one event has been recorded from 11 of these sources (linked points in Fig. (6–1)). These repetitions indicate an average standard deviation of about 0.06 km/sec. but may be twice that figure at low signal/noise ratios. With the exception of the natural events and a few marine shots (for which only a general location is known) distance errors are negligible. A linear regression through all the points suggests Va increases at 0.01 km/sec/km. The correlation coefficient (0.43) and standard deviation 0.4 km/sec. in conjunction with the expected errors ($<$ .12 km/sec.) indicate that Va varies at least as much due to other factors as it

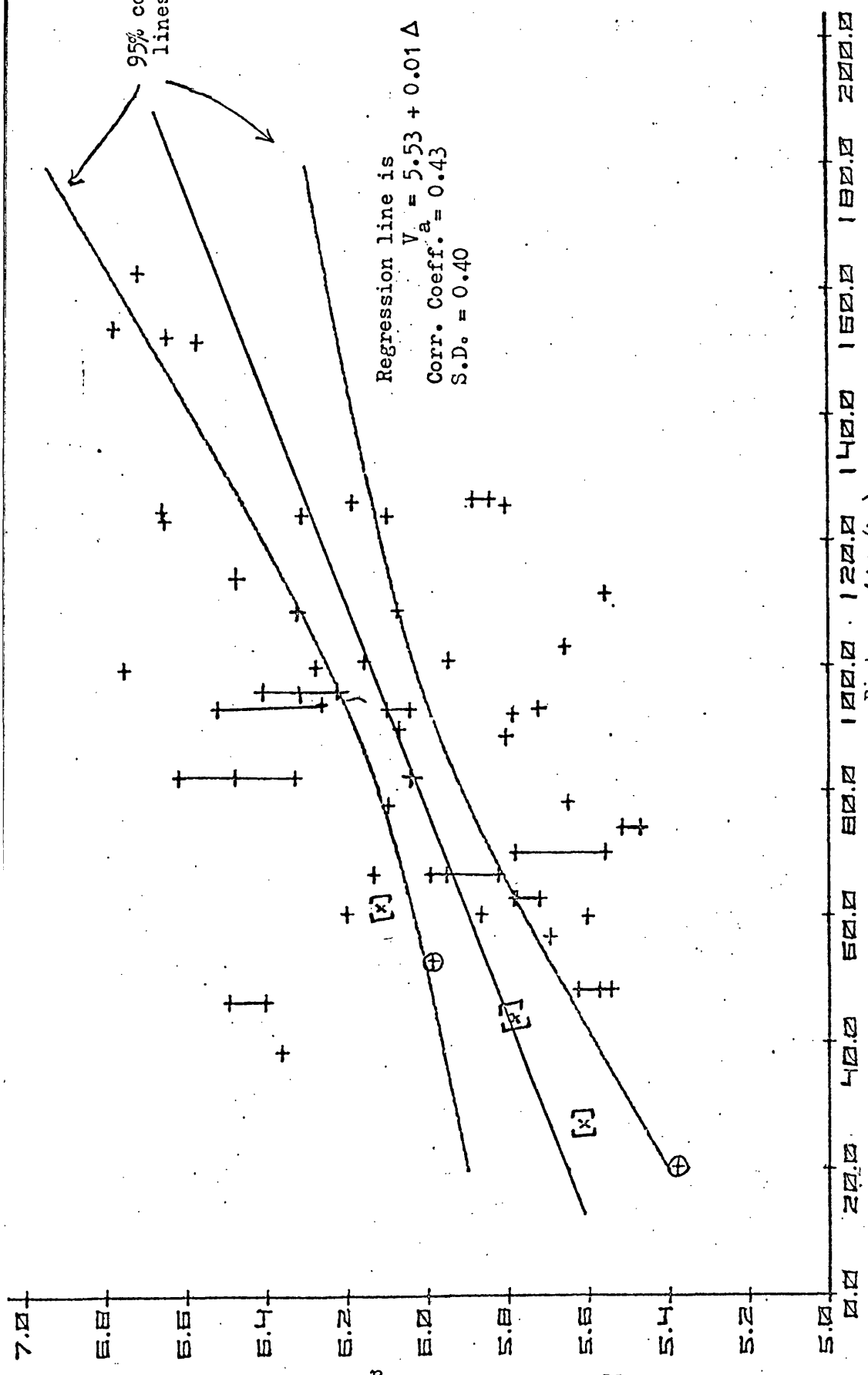

Fig. (6-1) Apparent velocity against distance for 62 events received at EKA. Repeats are linked and/or circled.
[x] Southern Uplands source received at Broughton, see Section (6.3.1)

does proportionally to distance. On a similar plot using different events but probably a few of the same sources, Jacob[31] recognised slow (5.5 - 6.0 km/sec.) and fast (6.44 km/sec. average) groups of 30 and 41 events respectively, with none in the 6.0 - 6.2 km/sec. interval, and fitted regression lines to each separately. Ten of the points on Fig (6-1), however, lie in this interval. Since the distance ranges of Jacob's fast and slow groups overlap it is no longer clear how to justify this separation. If the upper limit of the slow group is raised from 6.0 to 6.2 km/sec., a regression line through those points on Fig. (6-1) below that limit is, in fact, very close to that for Jacob's slow group but the correlation coefficient is not improved by comparison with taking all the events together and is considerably lower than that obtained by Jacob for the narrower velocity interval (0.43 compared with 0.78). It is concluded that more than half the variation in Va is still due to other factors than distance.

Despite the overlap in distance ranges between the fast and slow groups, where all are considered as first arrivals, Jacob proposed a model consisting of an increase in velocity with depth (5.5 to 6.0 km/sec.) to 12 km followed by a refractor having a velocity near the fast group average (6.4 km/sec.). To explain that the fast group sources approach closer to EKA along a NE-SW axis than a NW-SE one, he suggested that the refractor depth decreased with distance from EKA along the 'fast' axis and increased along the 'slow' one. Although the LISPB interpretation of a 6.4 km/sec. refractor limited to the Midland Valley at 7 km depth does not support this aspect of Jacob's model, the relationship on which it

was based is confirmed by the additional data reported here. In Fig. (6-2) a linear regression is drawn between apparent velocity and a function of azimuth i.e. the sine of the angle between arrival azimuth and a reference axis ($140^{\circ}/320^{\circ}$) which is approximately the normal to the trend of the Southern Uplands Fault and the Lower Palaeozoic structure. The correlation coefficient is 0.43 and the standard deviation 0.35 km/sec. The tendency for V_a to increase with range at constant azimuth can also be seen on this diagram. In this analysis events have only been limited to exclude those with $V_a > 6.9$ km/sec., i.e. $P_n \gg 6.9$ km/sec., see table (6-1). A few events from Jacob's paper for which the source azimuths could be identified have been included because they lie in otherwise unrepresented southerly quadrants i.e. they support the radial symmetry of the relationships. The azimuth of the LISPB line is shown on Fig. (6-2) and it appears in this orientation that 5.8 km/sec. $\lesssim V_a \lesssim$ 6.1 km/sec. i.e. the range of velocities which the LISPB interpretation assigns to the first 12 km under the Southern Uplands is restricted because of the orientation of the measurements.

6.2.2 Azimuthal Anomalies ($\Delta\theta$)

As mentioned earlier, in Section (5.1), it was found that waves travelling to EKA from different sources show azimuthal anomalies varying in sign and magnitude, where

Azimuth anomaly (shift) = (Direct - Calculated Propagation Vector)

Fig. (6-3) shows the relation between these anomalies and the direct

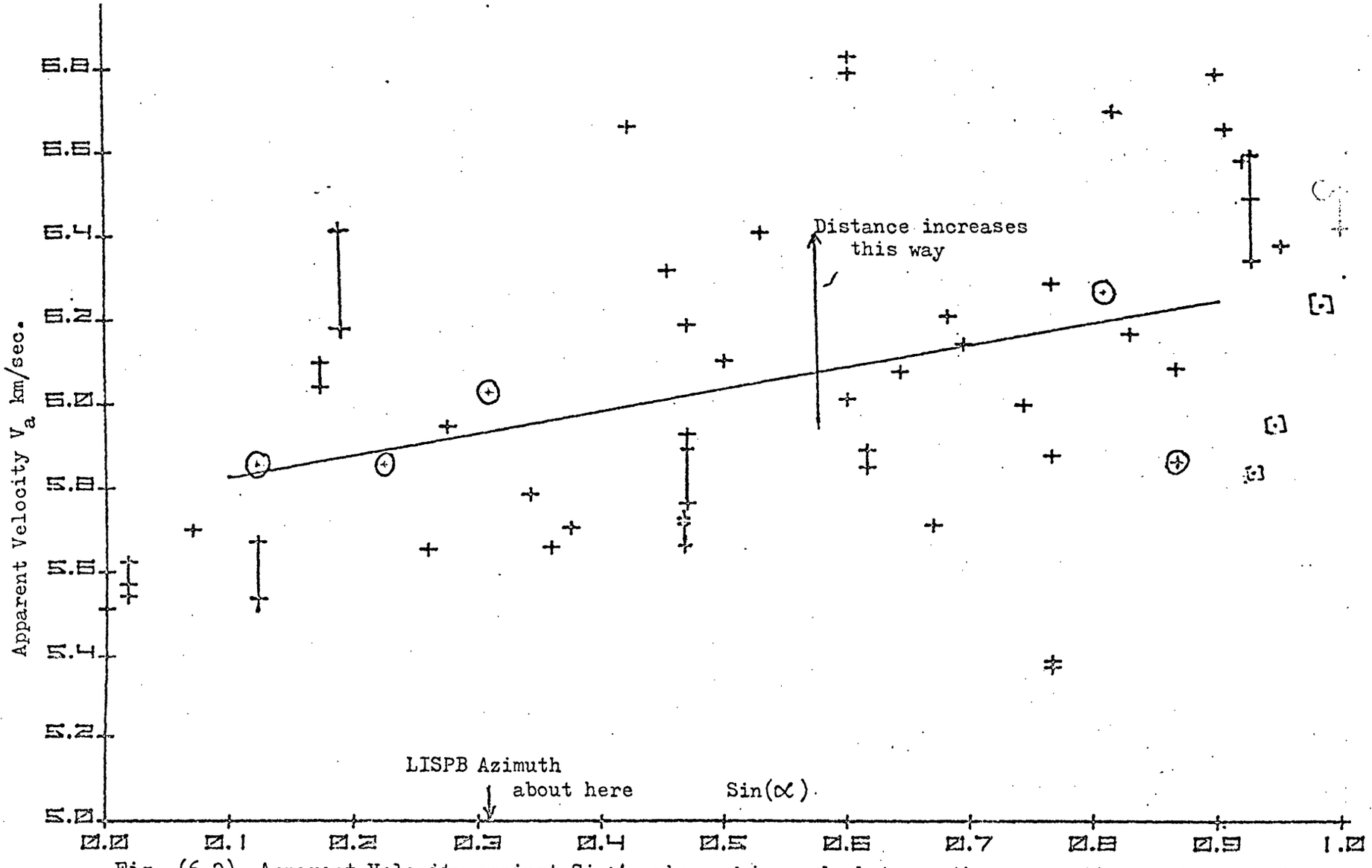

Fig. (6-2) Apparent Velocity against Sinα, whereα is angle between the propagation vector and the normal to the strike (140°/320°).
Regression line is V_a = 5.77 + 0.51 Sin , Corr. Coeff. = 0.43, S.D. = 0.35, ⊕ Points from Jacob's(31) data, [·] Southern Uplands source received at Broughton Array.

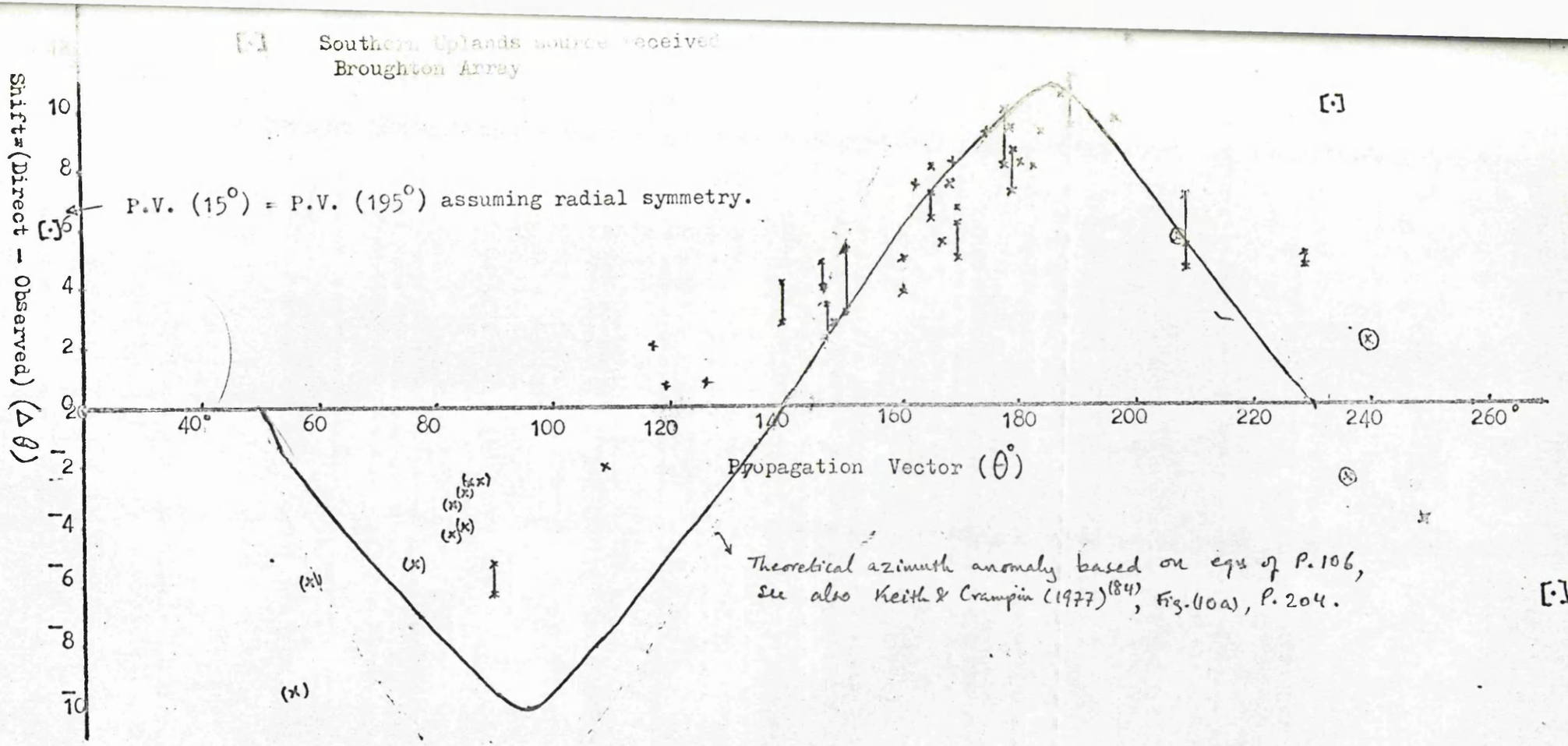

Fig. (6-3) Azimuth anomaly against propagation vector for all EKA local events

propagation vector (P.V.) as measured at the cross-over point of EKA, for all local events i.e. including all possible first-arrival phases, P_g, P* & P_n. It seems appropriate to include here rays from any depth, i.e. including P_n, since any azimuth anomalies they show may be produced by the velocity structure in a depth range common to them all.

The principal features of these observed anomalies are as follows:

(1) Seismic rays travelling at propagation vectors lying in the ranges 120° - 140° and 220° - 240° are not deflected, i.e. approximately normal and parallel to the geological strike.

(2) All rays with a propagation vector between about 130° - 230° seem to be deflected anti-clockwise. Deflection (shift) seems to increase systematically from 0° at about 130° (P.V.) into a maximum of about 11° somewhere around 180° (P.V.) and decreases afterwards.

(3) Rays travelling at propagation vectors less than 120° seem to be deflected clockwise. Deflection (shift) increases as propagation vector decreases, giving a maximum of -10° at about 55° (P.V.). Lack of data beyond that point makes the prediction of the state of the anomaly unresolved. On the other hand, the few points beyond 230° indicate a clockwise shift.

Azimuthal anomalies of different seismic waves have been observed, discussed and interpreted by different authors.

Otsuka (1966a)[70] observed azimuthal anomalies of some teleseisms recorded at the University of California network. These were found

to be cyclic functions of the direction of the source and with amplitude of 10^{o}. The author[70] discussed error sources and concluded that these anomalies cannot be attributed to measurement errors. In a following publication, Otsuka (1966b)[71] reported that the structural feature which is primarily responsible for these anomalies is located in the upper mantle within a depth of about 100 km. To account for these anomalies, the author[71] suggested a moderately dipping Moho underlain by a second deeper interface with a velocity decrease downward and with a steep dip towards the Ocean.

Niazi (1966)[72] reported that when a layer is overlying a half-space with a tilted interface, the refraction of seismic waves, from the half-space, generally results in their re-orientation away from the vertical plane of incidence with the following consequences:-

(1) The angle of emergence at the free surface will become azimuth dependent.

(2) The apparent direction of approach will be different from the true azimuth. The azimuthal variation also varies with azimuth.

The author[72] gave a mathematical formulation for the computation of apparent azimuth and the angle of incidence at the free surface and tabulated some numerical corrections to the observed apparent azimuth for a number of combinations of various dip angles and velocity contrasts.

Bolt & Nuttli (1966)[73] studied P-wave delay times at 12 California stations relative to Berkeley as functions of azimuth and computed best-fit sinusoids. In a later publication Nuttli & Bolt (1969)[74] concluded that variations in the depths to the top and bottom of the mantle low-velocity layer can account for the observed azimuthal anomalies.

Brown, Borg & Bath (1969)[75] studied apparent velocities in different azimuths and proposed a possible method of calculating true strike and dip of crustal boundaries. They developed a theory, partly for a sloping Moho only and partly for sloping Conrad and Moho with parallel strikes. They applied the theory to some observed P_n-arrivals and calculated the strike and dip of the Moho. They also concluded that if a sufficient number of P* arrivals can be observed, it would be possible to determine the strike and dip of the Conrad.

Ellis & Basham (1968)[76] reported azimuthal shifts as high as 18° from teleseisms recorded at four seismic stations in Central Alberta. They utilized Niazi's[72] approach to conclude that a (15° - 20°) dipping plane could explain such shifts.

From his studies of slowness and azimuth at the Uppsala Array, Brown (1973 a & b)[77,78] reported that near-surface lateral inhomogeneity was found from azimuth deviations to be small and equivalent to less than 3° dip on the Moho. He pointed out that to study the near-surface structure, azimuth is a better sounding parameter than slowness. In another publication, Brown (1973 c)[79] fitted sine curves to the travel time residuals of P-waves, from

teleseisms recorded at 13 Fennoscandian stations, with back azimuths as the independent variable. The result showed a clear regional trend towards apparently early arrivals from the north relative to those from the south. Ultimately the author[79] proposed two possible solutions

(1) systematic epicentral mislocation

(2) lateral inhomogeneity in P-velocity structure of the Fennoscandian crust and/or uppermost mantle.

In respect of EKA, however, since:

(1) for arrivals from $20 \leqslant \Delta \leqslant 150$ km i.e. approximately equivalent to depth penetrations ranging from 2 to 25 km, a consistent azimuth anomaly pattern is discernable (Fig. (6-3)),

(2) for arrivals in the velocity range $5.4 \leqslant v_a \leqslant 6.9$ km/sec, V_a tends to a maximum (6.28 km/sec.) along strikes and a minimum (5.71 km/sec.) normal to it i.e. a ratio of 0.92 which, in so far as data are available, appears to apply to all quadrants,

(3) for the close shot travel times a similar directional velocity variation (5.4 to 4.8 km/sec. as Vo on Blue (Fig. (5-6)) with a ratio of 0.88 km/sec.,

it seems likely and most economical of hypotheses to suggest that the azimuthal variation in propagation velocity (anisotropy) within the rocks under and around the array inferred from the close shot data is also responsible for the effects described on arrivals from more distant sources.

If it is considered that at any depth, Z , within these rocks that

the velocity, V_P, in the vertical plane (YZ) of the bedding is constant and greater than the velocity, V_N, normal to the bedding, then the seismic wavefronts should be considered as oblate spheroids rather than spheres. Then the azimuth, Φ, of the normal to the tangent plane at a point (x, y, z) on a wavefront surface is arctan $(Y. V_N^2/X. V_P^2)$ whereas that of the ray to the origin (source), Φ', is arctan (Y/X). Their difference $(\Phi' - \Phi)$ is then the apparent deflection or shift in the propagation vector. Under these assumptions these angles are independent of the vertical angle of approach. The shift, always towards the slow direction, would be up to 10° for $V_N/V_P = 0.85$. The assumed linear relationships between V_a and Δ, see Fig. (6-1), and V_a and sin (α), see Fig. (6-2) are likely to be biassed because not all azimuths are represented at all ranges. Such effects may be reduced if the V_a values are corrected for known variations in Vo, see Fig. (5-6), according to the relation:

$$\text{Sin (e)} = \frac{Vo}{V_a} = \frac{\bar{V}o}{\bar{V}_a}$$

Where "e" is the angle of emergence of a ray path. Taking Vo values from the Blue data shifted to a mean position between the Red and Blue points of Fig. (5-6), $(4.4 \lesssim Vo \lesssim 5.0$ km/sec.) a set of V_a values have been calculated for a mean $(\bar{V}o)$ value of 4.7 km/sec. For this purpose some of the events on Fig. (6-1) have been omitted. These are from sources over 50 km beyond the Southern Uplands Fault into the Midland Valley measured along their azimuths from EKA where the minimum time paths are likely to involve the 6.4 km/sec. basement (LISPB). One value from a nearer source (Duntilland, distance = 72 km) has been discarded as it is too low compared with two others from nearby and even compared with two from 20 km. Five of Jacob's

events from the south and one at short range from the west have been included on the Figure (6-3A). In fitting a regression line the two short range sources (< 20 km) have been excluded from the calculation. Its slope is now much less than in Fig. (6-1) and suggest a very slow rate of increase of velocity with depth (< 0.0030 km/sec./km) affecting ranges from 35 km out to 150 km. The initial rate of velocity increase with depth (0.8 km/sec./km), see Chapter V, could be maintained to a depth of about 1.6 km before reaching the 6.0 km/sec. value indicated at a range of 40 km, see Fig. (6-3A). The two arrivals from sources at about 20 km should then, but do not, reach this velocity.

It is, however, proposed that the apparent velocity with range variation into EKA taking azimuth into account is represented by Fig. (6-3A). If this is true, the seismic problem of recognising the presence or absence of a 6.4 km/sec. Midland Valley type basement under the Southern Uplands is not only difficult across strike (LISPB) but impossible along strike where such velocities are achieved within the Lower Palaeozoic.

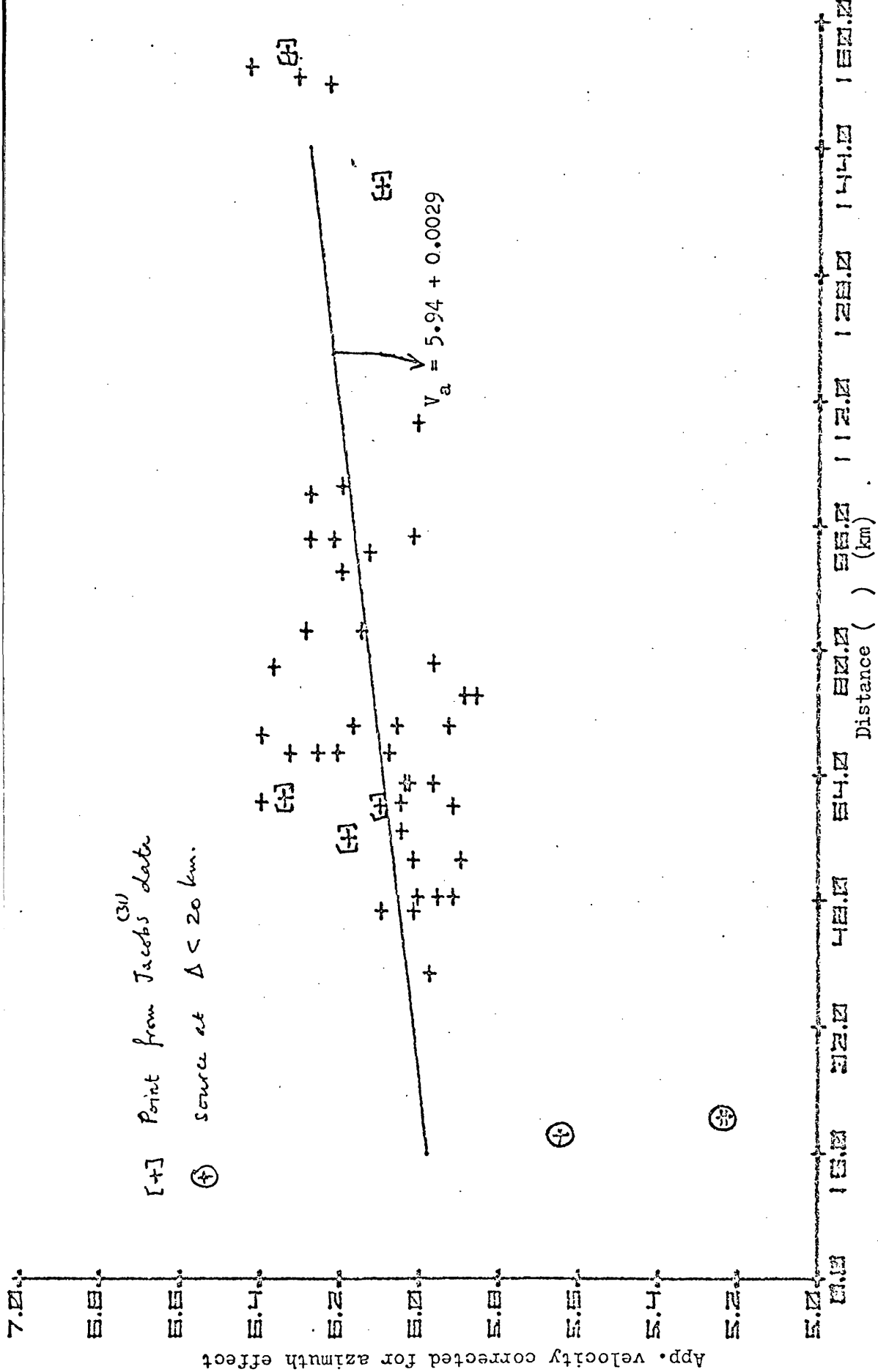

Fig. (6-3A) Apparent velocities corrected for azimuth effect against distance - EKA

6.3 Broughton Array

6.3.1 Apparent Velocity (V_a) against Distance (Δ)

Thirty events from 20 different sources are plotted in Fig. (6-4). The nine events which repeat a source (linked points) indicate a standard deviation of 0.08 km/sec. A least squares fit through all the points (Line 2) has a correlation coefficient of 0.79. The three abnormally low V_a values are for the only events originating within the Southern Uplands. Omitting these improves the correlation coefficient to (0.90) and shows V_a increasing at 0.024 km/sec./km from a projected 5.59 km/sec. at zero distance (Line 3). The standard deviation (0.1 km/sec.) is similar to that expected from repetitions of a source. The three events from the Southern Uplands (Line 1) suggest a parallel trend about 1 km/sec. slower. Plotted on Fig. (6-1) these three points are not as anomalous as they are on Fig. (6-4).

6.3.2 Apparent Velocity (V_a) against Propagation Vector (θ)

Taking all the points together, see Fig. (6-5), there is little apparent systematic variation. For the Southern Uplands' trio, that parallel with the strike has the highest V_a with the other two symmetrically disposed about it. Plotted on Fig. (6-2) these three points again are not anomalous.

Dividing those from the Midland Valley side of the array about the critical distance (50 km, see table (6-1)) suggests a possible minimum V_a normal to the strike for the longer range but not for the shorter range group.

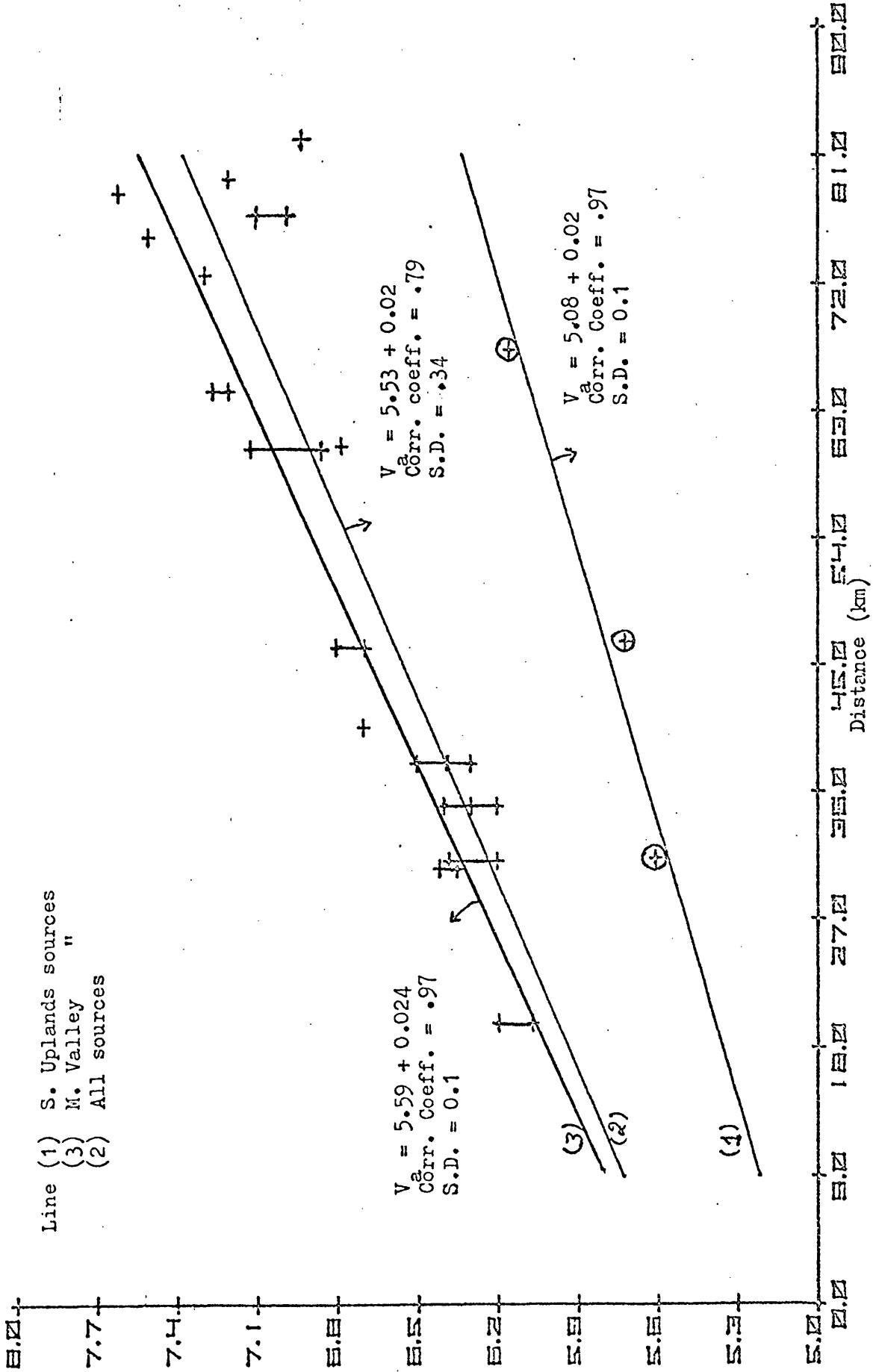

Fig. 7(6-4) Apparent velocity against distance for 30 local events received at Broughton Array.

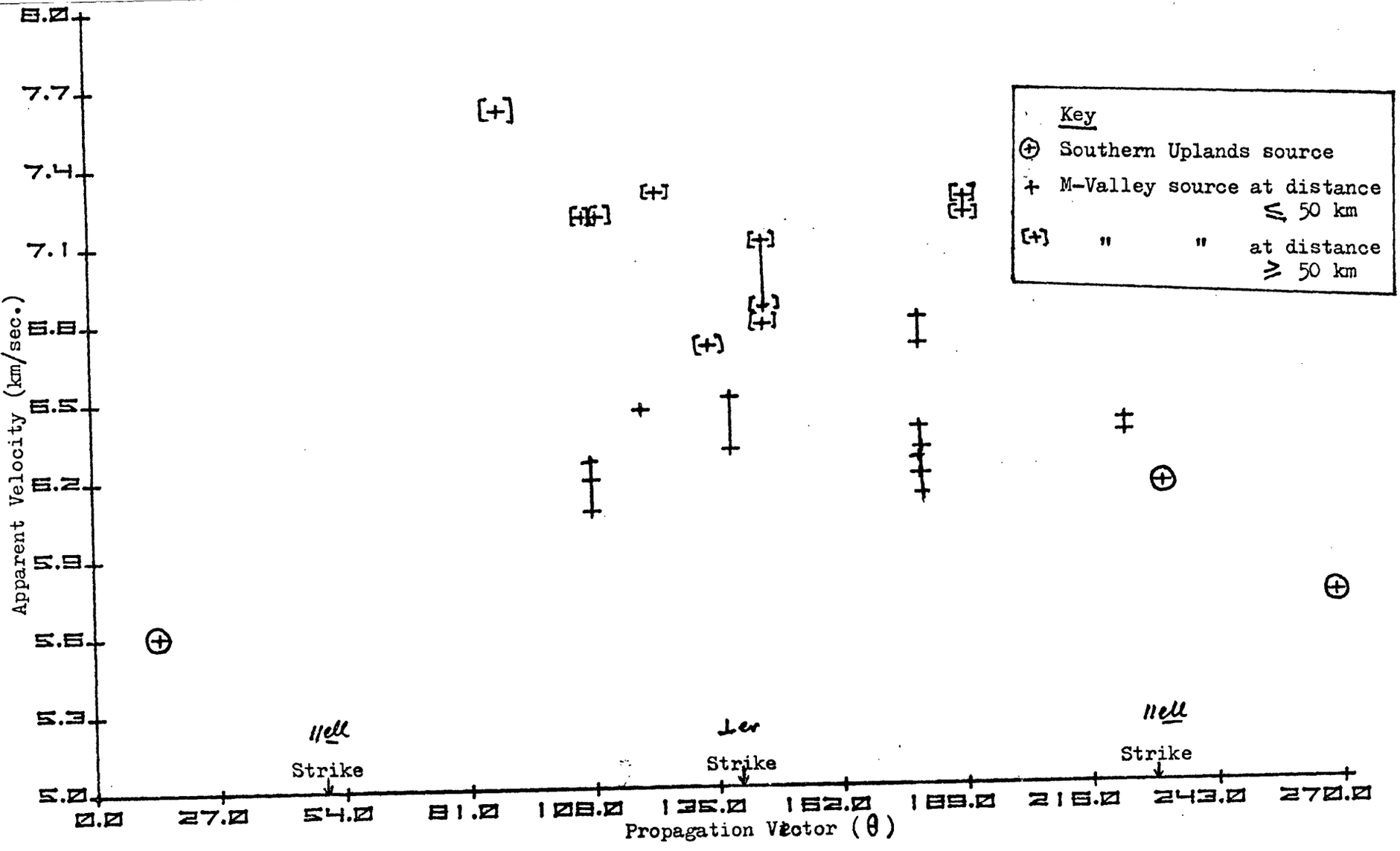

Fig. (6-5) Apparent velocity against propagation vector for events received at Broughton Array.

6.3.3 Azimuth Anomalies

Fig. (6-6) shows the relation between azimuth anomalies (as defined in Section (6.2.4)) and the propagation vector. One of the two most anomalous events is a Southern Uplands source and the other is a non-repeated 78.4 km distance quarry (Hillhouse). Taking all the points, there is no systematic anomaly change. Plotting the three Southern Uplands sources on Fig. (6-3), they seem to fit the Eskdalemuir pattern.

6.3.4 Conclusions and Comparison with EKA

When the apparent velocities measured at Broughton from Midland Valley sources are plotted over the lines representing the upper (parallel to strike, P) and lower (perpendicular to strike, N) velocity limits measured at EKA, see Fig. (6-7), it is clear that out to a range of 37 km, Broughton values lie within these limits. It is considered particularly significant that they lie very close to the parallel to strike value line at EKA. At EKA this direction lies in the plane of the essentially vertical bedding. Since the Lower Palaeozoic strata of the Midland Valley inliers are much less deformed than in the Southern Uplands, it is possible that the seismic waves from the north travel to Broughton also essentially in the plane of this bedding. At the same time this proposal explains the absence of azimuth anomaly at Broughton if this is to be associated with anisotropy along and across the bedding.

From 40 -- 80 km range, arrivals from the Midland Valley into Broughton have, without exception, higher apparent velocities than the fast limit into EKA from similar ranges. The alignment of the Broughton

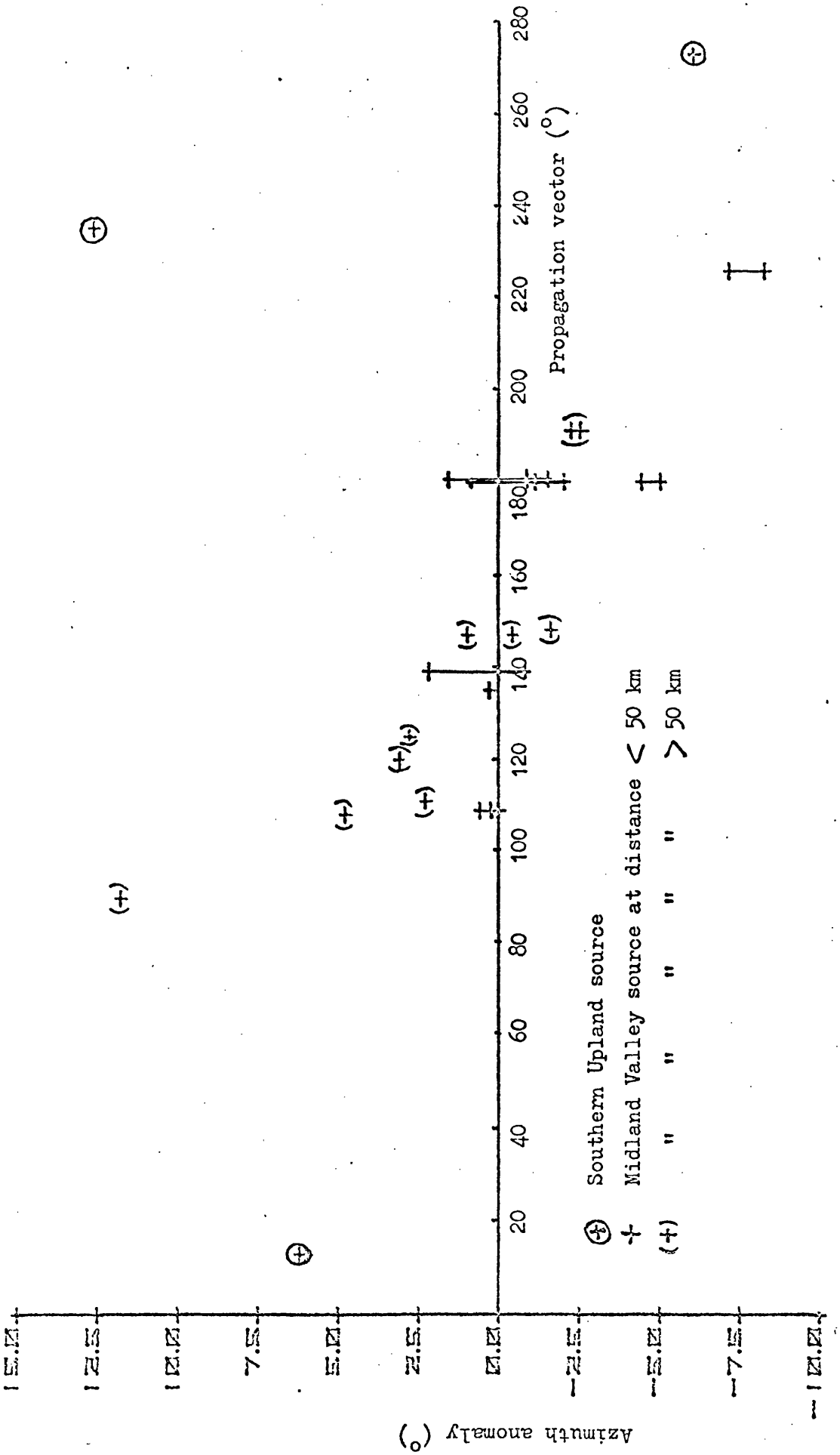

Fig. (6-6) Azimuth anomaly against propagation vector for 30 events received at Broughton

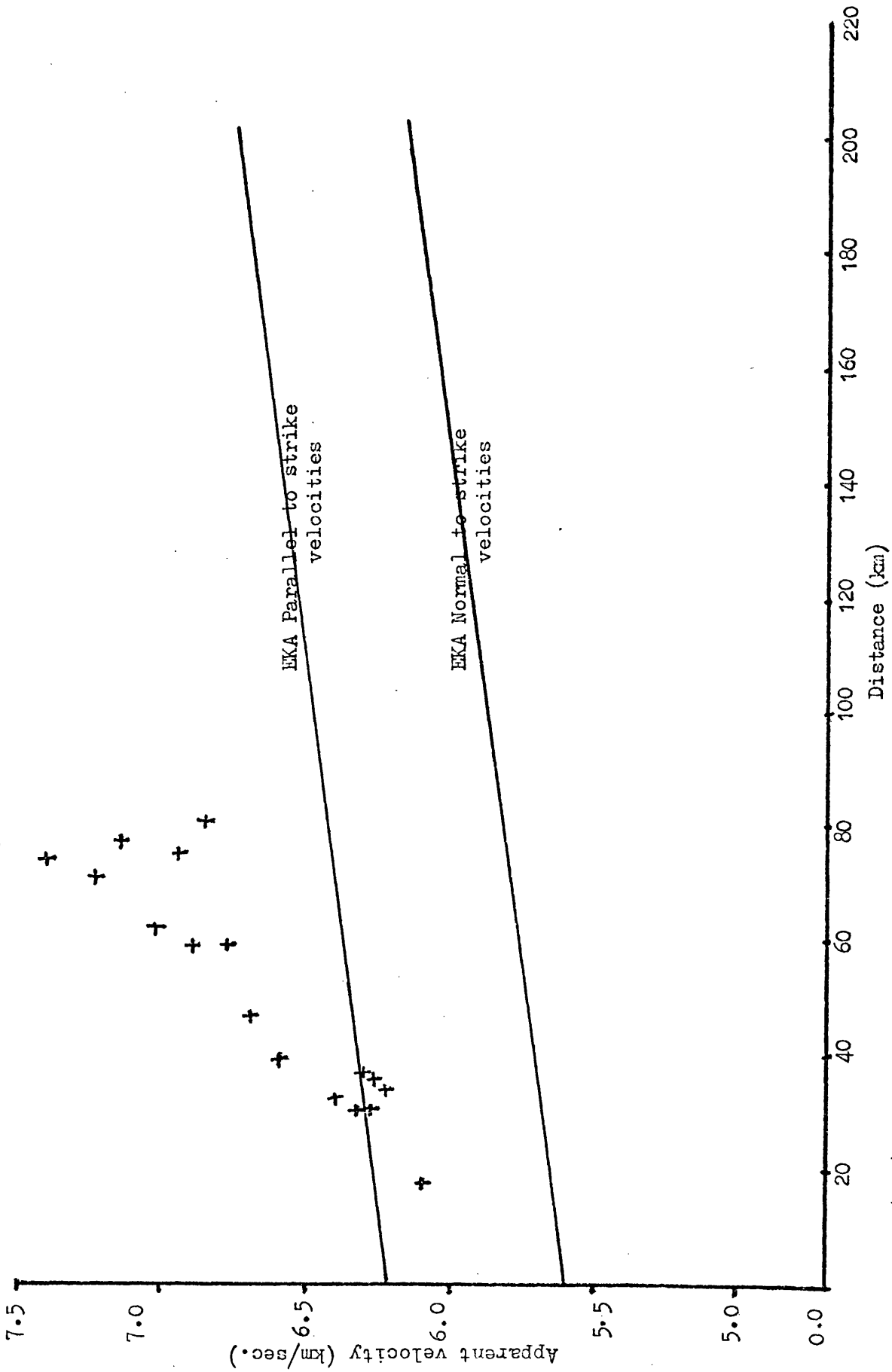

Fig. (6-7) Apparent velocities at Broughton compared with EKA velocities along strike and normal to it

events, Fig. (6-4) is probably fortuitous. The arrivals from $\Delta \leq 40$ km are better considered as refractions from a higher velocity basement (6.4 km/sec. at 7 - 8 km under the LISPB line) for which the critical distance is about right, see table (6-1). The apparent velocity values are, however, higher than expected from LISPB. As pointed out previously, the across strike orientation of the LISPB line in the Southern Uplands leads to velocities compatable with those deduced from the EKA measurements in that direction. As seen by LISPB the same velocity range (5.8 - 6.0 km/sec.), is found under the Midland Valley where it is again associated with Lower Palaeozoic rocks. At Broughton, however, velocities in this layer may range up to 6.3 km/sec. and the underlying basement velocities exceed 6.4 km/sec. These problems seem less severe than those which would be faced in accepting the high continuous rate of velocity increase with depth implied by the line on Fig. (6-4).

Dipping Interface(s) under Broughton Array

As an alternative, the rather high apparent velocities of waves received at Broughton Array from the Midland Valley side could have been magnified by approaching the array up-dip from the north. Considering an average solution where the 27 events of line 3, Fig. (6-4) are sub-divided into two groups, the first group includes 14 events at $\Delta \leq 40$ km, rays for which are unlikely to have reached the 6.4 km/sec basement. These have an average V_a of 6.32 ∓ 0.13 km/sec with a mean propagation vector of $162^\circ \mp 36^\circ$. The second group consists of 13 events at $\Delta > 40$ km with an average V_a of 6.92 ∓ 0.4 km/sec and a mean propagation vector of $143^\circ \mp 34^\circ$.

The indications of dipping plane effect are: (1) magnitude of V_a

(2) Azimuth shifts, shown on Fig. (6–6), is in reverse sense from EKA.

From the geological and seismic points of view, a dipping velocity structure in the vicinity of Broughton could be one of the following possibilities:–

(1) Relatively shallow boundary within the Lower Palaeozoic on which the array is situated with a velocity contrast base of " weathered " or fractured layer, cf. $\mp$ results of EKA close shots but with a dip towards the north.

(2) Upper Palaeozoic/Lower Palaeozoic discontinuity to the north of Southern Upland Fault around Biggar where the L.O.R.S. is seen at the outcrop. Such a discontinuity is unlikely to be deeper than 1km.

(3) Lower Palaeozoic/6.4 km/sec basement which is known to be at a depth of about 7–8 km.

If we consider a ray coming up from a refractor with velocity V_n (either 5.8 km/sec or 6.4 km/sec) through a refractor dipping with an angle (θ) and separating between two media with velocities V_o at the top and V_1 at the bottom then it can be easily shown that:

$$\tan(\theta) = \frac{V_o V_1/V_a - V_o V_1/V_n}{\frac{V_o}{V_n}\sqrt{V_n^2 - V_1^2} - \frac{V_1}{V_a}\sqrt{V_a^2 - V_o^2}} \qquad \longrightarrow (A)$$

Now if the first group arrive from the Lower Palaeozoic (5.8 km/sec) and the second group from the 6.4 km/sec basement, then a dipping interface towards $\frac{162^\circ + 143^\circ}{2} + 180^\circ = 332^\circ$ which will provide the V_a values, will have V_o & V_1 which satisfy

$$\tan(\theta) = \frac{V_o V_1/6.32 - V_o V_1/5.8}{\frac{V_o}{5.8}\sqrt{5.8^2 - V_1^2} - \frac{V_1}{6.32}\sqrt{6.32^2 - V_o^2}} = \frac{V_o V_1/6.92 - V_o V_1/6.4}{\frac{V_o}{6.4}\sqrt{6.4^2 - V_1^2} - \frac{V_1}{6.92}\sqrt{6.92^2 - V_o^2}}$$

which leads to a set of values of V_o & V_1. The maximum value of V_o

is 2.9 km/sec which leads to V_1 = 4.3 km/sec, i_c = 42.5° and θ = 5°. Such a refractor will have a depth less than 1 km in 10 km along dip.

Considering individual events from the first group, for example, Tams Loup is about 10° off true dip direction with V_a = 6.4 km/sec. This requires V_n to be about 6.0 km/sec to maintain a dip of about 5°. For Middleton which is about 75° off true dip direction, its 6.38 km/sec observed velocity requires also a 5° dip along its direction. It was found that, for this group, to satisfy equation A this requires (1) V_n is about 6.0 km/sec. (2) the dip of 5° of this shallow refractor to be maintained through the range of azimuths they span.

For the second group, i.e. arrivals from a refractor with V_n = 6.4 km/sec, those V_a's > 6.92 km/sec require a dip of not less than 5° with the specified V_0 & V_1. Since some of the strong events associate V_a > 7.0 km/sec with azimuths up to 60° from true updip direction (e.g. Hillhouse), this group also require a deeper interface (6.4 km/sec) with radiating dip in addition to the shallow one.

Therefore a model could be a choice of one or a combination of two of the following:

(1) Higher Lower Palaeozoic velocity than 5.8-6.0 km/sec.

(2) Higher basement velocity than 6.4 km/sec.

(3) Shallow dipping plane.

(4) Deeper dipping plane.

Until future work shows that shallow dipping plane exists or not or higher V_n values exist or not, the structure, as seen from this data, remains a choice between the above possibilities.

General Conclusion

Whilst the general proposition that the high average apparent velocities at Broughton may be due to a structural model involving true velocities consistent with LISPB/LOWNET is reasonable, there are complexities beyond a single dipping plane structure when the apparent velocities and azimuths of individual events are considered, i.e. almost certainly radiating dips and less certainly both a shallow and a deep interface.

With the present data such a model is, perhaps, to be preferred to one involving such high true velocities as Lower Palaeozoic $\bar{V}_a$ of 6.3 km/sec and basement $\bar{V}_a$ of 6.9 km/sec. The simplest way to choose between these alternatives would be a shallow refraction survey at the site of the Broughton Array.

6.4 Travel Times (EKA, Broughton & LOWNET)

Some preliminary calculations for simple models, in particular those describing velocity structure as continuous linear rates of velocity increase with depth have been made using the following equations

$$K = \frac{2}{x}\sqrt{V_a^2 - V_o^2} \quad \& \quad T = \frac{2}{K}\,\text{Sin h}^{-1}\,\frac{KX}{2V_o}$$

Where K is the velocity rate of increase in km/sec/km, V_o is the velocity, at the surface (zero depth), V_a is the apparent velocity, X is the horizontal distance and T is the travel time.

Assuming a mean surface velocity of 5.0 km/sec., K was calculated for each of 12 timed events recorded at EKA and from this their

Event's Name	Distance (km)	Apparent Velocity km/sec	Observed Tr. Time (sec)	Calctd. Tr. Time (sec)	Obs.-Calc (sec)	K km/sec/km
Craig Park	66.83	5.75	12.02	12.22	- 0.20	.05
Hillhouse	96.11	6.40	16.76	16.50	+ 0.26	.068
Boards Farm	93.31	6.52	16.59	16.90	- 0.31	.09
Cloburn	48.43	5.58	8.75	8.77	- 0.02	.04
Middleton	53.09	5.99	9.86	9.96	- 0.10	.124
Tams Loup	70.27	5.67	12.80	12.65	+ 0.15	.04
Kaimes	62.96	5.75	11.40	11.28	+ 0.12	.05
Douglasmuur	101.72	7.30	17.93	16.75	+ 0.18	.11
Murrayshall	99.63	6.70	17.90	17.87	+ 0.03	.09
Collace	126.85	6.0	21.91	22.42	- 0.51	.04
Loanhead	103.23	5.8	17.72	18.40	- 0.68	.04
Westfield	94.21	6.3	17.02	17.01	+ 0.01	.09

Table (6-2) Observed and theoretical travel times as calculated through a model with continuous linear increase of velocity with depth for timed events received at EKA.

travel times which show an average difference from the observed times of -0.09 sec., see table (6-2). The time differences between an assumed linear increase and Jacob's[31] non-linear function over his given velocity range 5.54 - 6.0 km/sec. for the top 12 km are only a few hundredth's of a second.

The timed events for which Figs. (6-3A) and (6-7) are supposed to apply cover a limited range of azimuths around the slow direction (108^{o} - 188^{o} (P.V.)). The low velocity gradient below a depth of 1.6 km suggests that travel times should match the apparent velocity of the refractor allowing for azimuth and delays in the top 1.6 km (0.33 sec). On this basis a mean $\bar{V}$ of 5.7 km/sec at a mean range of 57 km compares with an apparent velocity of 5.78 km/sec from Fig.(6-7).

Observed travel times into the Broughton Array and four LOWNET stations (GL, BL, AB & AU) from Midland Valley sources were compared with those calculated for the regional LOWNET model, see Section (2.4), for 12 events.

The mean difference (observed T.T. - calculated T.T.) at Broughton is $\bar{0}$ .24 sec., at (GL, BL, AU), also on the Southern Uplands Fault side of the Midland Valley, $\bar{0}$.23 sec. and for (AB) on the north side by the Highland Boundary Fault, $\bar{}$0.20 sec. It is concluded that the average velocity structure approaching Broughton is not significantly different from that approaching the quoted LOWNET stations.

Calculated travel times into Broughton based on K values (from measured V_a's and an assumed V_o = 5 km/sec.) have an average closer to the observed than those from the LOWNET model (0.09 sec. compared with $\bar{}$0.24 sec.) The rates of continuous vertical increase of velocity with depth (K $\approx$ 0.2 - 0.25 km/sec./km) are quite high.

The continuity of velocity increase with depth to below 7 - 8 km implied by the line of Fig. (6-4), however, has been rejected and the alignment of the Broughton points in the range 20 - 38 km suggests a low rate, see Fig. (6-7) (on EKA limit lines) in presumably the Lower Palaeozoic rocks above the basement. In the absence of shorter range data (20 km) there is little point in elaborating the model. Some continuous though non-linear function of velocity increase with depth from Old Red Sandstone into the underlying Lower Palaeozoic would, however, be consistent with the geologically observed gradation between them.

6.5 Conclusions

(1) Velocities in the Lower Palaeozoic rocks of the Southern Uplands are seen both from the close shots and the local events to vary from a maximum along a direction parallel to bedding (strike) and to a minimum at right angles. The ratio between these velocities is similar in both cases. This magnitude of anisotropy will provide azimuth anomalies of the observed magnitude and pattern.

(2) The velocity appears to increase rapidly (about 0.8 km/sec./km) down to a depth of 1 - 1.5 km and thereafter at a very slow rate of about 0.003 km/sec./km.

(3) This indicates along strike velocities in the Southern Uplands, approaching that of the 6.4 km/sec. refractor under the Midland Valley, at a range of about 75 km.

(4) The rather high apparent velocities measured at Broughton from the Midland Valley side may generally propose a structural model involving velocities consistent with LISPB & LOWNET with the existence of a shallow 4.3 km/sec refractor under

Broughton with a radiating dip of about 5° maintained through a wide azimuth range.

(5) If such a structure does not exist under Broughton area, then those high velocities from the Midland Valley side, which seem to agree with the along strike i.e. in the plane of the bedding velocities in the Southern Uplands, together with absence of systematic azimuth anomalies seem to be consistent with the Lower Palaeozoic structure under the Midland Valley being on average sub-horizontal. There the velocity of this refractor and the underlying basement appear to be greater than those found by LISPB.

(6) On the evidence presented here it is considered that the velocity of P waves within the Lower Palaeozoic rocks around EKA not only increases with depth but also varies with azimuth. Similar anisotropy dependent upon the attitude of the bedding in these rocks is to be expected elsewhere in the Southern Uplands and needs to be investigated before a complete interpretation of a seismic profile in any single azimuth can be achieved. Since it is not known whether the shallow structure under Broughton is a sufficient cause for the high apparent velocities observed there, it is recommended that this structure should be determined here and, routinely during future array work in the region. Until this point is resolved at Broughton the results there cannot be used to say how important it is to use arrays rather than linear profiles in seismically investigating the Lower Palaeozoic basement interface under the Midland Valley.

APPENDIX (1)

List of all source events received at EKA, Broughton and some/all LOWNET sensors.
X indicates that the event has been received at that station. Known origin times are either recorded (R) or calculated (C) through LOWNET. Origin times of the first 6 events were calculated without LOWNET.
X* indicates that the event has been received weekly at that station. Q = Quarry, N.E. = Natural Event.
Some of these events were repeated, see Appendices (5) and (6)

No.	Date	Event's Name	Coordinates	Origin Time			Received At						
				hr. m. sec.	C	R	EKA	Broughton	LOWNET EDI	AU	BH	GL	BL
(1)	8.6.76	EKA Shot(1)	325.920/603.530	13 06 28.05	X		X	-	-	-	-	-	-
(2)	6.9.76	" " (2)	325.250/605.510	11 20 02.50	X		X	-	-	-	-	-	-
(3)	6.9.76	" " (3)	328.150/609.100	13 48 40.82	X		X	-	-	-	-	-	-
(4)	6.9.76	" " (4)	328.750/605.830	15 34 45.10	X		X	-	-	-	-	-	-
(5)	6.9.76	" " (5)	325.250/605.510	17 24 45.70	X		X	-	-	-	-	-	-
(6)	6.9.76	" " (6)	332.140/602.710	19 21 46.75	X		X	-	-	-	-	-	-
(7)	3.2.77	Murrayshall Q	277.250/691.450	16 09 08.50		X	X*	X*	X	X	-	X*	X*

APPENDIX (1) (Contd.)

No.	Date	Event's Name	Coordinates	Origin Time hr. m. sec.	C	R	Received At EKA	Broughton	LOWNET EDI	AU	BH	GL	BL
(8)	9.2.77	Dumbuckhill	242.030/674.660	12 12 05.95		X	X*	X*	X*	X	-	X*	X*
(9)	10.2.77	Douglasmuir	252.400/674.780	12 49 38.66		X	X*	X*	-	-	-	-	-
(10)	14.2.77	Kaimes	313.12 /666.4	16 22 26.51		X	X*	X	X	X	-	X*	X
(11)	15.2.77	Tams Loup	288.230/663.780	12 57 51.41		X	X	X	X	X	_	X	X
(12)	23.2.77	Craig Park	312.720/670.280	16 45 32.57		X	X	X	X	X	X	X	X
(13)	10.3.77	Middleton	334.500/657.400	15 00 06.19		X	X	X	X	X	-	X	X
(14)	10.3.77	Boards Farm	279.450/685.430	17 07 11.11		X	X*	X*	X*	-	-	X*	X*
(15)	11.3.77	Craig Park	312.750/670.280	16 45 54.54		X	X	X	X	X	X	X	X
(16)	14.3.77	Cruicks	313.040/681.550	13 04 51.73		X	-	X	X	X	-	X	X

APPENDIX (1) (Contd.)

No.	Date	Event's Name	Coordinates	Origin Time hr. m. sec.	C	R	Received At EKA	Broughton	LOWNET EDI	AU	BH	GL	BL
(17)	16.3.77	Cloburn	294.710/641.350	12 28 49.01		X	X	X	X	X	X	X	X
(18)	16.3.77	Duntilland	284.240/663.560	14 52 59.86		X	X	X	-	-	-	-	-
(19)	25.3.77	Hillhouse	235.000/634.000	11 08 12.19		X	X	X	-	X	X	X	X
(20)	30.3.77	Westfield	321.260/699.280	14 26 54.80		X	X	X	X	X	X	X	X
(21)	30.3.77	Craig Park	312.670/670.280	15 39 56.70		X	X	X	X	X	X	X	X
(22)	1.4.77	Loanhead	236.580/655.420	11 03 21.45		X	X*	X*	-	-	X	-	-
(23)	6.4.77	Cloburn	294.600/641.330	11 32 40.09		X	X	X	X	X	X	X	X
(24)	28.4.77	Collace	320.960/731.610	19 03 33.00		X	X	-	X	X	X	X	X
(25)	11.2.77	Northfield	279.8 /685.420				X	X					

APPENDIX (1) (Contd.)

No.	Date	Event's Name	Coordinates	Origin Time hr. m. sec.	C	R	Received At EKA	Broughton	LOWNET EDI	AU	BH	GL	BL
(26)	23.3.77	Oxwellmains	366.2 /677.0				X	X					
(27)	25.12.77	Goat	317.450/686.800				X	X					
(28)	7.4.77	Craighouse	361.5 /635.5				X	X					
(29)	30.3.77	L*					X	X					
(30)	18.2.77	U/W					X	X					
(31)	14.4.77	Dunion	55.463°N/2.592°W				X	X					
(32)	16.2.77	Coatsgate	55.3333°N 3.4742°W				X	X					
(33)	3.5.74	Cairney Hill	285.30 /666.50	15 45 00.1	X		X						
(34)	23.5.74	Dollar NE	56.1422°N 3.615°W	18 35 00.9	X		X						

APPENDIX (1) (Contd.)

No.	Date	Event's Name	Coordinates	Origin Time hr. m. sec.	C	R	Received At EKA	Broughton	LOWNET EDI	AU	BH	GL	BL
(35)	10.5.74	Frairton Quarry	309·0 /723·0	15 43 25.9	X		X						
(36)	15.4.74	Newbattle	55.8725°N 3.077°W	23 04 54.6	X		X						
(37)	4.3.69	Rosewell NE·	329.06 /661.9	19 14 08.2	X		X						
(38)	18.9.69	Midlothian NE	332.8 /661.0	03 43 11.60	X		X						
(39)	6.7.76	Navy Shot(1)	356.2 /701.2				X						
(40)	23.6.76	Navy Shot(2)	365.0 /706.7				X						
(41)	7.5.74	NE·	295.0 /713.0				X						
(42)	29.4.74	NE·	297.5 /683.0	21 19 46.4	X		X						

APPENDIX (1) (Contd.)

No.	Date	Event's Name	Coordinates	Origin Time hr. m. sec.	C	R	Received At EKA	Broughton	LOWNET EDI	AU	BH	GL	BL
(43)	27.6.69	Dollar N.E.	305.0 /681.0				X						
(44)	27.6.69	Dollar N.E.	294.5 /693.0				X						
(45)	25.12.69	Midlothian N.E.	330.5 /672.0				X						
(46)	15.4.71	Glenalmond	295.0 /727.0				X						
(47)	17.4.71	Glenalmond	297.0 /727.2				X						
(48)	22.4.71	Glenalmond	295.7 /725.0				X						
(49)	7.9.76	Navy shot (I.M.)	369.0 /695.0				X						
(50)	8.4.71	Loch Awe	194.0 /713.5				X						

Appendix (2)

Dates and Arrival Times of EKA close shots

Shot No. & Date	Arrival times at																			
	R_1	2	3	4	5	6	7	8	9	R_{11}	B_1	2	3	4	5	6	7	8	9	B_{11}
(1)	13 hr 06' 28.0" +																			
8.6.76	.45	.41	.52	.67	.85	1.02	1.20	1.35	1.66		.33	.12	.15	.32	.51	.68	.86	1.12	1.19	1.52
(2)	11 hr 20' 02.0" +																			
6.9.76	.93	1.03	1.16	1.31	1.46	1.63	1.80	1.98	2.15	2.46	1.47	1.32	1.16	1.03	.90	.83	.84	.94	1.01	1.36
(3)	13 hr 48' 41.0" +																			
6.9.76	.78	.77	.80	.84	.93	1.05	1.17	1.32	1.45	1.65	1.24	1.09	.90	.74	.51	.39	.22	.05	.15	.21
(4)	15 hr 34' 45.0" +																			
6.9.76	.80	.66	.54	.46	.52	.65	.79	.97	1.12	1.45	.98	.82	.70	.56	.46	.43	.50	.56	.73	.04
(5)	17 hr 24' 45.0" +																			
6.9.76	.72	.90	1.13	1.31	1.49	1.68	1.87	2.06	2.23	2.56	1.31	1.16	1.01	.93	.96	1.07	1.23	1.38	1.53	1.85
(6)	19 hr 21' 47.0" +																			
6.9.76	1.25	1.08	.91	.73	.55	.39	.18	.02	.22	.11	1.0	.95	.98	.94	.96	.99	1.06	1.13	1.22	1.44

APPENDIX (3)

This program was used for the inversion of the T-X data for the inline shots of Chapter V and is based on Wiechert-Herglotz-Bateman integral, see Grant & West (1965)[64] p. 139. Input to it are travel times and distances. Output are velocities and depths, see Fig. (5-3B).

```
******* WATFIV BATCH JOB ************************************************
******* WATFIV BATCH JOB ************************************************
******* WATFIV BATCH JOB ************************************************
******* WATFIV BATCH JOB ************************************************

      £COMPILE        GALV07
      C       EL-ISA,RECEPTION
      C       PROGRAM UNB  HALL,GLASGOW,JUNE 1977
      C       WIECHERT-HERGLOTZ-BATEMAN INTEGRAL FOR INVERSION OF T-X DATA
 1            DIMENSION VINT(100),VPT(100),Z(100),T(100)
 2            REAL*8 TEXT(5)
 3            READ (5,104) NPR
 4            DO 50 K=1,NPR
 5            READ (5,106) TEXT
 6            WRITE (6,105) K,TEXT
 7            READ (5,100) N,XMAX
 8            READ (5,101) (T(J),J=1,N)
 9            WRITE (6,103)
10            VINT(1)=XMAX/T(1)/N
11            DO 20 J=2,N
12               VINT(J)=XMAX/(T(J)-T(J-1))/N
13         20 CONTINUE
14            M=N-1
15            DO 30 J=1,M
16               DIST=J*XMAX/N
17               VPT(J)=0.5*(VINT(J)+VINT(J+1))
18            Z(J)=0.0
19                DO 40 I=1,J
20                  X=VPT(J)/VINT(I)
21                  ACOSH=ALOG(X+SQRT(X**2-1.0))
22                  Z(J)=Z(J)+XMAX*ACOSH/N/3.1416
23         40             CONTINUE
24               WRITE(6,102) Z(J),VPT(J),T(J),DIST
25         30 CONTINUE
26         50 CONTINUE
27        100 FORMAT(2X,I3,F10.3)
28        101 FORMAT(2X,10F7.4)
29        102 FORMAT(10X,F7.3,10X,F7.3,14X,F7.4,8X,F7.3)
30        103 FORMAT(//6X,'DETERMINATION OF VELOCITY-DEPTH FUNCTION'/6X,'EY
           1HERT-HERGLOTZ-BATEMAN INTEGRAL'//6X,'DEPTH IN KM'4X,'VELOCITY
           1M PER S'4X,'TIME IN S'4X,'DISTANCE IN KM'/)
31        104 FORMAT(2X,I3)
32        105 FORMAT(////2X,'PROBLEM NUMBER ',I3,5A8)
33        106 FORMAT(5A8)
34            STOP
35            END

      £DATA
```

PROBLEM NUMBER 1 SHOT (6) RED ONLY 6/9/1976.

DETERMINATION OF VELOCITY-DEPTH FUNCTION
BY WIECHERT-HERGLOTZ-BATEMAN INTEGRAL

Output

Input

DEPTH IN KM	VELOCITY IN KM PER S	TIME IN S	DISTANCE IN KM
0.021	4.348	0.1160	0.500
0.073	4.466	0.2300	1.000
0.115	4.566	0.3400	1.500
0.135	4.591	0.4490	2.000
0.147	4.598	0.5578	2.500
0.159	4.602	0.6665	3.000
0.202	4.619	0.7751	3.500
0.421	4.792	0.8830	4.000
0.571	4.975	0.9840	4.500
0.729	5.132	1.0840	5.000
0.926	5.379	1.1790	5.500
1.042	5.525	1.2700	6.000
1.109	5.587	1.3600	6.500
1.185	5.650	1.4490	7.000
1.266	5.714	1.5370	7.500

PROBLEM NUMBER 2 SHOT (1) BLUE ONLY 6/9/1976.

DETERMINATION OF VELOCITY-DEPTH FUNCTION
BY WIECHERT-HERGLOTZ-BATEMAN INTEGRAL

DEPTH IN KM	VELOCITY IN KM PER S	TIME IN S	DISTANCE IN KM
0.034	4.869	0.1050	0.500
0.066	5.000	0.2055	1.000
0.090	5.038	0.3050	1.500
0.128	5.076	0.4040	2.000
0.249	5.239	0.5020	2.500
0.329	5.391	0.5950	3.000
0.361	5.420	0.6875	3.500
0.395	5.450	0.7795	4.000
0.440	5.479	0.8710	4.500
0.485	5.510	0.9620	5.000
0.536	5.540	1.0525	5.500
0.894	5.872	1.1425	6.000
1.117	6.192	1.2233	6.500
1.131	6.200	1.3040	7.000
1.148	6.207	1.3846	7.500

NUMBER 4 EKA (5) RED ONLY 6/9/76

RMINATION OF VELOCITY-DEPTH FUNCTION
IECHERT-HERGLOTZ-BATEMAN INTEGRAL

PTH IN KM	VELOCITY IN KM PER S	TIME IN S	DISTANCE IN KM
0.011	4.556	0.1100	0.500
0.029	4.577	0.2195	1.000
0.053	4.608	0.3285	1.500
0.125	4.673	0.4365	2.000
0.181	4.739	0.5425	2.500
0.231	4.785	0.6475	3.000
0.310	4.855	0.7515	3.500
0.403	4.951	0.8535	4.000
0.512	5.051	0.9535	4.500
0.621	5.155	1.0515	5.000
0.724	5.252	1.1475	5.500
0.858	5.366	1.2419	6.000
0.987	5.495	1.3339	6.500
1.067	5.587	1.4239	7.000
1.168	5.650	1.5129	7.500
1.255	5.714	1.6009	8.000
1.325	5.764	1.6879	8.500

NUMBER 5 EKA (3) BLUE ONLY (GRAPH) 6/9/76

RMINATION OF VELOCITY-DEPTH FUNCTION
IECHERT-HERGLOTZ-BATEMAN INTEGRAL

PTH IN KM	VELOCITY IN KM PER S	TIME IN S	DISTANCE IN KM
0.007	4.550	0.1100	0.500
0.015	4.556	0.2196	1.000
0.142	4.754	0.3295	1.500
0.225	4.975	0.4305	2.000
0.315	5.132	0.5305	2.500
0.458	5.409	0.6255	3.000
0.553	5.619	0.7155	3.500
0.631	5.685	0.8035	4.000
0.613	5.692	0.8914	4.500
0.828	5.698	0.9792	5.000
0.645	5.705	1.0669	5.500
0.663	5.711	1.1545	6.000
0.688	5.718	1.2420	6.500
0.705	5.724	1.3294	7.000

APPENDIX (4)

CALCULATION OF TIME OF ARRIVAL AT AN ARRAY ELEMENT FOR A NON-PLANE WAVE-FRONT

This appendix contains a listing of the program " CLOSE " which was used for the apparent velocity and propagation vector calculations, see Chapter VI. The program was written by Jacob (1969)[31] who gave the following theoretical treatment as the basis for the calculation of the delay in the time of arrival of a curved wavefront.

Correction for a Curved Wave-Front

Refering back to Fig. (4-2) the y-axis is NS and the x-axis is EW. Where the cross-over point of the array is (0, 0) in Cartesian co-ordinates and the position of the i^{th} seismometer is at (x_i, y_i) we have that the distance D from the source to the seismometer is

$$D = \left[(x_i + \Delta \sin \theta_w)^2 + (y_i + \Delta \cos \theta_w)^2\right]^{\frac{1}{2}}$$

and the difference between this and the distance of the source to the cross-over joint is $(\Delta - D)$. Therefore, for each seismometer, the time correction to be <u>added</u> to its arrival time is

$$\delta t_{i(xy)} = \frac{\Delta - \left[(x_i + \Delta \sin\theta_w)^2 + (y_i + \Delta \cos \theta_w)^2\right]^{\frac{1}{2}}}{V_a} \qquad (1)$$

If the azimuth, θ_z, of the shock is used instead of the propagation vector θ_w, change signs inside the inner brackets. In processing the signal on the array θ_f is used as this is what is " seen " by the array.

Correction for Altitude Differences

The delay due to relative altitude of the i^{th} seismometer is

$$\delta t_{i(z)} = \frac{z_i \cos}{V_1}$$

But, as $\sin \eta = V_1/V_a$ the correction term to be added is

$$\delta t_{i(z)} = -z_i \left(\frac{1}{V_1^2} - \frac{1}{V_a^2} \right)^{\frac{1}{2}} \qquad (2)$$

Summing equations (1) and (2) and allowing for experimental error, E_i, we get for the i^{th} seismometer

$$t_o - t_i = \delta t_i$$

$$= \frac{\Delta - \left[(x_i + \Delta \sin \theta_f)^2 + (y_i + \Delta \cos \theta_f)^2 \right]^{\frac{1}{2}}}{V_a}$$

$$- z_i \left(\frac{1}{V_1^2} - \frac{1}{V_a^2} \right)^{\frac{1}{2}} + E_i \qquad (3)$$

Write $\theta_f = \theta$ with subscript f understood. The equation (3) represents a conical wave front where $V_a > V_1$. This equation as it stands cannot be used to make a least squares fit to the data as it is non-lenear in terms of two of the unknowns. An iteration method has thus been used, successively correcting suggested values. Approximations are used which are acceptable as this is an iteration method. The first one is acceptable as it is an approximation to a small term in equation (3).

$$z_i \left(\frac{1}{V_1^2} - \frac{1}{V_a^2} \right)^{\frac{1}{2}} = \frac{z_i}{V_1} \left(1 - \frac{V_1^2}{V_a^2} \right)^{\frac{1}{2}}$$

$$= \frac{z_i}{V_1} \left(1 - \frac{V_1^2}{2V_a^2} - \frac{V_1^4}{8V_a^4} - \frac{V_1^6}{16V_a^6} \cdots\cdots\cdots\cdots \right)$$

so we can rewrite

$$t_o - t_i \approx E_i + \Delta (V_a + \delta V_a)^{-1}$$

$$- z_i \left(\frac{1}{V_1} - \frac{V_1^2}{2(V_a + \delta V_a)} - \frac{V_1^4}{8(V_a + \delta V_a)} - \frac{V_1^6}{16(V_a + \delta V_a)} \right)$$

$$- \left(V_a + \delta V_a\right)^{-1} \left[\left(x_i + \Delta \sin (\theta + \delta\theta) \right)^2 + \left(y_i + \Delta \cos(\theta + \delta\theta) \right)^2 \right]^{\frac{1}{2}} \quad (4)$$

Where V_a and θ are suggested values and δV_a and $\delta\theta$ are corrections.

Taking the contents of the square bracket.

$$[\ ] = x_i^2 + 2x_i \Delta \sin (\theta + \delta\theta) + \Delta^2 \sin^2 (\theta + \delta\theta) + y_i^2$$

$$+ 2\Delta\, y_i \cos (\theta + \delta\theta) + \Delta^2 \cos^2 (\theta + \delta\theta)$$

$$= x_i^2 + y_i^2 + \Delta^2 + 2\Delta (x_i \sin (\theta + \delta\theta) + y_i \cos (\theta + \delta\theta))$$

putting $\sin \delta\theta = \delta\theta$ and $\cos \delta\theta = 1$

$$\sin (\theta + \delta\theta) \approx \sin\theta + \delta\theta \cos\theta$$

$$\cos (\theta + \delta\theta) \approx \cos\theta + \delta\theta \sin\theta$$

so

$$[\ ] \approx x_i^2 + y_i^2 + \Delta^2 + 2\Delta (x_i \sin\theta + y_i \cos\theta) + 2\Delta\delta\theta (x_i \cos\theta - y_i \sin\theta)$$

putting

$$r_i = x_i^2 + y_i^2 + \Delta^2 + 2\Delta (x_i \sin\theta + y_i \cos\theta)$$

and

$$s_i = 2\Delta (x_i \cos\theta - y_i \sin\theta)$$

we have

$$[\ ] \approx [r_i + s_i \delta\theta]$$

$$\therefore [\ ]^{\frac{1}{2}} \approx r_i^{\frac{1}{2}} \left[1 + \frac{s_i \delta\theta}{r_i}\right]^{\frac{1}{2}} \quad (5)$$

Now maximum s_i is less than minimum r_i and $\delta\theta$ is normally small, so

$$\left| \frac{s_i \delta\theta}{r_i} \right| < 1$$

and equation (5) may be expanded. In the program $\delta\theta$ has in fact been limited to $\pm$ 0.2 radians. We may also expand in equation (4)

$$V_a + \delta V_a \;^{-1} \approx \frac{1}{V_a} - \frac{\delta V_a}{V_a^2}$$

$$\therefore\ t_o - t_i \approx E_i + \frac{1}{V_a}\left(\Delta - r_i^{\frac{1}{2}} - \frac{S_i \delta\theta}{2r_i^{\frac{1}{2}}} - \Delta\frac{\delta V_a}{V_a} + \frac{r_i^{\frac{1}{2}}\delta V_a}{V_a}\right.$$

$$\left. + \begin{matrix}\text{discarded}\\ \delta V_a \cdot \delta\theta \text{ term}\end{matrix}\right)$$

$$- \frac{z_i}{V_1}\left(1 - \frac{V_1^2}{2V_a^2}\left(1 + \frac{\delta V_a}{V_a}\right)^{-2} - \frac{V_1^4}{8V_a^4}\left(1 + \frac{\delta V_a}{V_a}\right)^{-4}\right.$$

$$\left. - \frac{V_1^6}{16V_a^6}\left(1 + \frac{\delta V_a}{V_a}\right)^{-6}\right) \qquad (6)$$

And putting $\left(1 + \frac{\delta V_a}{V_a}\right)^{-n} \approx 1 - n\frac{\delta V_a}{V_a}$

Where n = 2, 4, 6 in equation (6) we get

$$t_o - t_i \approx E_i + \frac{1}{V_a}\left(\Delta - r_i^{\frac{1}{2}}\right) - \frac{S_i\delta\theta}{2V_a r_i^{\frac{1}{2}}} - \frac{\delta V_a}{V_a^2}\left(\Delta - r_i^{\frac{1}{2}}\right)$$

$$- \frac{zi}{V_1}\left(1 - \frac{V_1^2}{2V_a^2}\left(1 - 2\frac{\delta V_a}{V_a}\right) - \frac{V_1^4}{8V_a^4}\left(1 - 4\frac{\delta V_a}{V_a}\right)\right.$$

$$\left. - \frac{V_1^6}{16V_a^6}\left(1 - 6\frac{\delta V_a}{V_a}\right)\right) \qquad (7)$$

rearranging equation (7) we get

$$E_i = P_i + u_i\,\delta\theta + w_i\,\delta V_a + t_o \quad \text{where } i = 1, 2, \ldots, n \qquad (8)$$

and the coefficients are as follows

$$P_i = -\left[t_i + \frac{1}{V_a}\left(\Delta - r_i^{\frac{1}{2}}\right) - \frac{z_i}{V_1}\left(1 - \frac{V_1^2}{2V_a^2} - \frac{V_1^4}{8V_a^4} - \frac{V_1^6}{16V_a^6}\right)\right]$$

$$u_i = \frac{S_i}{2V_a r_i^{\frac{1}{2}}}$$

$$w_i = \frac{1}{V_a^2}\left(\Delta - r_i^{\frac{1}{2}}\right) + z_i\left(\frac{V_1}{V_a^3} + \frac{V_1^3}{2V_a^5} + \frac{3V_1^5}{8V_a^7}\right)$$

and the normal equations are given by

$$\frac{\partial\left(\sum_i E_i^2\right)}{\partial(\delta\theta)} = \frac{\partial\left(\sum_i E_i^2\right)}{\partial(\delta V_a)} = \frac{\partial\left(\sum_i E_i^2\right)}{\partial(t_o)} = 0$$

i.e

$$\left(\sum_i u_i\right) t_o + \sum_i u_i p_i + \left(\sum_i u_i^2\right)\delta\theta + \left(\sum_i u_i w_i\right)\delta V_a = 0$$

$$\left(\sum w_i\right) t_o + \sum_i w_i p_i + \left(\sum_i u_i w_i\right)\delta\theta + \left(\sum_i w_i^2\right)\delta V_a = 0$$

$$nt_o + \sum_i p_i + \left(\sum_i u_i\right)\delta\theta + \left(\sum_i w_i\right)\delta V_a = 0$$

$$i = 1, 2, \ldots\ldots, n$$

Note that t_o is the actual time at the reference point (0, 0, 0) while $\delta\theta$ and δV_a are corrections to a suggested value.

Program " CLOSE " uses these equations and repeats the calculations until $\delta\theta < 0.005$ radians and $\delta V_a < 0.002$ km/s. $\delta\theta$ has been limited to $\pm$ 0.2 radians and δV_a limited to 0.5 km/s. in any one pass to make the process stable when the first suggestions are a long way from the truth. With this restriction the process has proved stable and converges rapidly. It works even if the suggested angle is 180^o wrong (an error that occurs when the azimuth is suggested instead of the propagation vector).

" CLOSE " can be made to work without altitude corrections by putting all $z_i = 0$ and it will treat the arrival as a plane wave if Δ is made large compared with the dimensions of the array. In the case

of EKA it is quite sufficient to put Δ = 500 km. If Δ is made unnecessarily large the program will be evaluating small differences between large quantities and accuracy will suffer. In the case of an unknown source an approximate value for Δ should be obtained from the P–S time interval.

N IV G LEVEL 21 MAIN DATE = 77187

```
      REAL EE(23),MM(23),HS(23)
      REAL X(23),Y(23),Z(23),S1(23),N1(23),S2(23),N2(23),P(23),U(2
      REAL PTOD
      INTEGER TITLE(80)
      INTEGER NN,ST(23),SUBF,PIT(23,4)
      INTEGER GENT
      REAL T(23)
      DIMENSION S(23),TCALC(23)
      WRITE (3,1)
    1 FORMAT(1H 'CLOSE SHOCK ARRAY PROCESSING'//)
      READ (2,2) ((PIT(I,J),J=1,4),X(I),Y(I),Z(I),I=1,23)
    2 FORMAT(4A1,3F7.4)
      READ (2,211) NUMBR
  211 FORMAT(I3)
      RTOD=57.295779513
      WRITE (3,4)
    4 FORMAT(1H ,22X,'PIT',5X,'X',9X,'Y',9X,'Z'/)
      DO 6 I=1,23
      WRITE (3,5) (PIT(I,J),J=1,4),X(I),Y(I),Z(I)
    5 FORMAT(1H ,20X,4A1,3F10.4)
    6 CONTINUE
      DO 13 MMM=1,NUMBR
      READ (2,12) TITLE
   12 FORMAT(80A1)
      WRITE (3,121) TITLE
  121 FORMAT(1H ,10X,80A1,///)
      DO 3 I=1,23
      T(I)=0.
      ST(I)=0
    3 CONTINUE
      READ (2,7)NN,SUBF,SCAF
    7 FORMAT(I2,I4,F7.1)
      WRITE (3,14)
   14 FORMAT(22X,'PIT',5X,'TIME'/)
      DO 8 N2=1,23
      IF(NN-N2)8,9,9
    9 READ (2,91) I,T(I)
   91 FORMAT(I2,F5.4)
      ST(I)=1
    8 CONTINUE
      DO 10 I=1,23
      IF(ST(I))10,10,11
   11 T(I)=(T(I)-SUBF)/SCAF
      WRITE (3,15) (PIT(I,J),J=1,4),T(I)
   15 FORMAT(1H ,20X,4A1,F10.3)
   10 CONTINUE
C
C     A TABLE OF PIT TITLE AND X,Y,Z COORDINATES, AND
C     A TABLE OF ARRIVAL TIMES AT THE PITS TO BE USED
C     HAVE NOW BEEN PRINTED.
C
      READ (2,16) VELA,THETA,DELTA,VEL1
   16 FORMAT(F3.1,F4.0,F6.2,F3.1)
C
C
  700 WRITE (3,17) VELA,THETA,DELTA
```

```
L  21          MAIN          DATE = 77167          23/26/22
   FORMAT(1H ,10X,'FIRST ESTIMATES ARE,VELOCITY =',F3.1,'KMS/SEC',
  1'PROPAGATION VECTOR =',F4.0,'DEGREES, WHILE DELTA =',F6.2,
  2'KMS'///)
   WRITE (3,172)VEL1
 2 FORMAT(1H ,5X,'SURFACE LAYER VELOCITY =',F3.1,'KMS/SEC'/)
   WRITE (3,18)
   FORMAT(1H ,14X,'THETA',5X,'DTHET',6X,'VELA',6X,'DVEL',6X,'TCP'/)
   THETA=THETA/R160
   DO 25 I=1,23
   IF(ST(I))25,25,26
   R1(I)=X(I)*X(I)+Y(I)*Y(I)+DELTA**2+2*DELTA*(X(I)*SIN(THETA)+Y(I)*C
  1OS(THETA))
   S1(I)=2*DELTA*(X(I)*COS(THETA)-Y(I)*SIN(THETA))
   R2(I)=Z(I)*(1-VEL1*VEL1/(2*VELA*VELA)+VEL1**4/(8*VELA**4)-VEL1**6/
  1(16*VELA**6))/VEL1
   S2(I)=VEL1*Z(I)*(1/(VELA**3)+VEL1*VEL1/(2*VELA**5)+3*VEL1**4/(8*
  1VELA**7))
   P(I)=-T(I)-(DELTA-SQRT(R1(I)))/VELA+R2(I)
   Q(I)=S1(I)/(VELA*SQRT(R1(I))*2)
   W(I)=(DELTA-SQRT(R1(I)))/VELA**2+S2(I)
 5 CONTINUE
   A=0
   B=0
   C=0
   D=0
   E=0
   F=0
   G=0
   H=0
   DO 31 I=1,23
   IF(ST(I))31,31,32
 2 A=A+Q(I)*P(I)
   B=B+Q(I)*Q(I)
   C=C+Q(I)*W(I)
   D=D+W(I)*P(I)
   E=E+P(I)
   F=F+W(I)*W(I)
   G=G+Q(I)
   H=H+W(I)
 1 CONTINUE
   A4=(D*B-A*C)*(B*G-NN*B)-(E*B-A*G)*(B*C-H*B)
   A5=(C*C-F*B)*(B*G-NN*B)-(B*C-H*B)**2
   DVEL=A4/A5
   TCP=((E*B-A*G)-(C*G-H*B)*DVEL)/(B*G-NN*B)
   DTHET=-(A+C*DVEL+G*TCP)/B
   IF(DVEL*DVEL-0.25)34,34,331
 1 IF(DVEL)332,332,333
 2 DVEL=-0.5
   GO TO 34
 3 DVEL=0.5
 4 IF(DTHET*DTHET-0.04)344,344,341
 1 IF(DTHET)342,342,343
 2 DTHET=-0.2
   GO TO 344
 3 DTHET=0.2
 4 THETA=THETA+DTHET
```

```
      VELA=VELA+DVEL
      WRITE (3,35) THETA,DTHET,VELA,DVEL,TCP
   35 FORMAT(1H ,10X,5F10.3)
      IF(DVEL*DVEL-0.000025)41,41,27
      IF(DTHET*DTHET-0.000004)42,42,27
      THETD=THETA*RTOD
      IF(THETD)421,424,422
      THETD=THETD+360.
      GO TO 424
      IF(THETD-360.)424,423,423
      THETD=THETD-360.
      WRITE (3,44) THETD,VELA
   44 FORMAT(1H ,'MEASURED VALUES',4X,'PROPAGATION VECTOR =
     1',F6.2,'DEGREES','APPARENT VELOCITY = ',F6.3,'KMS/SEC'/)
      WRITE (3,46) TCP
   46 FORMAT(1H ,'TIME AT CROSS-OVER POINT = ',F7.3,' SECONDS')

      THE APPARENT VELOCITY AND PROPAGATION VECTOR OF THE WAVE
      ACROSS THE ARRAY HAVE NOW BEEN CALCULATED. THE NEXT
      STEP IS TOCALCULATE WHAT THE ARRIVAL TIMES AT EACH
      PIT FOR THIS VELOCITY AND ANGLE SHOULD HAVE BEEN IF
      THERE WAS NO ERROR ( USE ORIGINAL EXACT,NOT APPROXIMATE
      EQUATIONSFOR THIS). HENCE RESIDUALS AND AN
      ESTIMATE OF THE VARIANCE. VALUE FOR RESIDUALS
      GOT FROM EQUATION 57A IN 'SKEW MULTILAYERING'.
    1 SCAR=0
      DO 55 I=1,23
      TCALC(I)=0.
      EE(I)=0.
      IF(ST(I))55,55,54
   54 B4(I)=SQRT((X(I)+DELTA*SIN(THETA))**2+(Y(I)+DELTA*COS(THETA))**2)
      B5(I)=Z(I)*SQRT(1/(VEL)*VEL)-1/(VEL4*VELA))
      TCALC(I)=TCP+B5(I)-(DELTA-B4(I))/VELA

      RESIDUAL = CALCULATED - OBSERVED

      EE(I)=TCALC(I)-T(I)
      SCAR=SCAR+EE(I)*EE(I)
      CONTINUE


    3 VAR=SCAR/(NN-1)


      T(23)=TCP
      WRITE (3,61)
   61 FORMAT(1H ,20X,'PIT',5X,'T CAL',5X,'E(I)'/)
      DO 63 I=1,23
      WRITE (3,62) (PIT(I,J),J=1,4),TCALC(I),EE(I)
   62 FORMAT(20X,4A1,2F10.3)
   63 CONTINUE
      WRITE (3,66) SCAR
   66 FORMAT(1H ,'SCAR =',E14.8/)
      WRITE (3,65) VAR
   65 FORMAT(1H ,'VARIANCE =',E14.8///)
      CONTINUE
      STOP
      END
```

APPENDIX (5)

List of all local events received at EKA Array, their distances, direct propagation vectors and travel times for some of these, as measured from the cross-over point and their apparent velocities and propagation vectors as calculated through Jacob's[31] program (see Appendix (4)). Some of those events with Low S/N ratio were rejected from the analysis.

No.	Event's Name	Distance (km)	Travel Time (sec)	Direct Propagation Vector (θ°)	Observed Prop. Vector	Apparent Velocity km/sec	Comments
1	Kaimes	62.96		168	161.6	5.718	
2	Kaimes	62.96		168	161.6	5.782	
3	Kaimes	62.96	11.399	168	162.0	5.775	
4	Craig Park	66.83	12.02	168	162.9	5.821	
5	Craig Park	66.83	12.02	168	162.0	5.950	
6	Craig Park	"	12.02	168	165.4	5.995	
7	Tams Loup	70.27		147	145.4	5.555	
8	Tams Loup	70.27		147	146	5.670	
9	Cairney Hill	74.16		145	141.2	5.481	
10	Cairney Hill	74.16		146	144.8	5.512	

APPENDIX (5) (Contd.)

No.	Event's Name	Distance (km)	Travel Time (sec)	Direct Propagation Vector (θ°)	Observed Prop. Vector	Apparent Velocity km/sec	Comments
11	Northfield	93.23	17.057	150.0	144.8	6.096	
12	Northfield	93.23		150.0	145.8	6.038	Low S/N Ratio
13	Boards Farm	93.31	16.59	150.0	152.5	6.518	"
14	Murrayshall	99.63	17.50	150.0	149.8	6.749	"
15	Douglasmuir	101.72	17.93	133.0	138.0	7.320	"
16	Dumbuckhill	109.63	19.22	129.5	129.4	6.25	Low S/N Ratio
17	High Craig	101.10		124.0	120	5.95	
18	Coatsgate	20.38		89.9	96.5	5.379	
19	Craighouse	46.57		227.4	222.7	6.492	
20	Hillhouse	96.11	16.76	108.0	109.9	6.40	
21	Middleton	53.09		188.0	181.0	5.985	
22	Cloburn	48.43	8.699	139.0	136.0	5.542	

APPENDIX (5) (Contd.)

No.	Event's Name	Distance (km)	Travel Time (sec)	Direct Propagation Vector (θ°)	Observed Prop. Vector	Apparent Velocity km/sec	Comments
23	Cloburn	48.43	8.699	139.0	136.2	5.624	
24	Cloburn	48.43	8.699	139.0	135.2	5.571	
25	Westfield	94.21		177.0	170.6	6.785	
26	Frairton	117.1		171.6	160.5	6.35	
27	Goat	82.1		173.0	164.5	6.02	
28	Westfield	94.21	17.02	177.0	169.2	6.358	
29	Oxwellmains	82.39		208.0	203.3	6.475	Low S/N Ratio
30	Oxwellmains	82.39		208.0	205.2	6.326	
31	Navy Shot	100.95	18.2	196	186.3	6.152	
32	Navy Shot	109.15	18.85	200	184.2	6.069	
33	Collace	126.85		177.5	168.8	5.839	
34	Collace	126.85	21.92	177.5	171.5	5.882	

APPENDIX (5) (Contd.)

No.	Event's Name	Distance (km)	Travel Time (sec)	Direct Propagation Vector (θ°)	Observed Prop. Vector	Apparent Velocity km/sec	Comments
35	Dollar N. E.	78.28		155.0	156.7	5.647	
36	Dollar "	92.47		160.0	151.5	5.782	
37	Dollar "	94.65		162.0	154.6	5.692	
38	Rosewell "	56.83		182.0	173.7	5.693	
39	Midlothian "	60.50		183.0	169.1	6.198	
40	Midlothian "	66.75		184.0	174.8	6.131	
41	Newbattle	60.40		190.0	174.6	5.863	
42	Glenalmond	126.42	21.80	168.0	159.2	6.182	
43	Glenalmond	124.37	21.42	167.0	159.4	6.309	
44	Glenalmond	123.54	21.24	167.8	162.1	6.649	
45	Natural Event	125.30	20.16	164.5	158.0	6.655	

APPENDIX (5) (Contd.)

No.	Event's Name	Distance (km)	Travel Time (sec)	Direct Propagation Vector (θ°)	Observed Prop. Vector	Apparent Velocity km/sec	Comments
46	Loch Awe	163.13	22.33	125.5	125.9	6.712	
47	SOSP(II) Shot (25)	152.13	25.437	73.0	72.3	6.565	
48	" (26)	153.03	25.640	74.5	76.1	6.641	
49	" (27)	154.28	25.390	75.9	81.2	6.772	
50	Isle of May	100.0			195.9	6.273	
51	U/W	90.0			182.4	6.066	
52	L*	60.0			147.6	5.601	
53	Cruicks	77.84		170.0	167.6	6.094	
54	Loanhead	17.70	103.23	119.3	118.35	5.653	Low S/N Ratio
55	Craighouse	46.57		227.4	222.40	6.402	
56	Dunion	38.70		248.0	252.0	6.361	

APPENDIX (5) (Contd.)

No.	Event's Name	Distance (km)	Travel Time (sec)	Direct Propagation Vector (^{o})	Observed Prop. Vector	Apparent Velocity km/sec	Comments
57	Duntilland	72.35		144	146.8	4.955	
58	Coatsgate	20.38		89.9	95.5	5.365	
59	Middleton	53.09		188.0	180.5	5.870	
60	Westfield	94.21		177.0	168.5	6.09	
61	Westfield	94.21		177.0	170	6.15	
62	Oxwellmains	82.39		208.0	203	6.616	

APPENDIX (6)

List of all local events received at Broughton Array, their distances, direct propagation vectors and travel times for some of these, as measured from the cross-over point and their apparent velocities and propagation vectors as calculated through Jacob's[31] program (see Appendix (4)

No.	Event's Name	Distance (km)	Travel Time (sec)	Direct Propagation Vector (θ°)	Observed Prop. Vector	Apparent Velocity km/sec	Comments
1	Middleton	30.55	5.818	224	232.8	6.352	
2	Middleton	30.55		224	231.4	6.417	
3	Douglasmuir	72.64	12.7	123	120	7.289	Low S/N Ratio
4	Loanhead	79.32	14.01	107	102.4	7.200	"
5	Northfield	60.32		146.0	146.3	7.119	"
6	Boards Farm	60.52	10.769	146	145.0	6.78	"
7	Murrayshall	66.75	11.910	147.0	146.8	6.140	"
8	Dumbuckhill	81.48	14.36	119.0	115.8	6.455	"
9	Cruicks	76.22	8.316	179.6	185.4	6.80	
10	Cruicks	76.20		179.6	184.8	6.694	

APPENDIX (6) (Contd.)

No.	Event's Name	Distance (km)	Travel Time (sec)	Direct Propagation Vector (θ°)	Observed Prop. Vector	Apparent Velocity km/sec	Comments
11	Kaimes	31.08	5.83	179.5	181.9	6.380	
12	Kaimes	31.08		179.5	181.8	6.288	
13	Kaimes	31.08		179.5	178.6	6.142	
14	Coatsgate	31.25		14.0	7.7	5.607	
15	Tams Loup	37.98	7.19	138.5	136.0	6.542	
16	Tams Loup	37.98		138.5	138.5	6.277	
17	Tams Loup	〃		〃	138	6.38	
18	Hillhouse	78.39	13.395	89	77.1	7.612	
19	Oxwellmains	67.38		232	219	6.15	Low S/N Ratio
20	Craighouse	46.63		268.8	275.5	5.718	
21	Westfield	64.43		190.0	192.1	7.262	
22	Westfield	64.43		190	192.5	7.20	

APPENDIX (6) (Contd.)

No.	Event's Name	Distance (km)	Travel Time (sec)	Direct Propagation Vector (θ°)	Observed Prop. Vector	Apparent Velocity km/sec	Comments
23	Craig Park	34.97	6.480	180	181.6	6.360	
24	Craig Park	34.97	6.510	180	178.4	6.296	
25	Craig Park	34.97	6.460	180	179.0	6.417	
26	Cloburn	19.72		108	107.7	6.313	
27	Cloburn	19.72	3.77	108	107.5	6.071	
28	Cloburn	19.72	3.77	108	108.0	6.196	
29	Duntilland	40.58	7.543	134	134.3	6.731	
30	High Craig	75.30		110	107.8	6.842	Low S/N Ratio

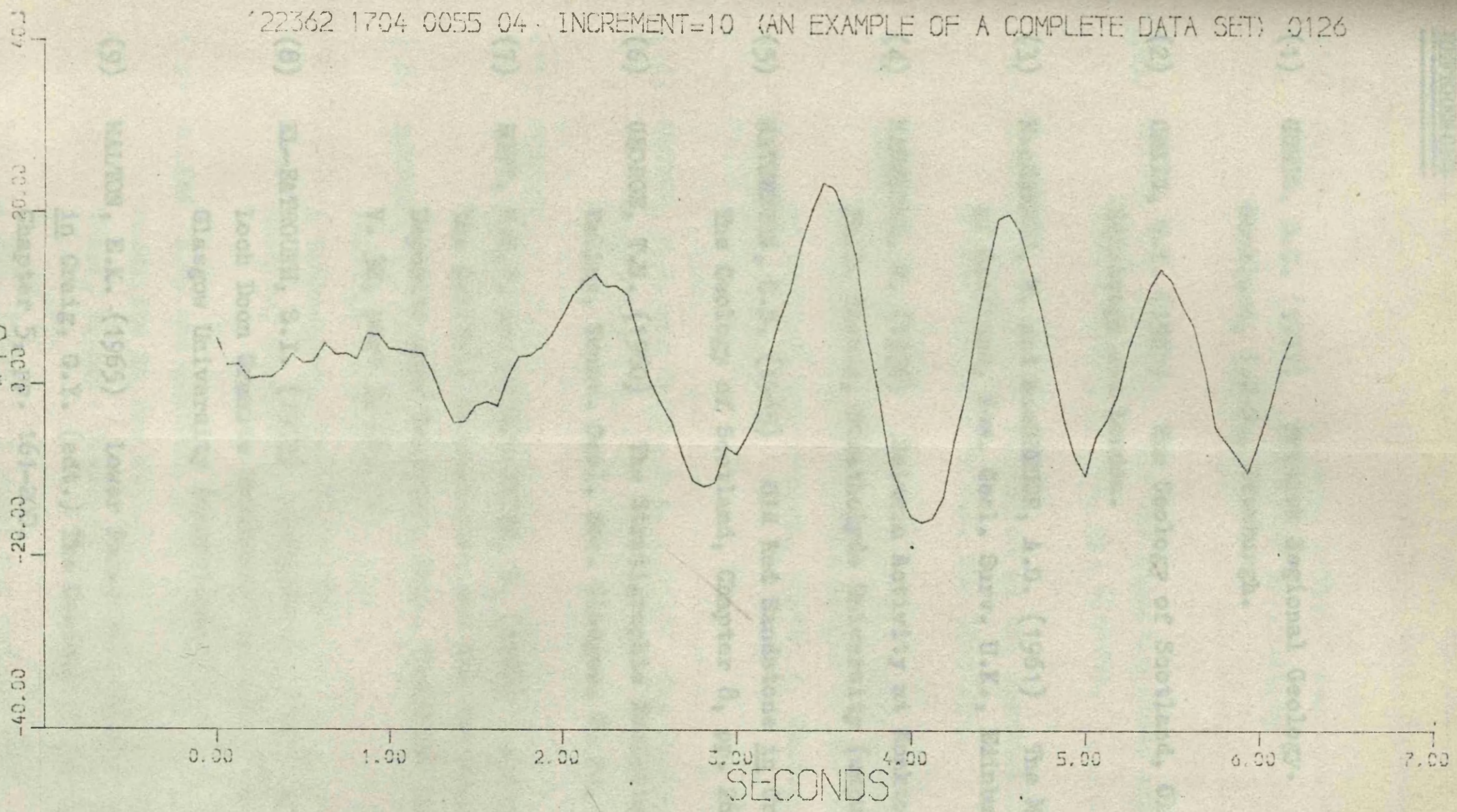

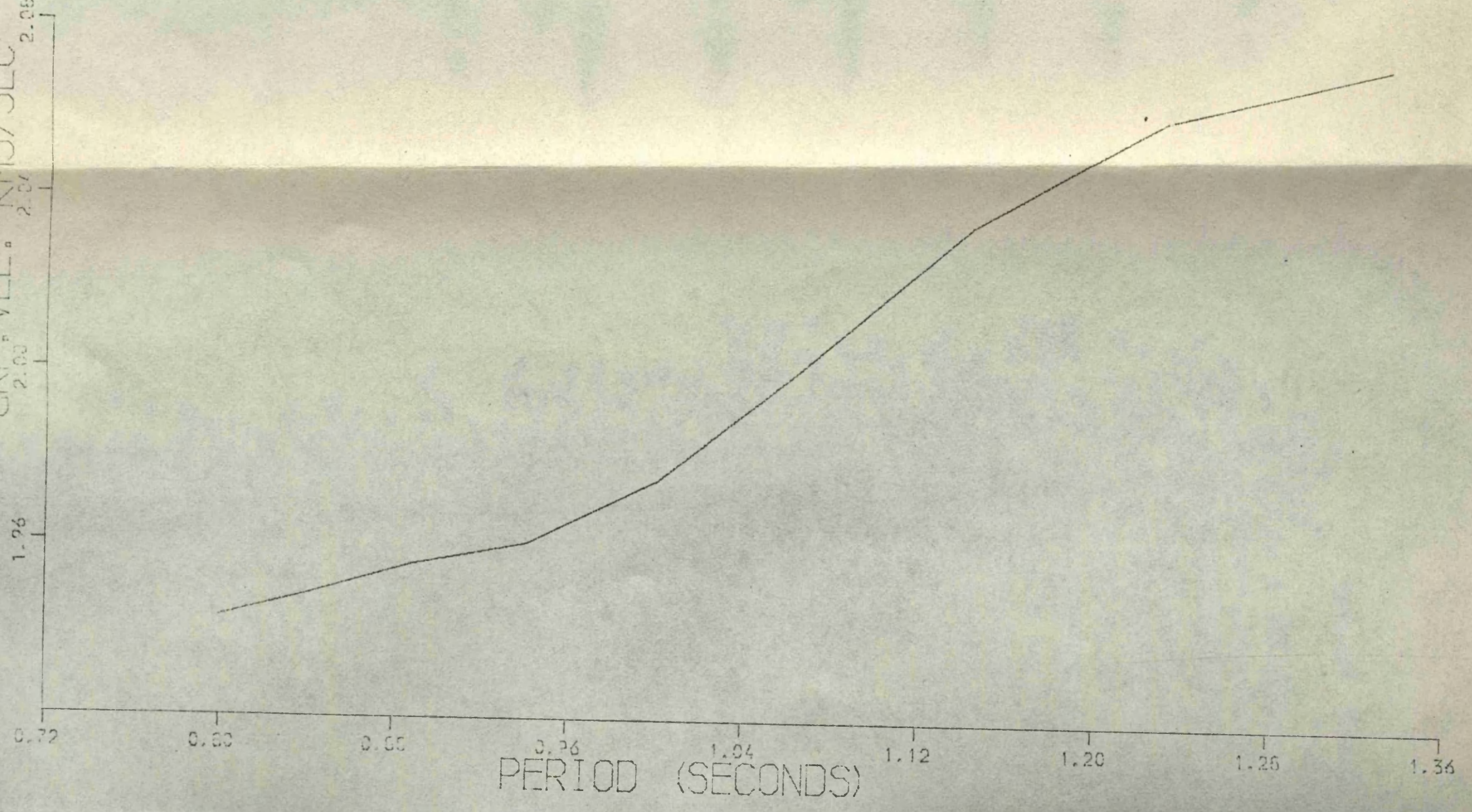

Appendix (7) Dispersed Rayleigh waves recorded at EKA from a Midland Valley source (natural event) and its dispersion curve as calculated through the program referred to in Chapter I, see Burton & Blamey (1972)[80].

REFERENCES

(1) GREIG, D.C. (1971) British Regional Geology. The South of Scotland, I.G.S., Edinburgh.

(2) CRAIG, G.Y. (1965) The Geology of Scotland, Oliver and Boyd, Edinburgh and London.

(3) MacGREGOR, M. and MacGREGOR, A.G. (1961) The Midland Valley of Scotland, Mem. Geol. Surv. U.K., Edinburgh.

(4) MASHKOUR, M. (1976) Seismic Activity at Monktonhall Colliery, Ph.D. Thesis, Strathclyde University (unpublished).

(5) WATERSTON, C.D. (1965) Old Red Sandstone in Craig, G.Y. (edt.) The Geology of Scotland, Chapter 8, pp. 269-308.

(6) GEORGE, T.N. (1960) The Stratigraphic Evolution of the Midland Valley, Trans. Geol. Soc. Glasgow, V. 24, pp. 32-107.

(7) BOTT, M.H.P. and MASSON-SMITH, D. (1960) A Gravity Survey of the Criffell Granodiorite and the New Red Sandstone Deposits near Dumfries, Proc. Yorkshire Geol. Soc., V. 32, part 3, No. 13.

(8) EL-BATROUKH, S.I. (1975) Geophysical Investigations on Loch Doon Granite South-West Scotland, Ph.D. Thesis, Glasgow University (unpublished).

(9) WALTON, E.K. (1965) Lower Palaeozoic Rocks - Stratigraphy in Craig, G.Y. (edt.) The Geology of Scotland, Chapter 5, pp. 161-200.

(10) LAPWORTH, C. (1882) The Girvan Succession, Q.J. Geol. Soc. London, V. 38, pp. 537-666.

(11) PEACH, B.N. and HORNE, J. (1899) The Silurian Rocks of Britain, V. 1, Scotland Mem. Geol. Survey.

(12) CRAIG, G.Y. and WALTON, E.K. (1959) Sequence and Structure in the Silurian Rocks of Kirkcudbrightshire, Geol. Mag., V. 96, pp. 209-220.

(13) WILSON, J.T. (1966) Did the Atlantic Close and then Re-open? Nature Lond., V. 211, pp. 676-681.

(14) DEWEY, J.F. (1969) Evolution of the Appalachian/Caledonian Orogen, Nature, V. 222, pp. 124-129.

(15) DEWEY, J.F. (1971) A Model for the Lower Palaeozoic Evolution of the Southern Margin of the Early Caledonides of Scotland and Ireland, Scott. J. Geology, V. 7, pp. 219-240.

(16) CHURCH, W.R. and GAYER, R.A. (1973) The Ballantrae Ophiolite, Geol. Map., V. 110, pp. 497-510.

(17) MOSELEY, F. (1977) Caledonian Plate Tectonics and the Place of the English Lake District, Geol. Soc. Am.

(18) BAMFORD, D., FABER, S., JACOB, B., KAMINSKI, W., NUNN, K., PRODEHL, C., FUCHS, K., KING, R., and WILLMORE, P. (1976) A Lithospheric Seismic Profile in Britain: I. Preliminary Results, Geophys. J.R. Astr. Soc., V. 44, pp. 145-160.

(19) McLEAN, A.C. and QURESHI, I.R. (1966) Regional Gravity Anomalies in the Western Midland Valley of Scotland, Trans. R. Soc. Edinburgh, V. 66, pp. 267-283.

(20) POWELL, D.W. (1971) A Model for the Lower Palaeozoic Evolution of the Southern Margin of the Early Caledonides of Scotland and Ireland, Scott. J. Geology, V. 7, pp. 369-372.

(21) BAMFORD, D., NUNN, K., PRODEHL, C., and JACOB, B. (1977) LISPB - III. Upper crustal structure of Northern Britain, J. Geol. Soc. Lond., V. 133, pp. 481-488.

(22) HALL, J. (1971) Seismic studies in the region of the Firth of Clyde, Ph.D. Thesis, Glasgow University (unpublished).

(23) McLEAN, A.C. (1961) Density measurements of rocks in South-West Scotland, Proc. Roy. Soc. Edinb., V. 68, pp. 103-110.

(24) KEY, F.A., MARSHALL, P. D. and McDOWALL, A.J. (1964) Two recent British earthquakes recorded at the U.K. Atomic Energy Authority Seismometer Array at Eskdalemuir, Nature, V. 201, No. 4918, pp. 484-485.

(25) AGGER, H.E. and KEY, F.A. (1964-5) The Glasgow area earthquake recorded at the U.K.A.E.A. Seismometer Array at Eskdalemuir, Geophys. J. Roy. Astr. Soc., V. 9, pp. 537-539.

(26) AGGER, H.E. and CARPENTER, E.W. (1964-5) A crustal study in the vicinity of the Eskdalemuir Seismological Array Station, Geophys. R. Roy. Astr. Soc., V. 9, pp. 69-83.

(27) KEY, F.A. (1967) Signal generated noise recorded at the Eskdalemuir Seismometer Station, Bull. Seism. Soc. Amr., V. 57, No. 1, pp. 27-37.

(28) HUDSON, J.A. (1967) Scattered surface waves from a surface obstacle, Geophys. J. Roy. Astr. Soc., V. 13, pp. 441-458.

(29) BOTT, M.H.P. (1968) The geological structure of the Irish Sea basin. In Donovan, D.T. (edt.) Geology of shelf seas, Chapter 7, pp. 93-115, Oliver and Boyd, Edinburgh.

(30) BLUNDELL, D.J. and PARKS, R. (1969) A study of the crustal structure beneath the Irish Sea, Geophys. J. Roy. Astr. Soc., V. 17, pp. 45-62.

(31) JACOB, A.W.B. (1969) Crustal phase velocities observed at the Eskdalemuir Seismic Array, Geophys. J. Roy. Astr. Soc., V. 18, pp. 189-197.

(32) JOHNSON, L.E. and GILBERT, F. (1972) Inversion and inference for teleseismic ray data, in Bolt, A.A. (edt.) Methods in computational physics, V. 12, pp. 231-266, Academic Press, New York and London.

(33) CORBISHLEY, D.J. (1970) Multiple array measurements of the P-wave travel-time derivative, Geophys. J. Roy. Astr. Soc., V. 19, pp. 1-14.

(34) CORBISHLEY, D.J. (1970) Structure under seismic arrays, Geophys. J. Roy. Astr. Soc., V. 21, pp. 415-425.

(35) WILLMORE, P.L. (1973) Crustal studies in the region of the British Isles, Tectonophysics, V. 20, pp. 341-357.

(36) CRAMPIN, S., JACOB, A.W.B., MILLER, A. and NEILSON, G. (1970) The LOWNET radio-linked seismometer network in Scotland, Geophys. J.R. Astr. Soc., V. 21, pp. 207-216.

(37) BORG, H. and BATH, M. (1971) The Uppsala Seismograph Array Station, Pur. & Appl. Geophys., V. 89, pp. 19-31.

(38) BATH, M. (1974) Developments in solid earth geophysics, V. 7: Spectral analysis in geophysics, Elsevier, Amsterdam, Oxford, New York.

(39) PRESS, F. (1956 b) Determination of crustal structure from phase velocity of Rayleigh waves. Part I: Southern California, Bull. Geol. Soc. Amr., V. 67, pp. 1647-1658.

(40) WILSON, J.T. (1967) Seismic detection of nuclear explosions, in Runcorn, S.K., International Dictionary of Geophysics, V. 2, pp. 1343-1345, Pergamon Press, Oxford.

(41) BIRTILL, J.W. and WHITEWAY, F.E. (1965) The application of seismic arrays to the analysis of seismic body waves. Phil. Trans. Roy. Soc. A V. 258, pp. 421-493.

(42) WILLMORE, P.L. (1962) Nature, Lond., V. 195, pp. 1250-1252.

(43) TRUSCOTT, J.R. (1964-5) The Eskdalemuir Seismological Station, Geophys. J. Roy. Astr. Soc., V. 9, pp. 59-68.

(44) CAPON, J. (1973) Signal processing and frequency-wavenumber spectrum analysis for a large aperture seismic array, in Bolt, B.A. (edt.) Methods in computational Physics, V. 13, pp. 1-59, Academic Press, New York and London.

(45) JANSSON, B. and HUSEBYE, E.S. (1968) Application of array data processing techniques to a network of ordinary seismograph stations, Pure & Appl. Geophys., V. 69, pp. 80-99.

(46) KEEN, C.G., MONTGOMERY, J., MOWAT, M.W., MULLARD, J.E. and PLAT, D.C. (1965) British seismometer array recording systems, Radio Elect. Eng., V. 30, pp. 297-306.

(47) WIECHERT, D.H., MANCHEE, E.B. and WHITHAM, K. (1967) Digital experiments at twice real time speed on the capabilities of the Yellowknife Seismic Array, Geophys. J., V. 13, pp. 277-295.

(48) SAVIT, C.H., BRUSTAD, J.T. and SIDER, J. (1958) The moveout filter, Geophysics, V. 23, pp. 1-25.

(49) MUIRHEAD, K.J. and DATT, R. (1976) The N-th root process applied to seismic array data, Geophys. J. Roy. Astr. Soc., V. 47, pp. 197-210.

(50) MUIRHEAD, K.J. (1968 a) Eliminating false alarms when detecting seismic events automatically, Nature, V. 186, pp. 704.

(51) IYER, H.M. (1968) Determination of frequency-wavenumber spectra using seismic arrays, Geophys. J. Roy. Astr. Soc., V. 16, pp. 97-117.

(52) HAUBRICH, R.A. (1968) Array design, Bull. Seism. Soc. Amr., V. 58, No. 3, pp. 977-991.

(53) Internal Report, AWRE, Blacknest.

(54) DAVISON, C. (1924) A history of British earthquakes, Cambridge University Press.

(55) DOLLAR, A.T.J. (1950) A catalogue of Scottish earthquakes, 1916-1949, Trans. Geol. Soc. Glasgow, V. 21, pp. 283-361.

(56) CRAMPIN and WILLMORE (1973) Dollar earthquakes.

(57) CRAMPIN, S. (1970) A method for the location of near seismic events using travel-times along ray paths, Geophys. J., V. 21, pp. 535-539.

(58) CRAMPIN, S. (1973) FAMG: A computer program for the location of local earthquakes recorded by large-aperture low-density seismic networks, Deport No. 33, Global Seismology Unit, I.G.S., Edinburgh.

(59) WALTON, E.K. (1961) Some aspects of the succession and structure in the Lower Palaeozoic rocks of the Southern Uplands of Scotland, Geol. Rdsch., V. 50, pp. 63-77.

(60) Directory of Quarries and Pits, (20th edt.), The Quarry Managers' Journal Ltd., London.

(61) Members Directory (1976) The British Quarrying and Slag Federation Ltd., London.

(62) HOULISTON, D.J., LAUGHLIN, J. and WAUGH, G. (1976) Developments of the seismic data-processing system of the Institute of Geological Sciences in Edinburgh, Internal Report, No. 14, I.G.S., Edinburgh.

(63) HAGEDOORN, J.G. (1959) The plus-minus method of interpreting seismic refraction sections, Geophys. Prosp., V. 1, pp. 158-182.

(64) GRANT, F.S. and WEST, G.F. (1965) Interpretational theory is applied geophysics, McGraw-Hill, New York.

(65) ANDERSON, L. and LIEBERMANN, R.C. (1968) Sound velocities in rocks and minerals: Experimental methods, extrapolations to very high pressures and results, in Mason, W.P. (edt.) Physical Acoustics, V. IV, Part B, pp. 329-472.

(66) SMITHSON, S.B. and SHIVE, P.N. (1975) Field measurements of compressional wave velocities in common crystalline rocks, Earth Planet, Sci. Lett., V. 27, pp. 170-176.

(67) HALL, J. and AL-HADDAD, F.M. (1976) Seismic velocities in the Lewisian metamorphic complex, north west Britain - 'in situ' measurements, Scott. J. Geol., V. 12, No. 4, pp. 305-314.

(68) SCHENK, V. and SCHENKOVA (1974) Stress wave velocity and crack system of a medium, Geophys. Prosp., V. 22, No. 4, pp. 710-721.

(69) NETTLETON, L.L. (1940) Geophysical prospecting for oil, McGraw-Hill, New York and London.

(70) OTSUKA, M. (1966) Azimuth and slowness anomalies of seismic waves measured on the Central California Seismographic Array, Part I. Observations, Bull. Seism. Soc. Amr., V. 56, No. 1, pp. 223-239.

(71) OTUSKA, M. (1966) Azimuths and slowness anomalies of seismic waves measured on the Central California Seismographic Array, Part II. Interpretation, Bull, Seism. Soc. Amr., V. 56, No. 3, pp. 655-675.

(72) NIAZI, M. (1966) Corrections to apparent azimuths and travel-time gradients for a dipping Mohorovicic Discontinuity, Bull. Seism. Soc. Amr., V. 56, No. 2, pp. 491-509.

(73) BOLT, B.A. and NUTTLI, O.W. (1966) P-wave residuals as a function of azimuth, 1, Observations, J. Geophys. R., V. 71, pp. 597-7-

(74) NUTTLI, O.W. and BOLT, B.A. (1966) P-wave residuals as a function of azimuth, 2. Undulations of the mantle low-velocity layer as an explanation, J. Geophys. R., V. 74, pp. 6594-

(75) BROWN, R.J., BORG, H. and BATH, M. (1969) Strike and dip of crustal boundaries - A method and its application, Pure and Appl. Geophysics, V. 88, pp. 60-74.

(76) ELLIS, R.M. and BASHAM, B.W. (1968) Crustal characteristics from short-period P-waves, Bull. Seism. Soc. Amr., V. 58, No. 5, pp. 1681-1700.

(77) BROWN, R.J. (1973 b) Slowness and azimuth at the Uppsala array, Part I: Array calibration and event location, Pure and Appl. Geophys., V. 105, pp. 759-769.

(78) BROWN, R.J. (1973 c) Slowness and azimuth at the Uppsala array, Part 2: Structural studies, Pure & Appl. Geophys., V. 109, pp. 1623-1637.

(79) BROWN, R.J. (1973 d) Azimuthally varying P-wave travel-time residuals in Fennoscandia and lateral inhomogeneity, Pure & Appl. Geophysics, V. 105, pp. 741-758.

(80) BURTON, P.W. and BLAMEY, C. (1972) A computer program to determine the spectrum and a dispersion characteristic of a transient signal, AWRE report No. 048/72, AWRE, Aldermaston.

(81) The Eskdalemuir Array, Internal Report, M.O.D., Blacknest

(82) CRAMPIN, S. (1976) A comment on " The early structural evolution and anisotropy of the oceanic Upper Mantle", Geophys. J. R. Astr. Soc., V. 46, pp. 193-197.

(83) CRAMPIN, S. (1977) A review of the effects of anisotropic layering on the propagation of seismic waves, Geophys. J. R. Astr. Soc., V. 49, pp. 9-27.

(84) KEITH, C.M. and CRAMPIN, S. (1977) Seismic body waves in anisotropic media - I, Geophys. J.R. Astr. Soc., V. 49, pp. 181-208.